Universidad Autónoma de Madrid
Departamento de Bioquímica

Polycomb RING1B complexes in hematopoietic cells

TESIS DOCTORAL

Katarzyna Starowicz

Madrid, 2017

Departamento de Bioquímica
Facultad de Medicina
Universidad Autónoma de Madrid

Polycomb RING1B complexes in hematopoietic cells

Memoria presentada por Katarzyna Starowicz, licenciada en Biología, para optar al grado de Doctor en Biociencias Moleculares por Universidad Autónoma de Madrid

Directores de tesis:
Miguel Ángel Vidal Caballero
(Centro de Investigaciones Biológicas - CSIC)
Carmela Calés Bourdet
(Instituto de Investigaciones Biomédicas – UAM-CSIC)

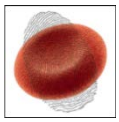

HEM_ID
HEMATOPOIETIC
CELL
IDENTITY

La presente Tesis Doctoral con título: **Polycomb RING1B complexes in hematopoietic cells** ha sido realizada por Katarzyna Starowicz bajo la dirección del Dr. Miguel Ángel Vidal Caballero y de la Dra. Carmela Calés Bourdet, pertenecientes el departamento de Biología Celular y Molecular del Centro de Investigaciones Biológicas (CSIC) y al departamento de Biología del Cáncer de Instituto de Investigaciones Biomédicas (CSIC-UAM), respectivamente.

El desarrollo del trabajo ha sido posible gracias a la financiación concedida por el Marie Skłodowska-Curie Actions con la beca FP7-PEOPLE-2011-ITN (grant number 289611) así como a través del Ministerio de Economía y Competitividad (MINECO) gracias al proyecto SAF2013-47997-P y al proyecto SAF2016-80486-P

V°B° de los directores de la tesis:

Dr. Miguel Ángel Vidal Caballero

Dra. Carmela Calés Bourdet

Acknowledgements

Mojej rodzinie
Moim przyjaciołom

ACKNOWLEDGEMENTS

Este trabajo ha sido elaborado durante los últimos 5 años, no existiría sin el apoyo y la presencia de algunas personas maravillosas en mi vida.

En primer lugar quiero agradecer a mis directores de tesis: Dr. Miguel Vidal y Dra. Carmela Calés por darme la oportunidad de realizar este trabajo en vuestros laboratorios, enseñarme lo complicado del mundo Polycomb y hematopoyesis. Al igual que por todos los tipos de ayuda que me disteis durante estos 5 años (no solo en el trabajo), por perdonarme mis fallos, por corregir mis errores y lo más importante de todo por " believe in me". Me acuerdo que cuando llegue a Madrid hace 5 años, estaba totalmente sola y vosotros me habéis tratado como familia y gracias a esto no me sentía como una "guiri" en España. En realidad para mí sois como una "segunda familia" y gracias a vosotros me he desarrollado como científica pero también como persona.

We thank Dr. Haruhiko Koseki from RIKEN Center in Yokohama for help with derivation of BirA and Ring1B^{bio} mice and also Dr. Mariano Barbacid from CNIO for the *CreER*^{T2}mouse line. We thank also Dr Keiryn L. Bennett (CeMM) for help with mass spectrometry analysis.

También quiero agradecer a mis compis del labo 106 Zahiri, Moni y a Fabio por escucharme y apoyarme en todas las ocasiones. Sin vosotros estos últimos 5 años seguro que hubiesen sido mucho más duros. Tu Zahiri, mi peliroja (antiguamente), desde mi primer día en el labo intentabas que me sintiera en Madrid como en casa y estabas siempre a mi lado.

A las niñas de 1.4.2 Lucia y Sandra por ayudarme y escucharme cuando estuvimos analizando muestras en citometro o trabajando con los bichetes. Espero que os vayan bien vuestras tesis y sin grandes complicaciones.

Al personal del animalario por toda la ayuda con los ratones y también por apoyarme y escucharme en momentos duros.

A mis compañeros del CIB – Teresa, María P. (las vecinas del 105), Ana, Bea y Lore por escucharme y por toda la ayuda que me disteis últimos 5 anos

To my HEM_ID friends (students and PIs) to share with me this great experience. Our meetings were always unique in scientific and personal meaning. I hope to see you soon again because I really miss you guys.

Mojej rodzinie, w szczególności moim rodzicom gdyby nie oni myśle że ta praca nigdy by nie powstała. Jestem wam ogromnie wdzięczna za całe wsparcie jakie mi dajecie przez całe dotychczasowe życie a także za wiare w moją osobę mimo że nie jestem dzieckiem idealnym. Mojej sister Karolci, szwagrowi Piotrkowi i Ali za wszelaką pomoc, wysłuchiwanie moich narzekań i bycie zawsze obok. Dzieki wam jestem lepszym człowiekiem.

Moim Paskudnikom, za wsparcie przez te wszytskie lata (nie tylko te 5). Za bycie przy mnie w tym dobrych i złych momentach. Za cierpliwość do mojej osoby i moich gorzkich żali. Gdyby nie wy laski to nie wiem jakbym to wszystko wytrzymala bo jak mówi Korek „science to nie rurki z kremem". Dziękuje wam wszystkim a w szczególności Korkowi, Wronie i Lani (bosh, nie wiem jak wytrzymujesz ze mna od prawie 25 lat).

A ti Pedro, por aparecer en mi vida en el momento más inesperado y estar aquí hasta ahora, momento en el cual escribo estas palabras. Gracias por estar conmigo en los momentos felices y también por estar en los momentos duros, por apoyarme y aguantarme todos estos años que no han sido fáciles, y por tener fe en mí.

Gracias a todos vosotros he podido elaborar este trabajo. Os quiero mucho…

And last but not least, a MSC Actions of European Commision y Ministerio de Economía y Competitividad por financiar mi trabajo.

Summary
(Resumen)

SUMMARY

RING1A and RING1B paralogous proteins are part of the heterodimeric RING finger-type E3 ligases present in type I Polycomb Repressive Complexes (PRC1). They are responsible for the monoubiquitylation of histone H2A that correlates with the transcriptional repression of PRC1 targets. PRC1 are biochemically heterogeneous entities which have RING1A/RING1B as core components present in all of their forms. PRC1 complexes are grouped into canonical and non-canonical complexes depending on subunits content and therefore functionally distinct. The known biochemical heterogeneity and regulatory complexity of PRC1 assemblies arises from cell types departed (tumoral established lines) from in vivo cells. We thus asked how faithfully the accepted PRC1 complexes represent those extant in non- or less-altered cell types. For this purpose, we set up an experimental system to investigate PRC1 within the hematopoietic compartment, in primary cells of different lineage and/or different stage of maturation. We used a mouse line that expresses a RING1B variant that can be biotinylated by a ubiquitously expressed prokaryotic biotin ligase. The biotinylatable RING1B, knocked-in at the RING1B locus, is subject to the same controls as the endogenous gene, thus representing a situation as close to the physiological state as possible. Selected hematopoietic cell types obtained from these mice, and ex-vivo expanded populations of progenitors were used to prepare nuclear extracts from which RING1B and associated proteins were isolated using streptavidin beads. We found that levels of PRC1 subunits change from one cell type to another. Our results show that RING1A and RING1B segregate, for the most part, into different complexes. Likewise, the differences in distribution of PRC1 subunits throughout density gradients vary with cell types, without a perceivable pattern. During our attempts of studying the content of PRC1 subunits in RING1B complexes, we found that PRC1 assemblies in hematopoietic cells are more unstable than complexes in the cell lines commonly used. In summary, the data point at the presence of complexes of heterogeneous composition related to different maturation stages and different of the nowadays accepted, paradigmatic PRC1.

RESUMEN

Las proteina ligasas E3 de la clase I de complejos represivos Polycomb (PRC1) son heterodímeros de proteínas que siempre contienen o RING1A o su homólogo RING1B. La actividad protein ligasa de PRC1 es responsable de la monoubiquitinación de la histona H2A. Los complejos PRC1 son entidades bioquímicamente heterogéneas, agrupándose en dos grandes categorías, canónica y no canónica, definidas por capacidades que más allá de la modificación de H2A, presentan funciones exclusivas. La mayor parte del conocimiento actual sobre complejos PRC1 deriva de estudios con líneas celulares establecidas a partir de tumores o tipos celulares singulares, como las células madre embrionarias que, en conjunto, difieren de los tipos celulares que se encuentran in vivo. Nosotros nos hemos preguntado si lo que conocemos de PRC1 es una fiel representación de células no alteradas como las que pueden encontrarse in vivo o con alteraciones mínimas. Para ello diseñamos un sistema experimental para estudiar PRC1 en células primarias de diferente linaje y/o diferente estado de maduración dentro del compartimento hematopoyético. El sistema se basa en una línea de ratones genéticamente manipulados para conseguir la expresión de una forma de RING1B que se puede biotinilar endógenamente y, de esta manera, aislarse con facilidad mediante el uso de bolas con estreptavidina inmovilizada. Como la variante de RING1B resulta de la modificación del gen endógeno, se puede esperar que tanto su regulación como sus niveles se asemejen a los del producto del gen salvaje, es decir, las condiciones extremadamente próximas a las fisiológicas. Varios tipos celulares hematopoyéticos seleccionados asì como sus derivados expandidos ex-vivo se utilizaron para la preparación de extractos en los que determinamos niveles de subunidades PRC1 y sus asociaciones en complejos. Hemos encontrado que la expresión de subunidades varía con el tipo celular y que sus niveles disminuyen, en células primarias con la diferenciación. También vemos que la mayoría de los complejos que contienen RING1B son independientes de los que contienen RING1A, lo que sugiere diferencias funcionales no anticipadas, dada la redundancia de parálogos identificados. Al aislar complejos que contienen RING1B, hemos observado que las distintas subunidades PRC1 se asocian entre sí y a RING1B con afinidades mucho menores que las mostradas en complejos de células de líneas establecidas. Junto a la diversidad relacionada con el estado de maduración, estos estudios apuntan a la presencia de complejos parcialmente distintos de los que constituyen el actual paradigma PRC1.

Index

INDEX

Abbreviations

ABREVIATIONS

4'-OHT – 4' hydroxytamoxifen

AUTS2 - Autism Susceptibility Candidate 2

BMI1 – B lymphoma Mo-MLV insertion region 1 homolog

BCOR – BCL6 corepressor

CBFβ – core binding factor beta

CBX – chromodomain protein

CHD – chromodomain helicase

CKIIa - casein kinase subunit 2 a

DCAF7 - DDB1- and CUL4-associated factor 7

DMEM- Dulbecco's modified Eagle medium

DTT – ditiotreitol

EDTA- Ethylenediaminetetraacetic acid

EtOH- ethanol

EZH – Enhancer of Zeste

E2F6 - E2F Transcription Factor 6

FBRS – probable fibrosin 1

FCS – fetal calf serum

IL-3 – interleukin 3

IL6 – interleukin 6

IMDM - Iscove's Modified Dulbecco's Media

ISWI - imitation SWI

GM-CSF – granulocyte macrophages colony stimulating factor

KDM2B – Lysine specific demethylase 2B

KMT2A - Histone-lysine N-methyltransferase 2A

L3MBTL- Lethal(3)malignant brain tumor-like protein

LPS – lipopolysacharide

MAX - Myc-associated factor X

M-CSF – macrophages colony stimulating factor

MGA - MAX gene-associated protein

MLL – mixed-lineage leukemia 1 = KMT2A

NaCl – sodium chloride

NP40 = Igepal

NUP98 – Nucleoporin 98

PcG – Polycomb Group

PCGF – Polycomb group RING finger

PCR- polymerase chain reaction

PHC - Polyhomeiotic

PRC1- Polycomb repressive complex 1

PRC2 – Polycomb repressive complex 2

PRE – Polycomb responsive element

RING1A – Really interesting new gene 1A

RING1B - Really interesting new gene 1B

RPMI 1640 - Roswell Park Memorial Institute medium 1640

RYBP – Ring1 and YY1- binding protein

SAM – sterile alpha motive

SCF – stem cell factor

SCM – Polycomb protein SCM

SDS- sodium dodecyl sulfate

SKP1 - S-phase kinase-associated protein 1

SWI/SNF - SWItch/Sucrose Non-Fermentable

WDR5 - WD repeat-containing protein 5

YAF2 – homologue of RYBP

YY1 – yin and yang 1

Introduction

INTRODUCTION

The genetic material, in eukaryotes, is organized as long nucleoprotein complex(es) that display complicated form topological conformations. Access to DNA, the template of all encoded products that determine a cellular identity is, therefore, one of the key elements in gene regulation. At the most elemental level, chromatin is but a string of DNA wrapped around an octamer of duplicated dimers of histones H2A-H2B and histones H3-H4. A large collection of proteins, forming a variety of complexes endowed with diverse enzymatic activities, is devoted to chromatin regulation. The protein complexes they form are known as chromatin regulators. They modify chromatin, from local to high-order structures through a highly regulated, interconnected network of protein-protein interactions and enzymatic activities. As a result, cis-acting control regions, i.e. promoters and enhancers, the sequences that DNA binding proteins bind to among the collection of chromatin regulators, the Polycomb system stands out historically by their association with developmental processes.

1. THE POLYCOMB SISTEM OF CHROMATIN REGULATORS

The so-called Polycomb system was initially defined genetically, grouping mutations isolated in developmental studies with the fly Drosophila melanogaster (Lewis, 1978).After molecular cloning of the Polycomb group (PcG) of genes, it was apparent the multiplicity of unrelated proteins involved. Functionally, the derepression of Hox genes in Polycomb mutant larvae and the alterations seen in adult flies led to the classification of the products of PcG genes as transcriptional repressors (Jürgens, 1985). It is, precisely, the phenotype of adult mutant male flies, showing additional sex combs in their first and second pair of legs what coined the term Polycomb to name the group of genes that when mutated showed similar phenotypes. PcG products assemble in protein complexes, as assessed following biochemical purification, in a way consistent with the interactions observed during genetic analysis. Importantly, work in other system models soon showed evolutionary conservation so that PcG products are found in plants, metazoans and even (some of them, at least) in yeast (Alonso et al., 2007; Levine et al., 2002). PcG proteins form two major types of complexes termed Polycomb repressive complexes (PRC) (Levine et al., 2002). The two types, contain non-overlapping sets of proteins. One class of complexes, PRC2, was first associated with an enzymatic activity that di- and try-methylates lysine 27 of histone H3 (H3K27me3) (R. Cao & Zhang, 2004; Czermin et al., 2002). The other class of complexes, PRC1, can also modify histones, but through

monoubiquitylation of histone H2A (H2AUb) (de Napoles et al., 2004; Wang et al.,2004).. These modifications and the protein domains responsible are the most conserved portions of PcG proteins throughout evolution.

While PRC1 and PRC2 do not normally associate physically, they colocalize, to some extent, on chromatin (Ram et al., 2011). Functionally PRC1 and PRC2 show mutual interdependence at certain sites (Farcas et al., 2012; Tavares et al., 2012). As other chromatin regulators, PRC1 and PRC2 contain, in addition to the mentioned enzymatic activities, subunits that recognize and associate to specific modifications of histone tails (Bernstein et al., 2006; Kaustov et al., 2011; Min et al.,, 2003), subunits that bind non-specifically DNA or RNA and also subunits engaged in protein-protein contacts (Aranda, Mas, & Croce, 2015; Farcas et al., 2012; Kaneko et al., 2014; Neira et al., 2009; Yap et al., 2010; Yu et al., 2012). Although initially identified as transcriptional repressors, recent evidence points at PRC1 associated also to transcriptionally active loci (Creppe et al., 2014; Frangini et al., 2013; Kloet et al., 2016; Loubiere et al., 2016; Morey et al., 2015). Despite intense work in many laboratories, the mechanisms underlying the activity(es) of PRCs are poorly characterized. This includes their recruitment to targets and their influence on the transcriptional process. In mammalian cells most work on the Polycomb system has been carried out on the model of embryonic stem cells (ESCs), a pluripotent cell type of transient existence in the preimplantation embryo that can be maintained in vitro, as sustained in time under conditions that hold their tendency to differentiation. It is because they make an excellent model to study in vitro differentiation that they are so broadly used.

2. PRC RECRUITING TO GENOMIC SITES

In flies, PRC is recruited to so-called Polycomb response elements, short sequences enriched in DNA binding sites (Zink & Paro 1989; Ringrose & Paro, 2007) however, similar sites are not known in mammalian cells. Instead, PcG complexes locate preferentially to singular genomic regions, CpG islands (CGIs) of hundred to few kilobases of sequences enriched in the dinucleotide CpG, that, in contrast to sites not so enriched in CpG are free of DNA methylation (Farcas et al., 2012). About half of the mammalian promoters are contained within CGIs probably due to its unique structure that makes them ideal platforms for gene regulation (Deaton & Bird, 2011). PcG complexes locate to CGIs because of KDM2B, a DNA binding protein with a domain that specifically recognizes unmethylated CpG sequences and

that purifies with a subset of PRC1 complexes (Farcas et al., 2012). Regulatory events not fully characterized restrict the presence of PRC1 complexes to some of this sites bound by KDM2B. Binding of PRC1 at these sites is accompanied by H2AUb, which in turn is recognized by a subunit of PRC2, leading to allosteric activation of the methyltransferase activity of PRC2 subunit EZH2 (Kalb et al., 2014). Subsequent methylation of H3K27, in turn, increases the residence time of some PRC1 complexes at these sites through the recognition of PRC2-modified H3K27me3 (Blackledge et al., 2014; Kalb et al., 2014). In this way a self-reinforcing mechanism is at play at, at least, some regions, although there are other sites where PRC1 and PRC2 do not colocalize (Ku et al., 2008; van den Boom et al., 2016). In addition to CGIs, other DNA sequences are used for transcription-factor mediated recruiting (Suzuki et al., 2016; Yu et al., 2012) but these have not been established as general ways of recruiting.

3. PRC TRANSCRIPTIONAL ACTIVITY

Two main paths have been explored to explain PRC repression. One, on transcription initiation, proposes that PRC1, or its histone modification interact with the assembly of the pre initiation complex (Lehmann et al., 2012) or the pausing of RNA polymerase II (Stock et al., 2007). Derived from work with ESCs, Polycomb involvement in either mechanisms is not settled (Jadhav et al., 2016).

The second mechanism for transcriptional repression is based on the ability to compact chromatin, normally dependent on protein-protein interactions. The presence of subunits with such an ability on some PRC1 complexes leads to functionally relevant alterations of chromatin structure (Boettiger et al., 2016; Isono et al., 2013; Lau et al., 2017). PRC1 participates also from long-distance contacts between genomic sites, such as those between enhancer and promoters. Their involvement may result in transcriptional activity that can be modulated (Kondo et al., 2014; Schoenfelder et al., 2015).

4. NO TRANSCRIPTIONAL FUNCTIONS OF POLYCOMB COMPLEXES

The PRC1 complexes always were described as chromatin remodelers which regulate gene transcription. Last discovers show that these proteins also have other functions which is not associated with transcription machinery. RING1A and RING1B were found to be involved in DNA replication (Bravo et al., 2015; Piunti et al., 2014). PCGF4, other component of PRC1

complexes is regulating oxidative stress in hematopoietic compartment (Liu et al., 2009; Nakamura et al., 2012) but also DNA damage response (DDR) pathway (X. Lin et al., 2015; Liu et al., 2009). Also CBX8 was found to be involved in DDR (Oza et al., 2016). The new evidences about novel PRC1 functions shows that there are still remaining questions to answer about nature of Polycomb proteins.

5. PRC1 COMPLEXES

RING1A and RING1B proteins, with the enzymatic activity of E3 ligase, are a core component of PRC1 complexes. These proteins were co-purified with all Polycomb proteins, what suggest that plays the main role in Polycomb machinery. Their structure, contain several motifs allowing other PRC1 subunits interact. On the N-terminus, the RING finger motif is found (Saurin et al., 1996) and is used for interaction with PCGF paralogs. The C-terminus hold the RAWUL domain (Ring-finger And WD40 associated Ubiquitin-Like (Sanchez-Pulido et al., 2008), which participate in interactions with the other PRC1 subunits.

5.1 Ubiquitination mediated by RING1A and RING1B

The PRC1 E3 ligase module contains RING1A or RING1B which interact through their RING finger domain with one of the six Polycomb group RING finger proteins (PCGFs)(Buchwald et al., 2006; Li et al., 2006). Ubiquitination of proteins is a multi-step process, in which E3 ligase transfer ubiquitin from the E2 element, specific conjugating enzyme, or ubiquitin carrier (Metzger et al., 2014). PRC1 E3 ligases work with UBCH5, specific E2 component, which interact exclusively with RING1A or RING1B (Buchwald et al., 2006). The PCGF proteins do not interact directly with E2 module but stimulate enzymatic activity of RING proteins, which deposit ubiquitin on H2AK119. Ubiquitination of H2A was associated with transcriptional repression, because mutation in RING1B leads to loss of H2Ak119ub and activation of Hox genes (Cao et al., 2005, Wang et al., 2004).

5.2 PRC1 heterogeneity (Canonical vs non-canonical)

Each subunit of Polycomb complex characterized in *Drosophila* has multiple orthologs in the mammalian genome (Otte & Kwaks, 2003; Sparmann & van Lohuizen, 2006), which indicate a wide range of possible associations. Depending on the structural composition, PRC1 complexes are grouped into two main types: canonical- and non-canonical-PRC1. Canonical

PRC1 refer to the first complex, purified from HeLa cells containing various CBX proteins (homologs of Pc), RING1A and RING1B – subunits with activity analogous to dRing, homologs of Ph (PHC1,2,3) and BMI1/PCGF4 - homolog of Psc.

The complexes composition and interactions between subunits was poorly understood during the years. Various groups were working on biochemical identification of PRC1 using the affinity tag purification method. In subunit-independent manner the RING1A/B proteins were co-purified and new interactions was identified. The composition and interactions between Polycomb proteins were characterized by investigations on subunits as PCGF2 (Elderkin et al., 2007), PCGF4 (Wiederschain et al., 2007), E2F6 (Ogawa et al., 2002), BCOR and PCGF1 (Gearhart et al., 2006). A mile step in the Polycomb research was the isolation of the RING1B complexes and identification of a high number of novel interactions. Additionally, identification of new complex containing KDM2B/FBXL10 and BCOR was assessed in the study (Sánchez et al., 2007). At the time there was no evidence explaining the complexity of interactions. Recent results, published by Hauri and colleagues where they perform complete analysis of Polycomb ineractome in human cells shown how miscellaneous Polycomb interaction network could be (Hauri et al., 2016).

	Canonical PRC1 (PRC1.2, PRC1.4)	**Non-canonical PRC1 (PRC1.3,PRC1.5, PRC1.6)**
core components	RING1A, RING1B	RING1A, RING1B
PCGF proteins	PCGF2/MEL18 (PRC1.2/1.4) PCGF4/BMI1 (PRC1.2/1.4)	PCGF1/NSPC1 (PRC1.1) PCGF3 (PRC1.3) PCGF5 (PRC1.5) PCGF6/MBLR (PRC1.6)
chromodomain proteins	CBX2/M33, CBX4/PC4, CBX6, CBX7, CBX8 (PRC1.2/1.4)	CBX8 (PRC1.1), CBX3/HP1γ (PRC1.6)
Polyhomeiotic homologs	PHC1, PHC2, PHC3 (PRC1.2/1.4)	
Sex Comb on Midleg homologs	SCML2,SCMH1,SFMBT1(PRC1.4)	
DNA-binding proteins		KDM2B/FBXL10 (PRC1.1) MGA-MAX, E2F6-TDFP1(PRC1.6)
Other subunits	RYBP	RYBP, YAF2 (PRC1.1,3,5,6) L3MBTL2, WDR5 (PRC1.6) SKP1, BCOR (PRC1.1) AUTS2,CSNK2A1/CK2a(PRC1.5)

Table I. Canonical and non-canonical PRC1 subunits

For long time PRC1 complexes did not have clear and simply classification. The recent one, is based on the six family members of the PCGF (Gao et al., 2012). Gao and colleagues purified each of PCGFs with a set of associated proteins, that are present in each of PRC1 complexes. They suggested to name complexes from PRC1.1 to PRC1.6, depending on PCGF homolog. In Table I are presented all subunits divide into categories: canonical and non-canonical.

The CBX paralogs, which associate with RING proteins by their RAWUL domain have in their structure chromo (CHRomatin Organization Modifier) domain which could recognized H3K27me3 CBX (Yap & Zhou, 2011) Interaction of CBX proteins with other PRC1 components is mutually exclusive (Vandamme et al., 2011). Chromodomains of CBX proteins have different affinity to recognize H3K27me3 (Bernstein et al., 2006; Kaustov et al., 2011). Studies in embryonic stem cells (ESC) shows that CBX7 and CBX8 recruitment is efficient, whereas CBX2, CBX4 and CBX6 not (Zhen et al., 2016). CBX proteins form part of canonical PRC1 (preferentially) however, they are also found in non-canonical complexes (Beguelin et al., 2016).

RYBP and their paralog YAF2 (García et al., 1999) are two proteins which also interact with RING1A/B by association to their RAWUL domain. Participation of this proteins in PRC1 complexes is mutually exclusive with CBX proteins (Tavares et al., 2012). RYBP was found to bound to DNA (Neira et al., 2009). It was also proposed to recruit PRC1 complexes to chromatin, however the mechanism is not well characterized (Tavares et al., 2012).

5.3 Is function dependent on the composition?

Since the composition of PRC1 complexes was defined, it was suggested that different complexes may have distinct functions (Luis et al., 2012). Study on genomic localization the PCGFFs homologues has shown that promoters are bound exclusively or predominantly by only one PCGF (Gao et al., 2012). Those results could imply that every complex has a specific target and biological function. The comparison of chromatin occupancy by PRC1-RYBP and PRC1-CBX7 complexes has demonstrated that this two distinct complexes can colocalize at genomic loci but in general occupy specific for each targets (Morey et al.,2013). Also it is known that RING1A has an ability to compensate RING1B deletion in ES cells, however that is not happen with CBXs proteins. Each of the CBX proteins has it specific function that cannot

be carried by other members of the family (Creppe et al., 2014; Klauke et al., 2013; Morey et al., 2013).

5.4 Changes in composition during differentiation

In the context of Polycomb, little is known about the role of heterogeneity of PRC1 in differentiation. In ESC and hematopoietic system, CBX7 is involved in self-renewal, but during lineage commitment is repressed and replaced by its paralogs (CBX2, CBX4 or CBX8) (Klauke et al., 2013; Morey et al., 2012). Interestingly, in those cells, CBX6 is transcriptionally active protein not interacting with PRC1 subunits and just 5% of its genomic occupancy is associated with Polycomb proteins (Morey et al., 2012). That result suggests that the CBX6 has non-Polycomb linked role in those cell types. Changes in composition and targets of PCGF2-containing complexes during cardiac differentiation shown that PRC1 complexes could play a different role on each step of the process (Morey et al., 2015). This study proposes that specific PRC1 complexes control different cell types, influencing biological processes during differentiation of the cells via activation or repression of the gene transcription.

Proteomic and genomic studies dedicated to a characterization of PRC1 complexes during differentiation of ESC to neural cells have revealed that PRC1 complexes are cell type specific (Kloet et al., 2016). Using label-free quantitative proteomic approach, the group demonstrated dramatic changes in PCGFs and CBX protein during differentiation. PCGF6 is exchanged by PCGF4 and CBX7, which is present only in ESC, is replaced by CBX6 in the neural cells. Other examples, highlights, those subunits PHC2 and 3 are present only in differentiated neural cells. Genomic studies has shown that in both cell types PRC1 complexes binds to different targets, confirming the specific function of each complex.

5.5 Association with non-Polycomb proteins

Multiple proteomic analysis identified interactors of RING1B which are PRC1 subunits but also proteins which did not belong to the Polycomb family. Various group demonstrate that RING1B could interact with other chromatin remodelers, members of SWI/SNF family complexes (Stanton et al., 2016).. Other interactors which were found to be associated to RING1B probably plays role in Polycomb machinery which could be recruitment mechanism or specific role of PRC1. This is still remaining question.

It is important to note that most of the above body of knowledge on the nature of PRC1 complexes (and also of their function) derives from work in a limited and selective cell types. Despite evolutionary conservation, the Drosophila model cannot shed light on, for example, the mammalian system given the large differences in PRC1 subunits (the conserved regions are, basically, restricted to functional domains, such as RING fingers, chromodomains or SAM domains). Mammalian systems on which PRC1 has been studied include, in addition to ESCs, the humoral cell lines such as human kidney embryo 293 cells, HeLa or MEL (murine erythroleukemia). The content of these cells in PRC1 subunits (and, in general, of most proteins) is much higher than that in in vivo cells. Besides, their unusual nature (ESCs, cells can only deploy a subset of regulatory pathways, channeled towards their transformed phenotype.

With this in mind, we set out to investigate the nature of PRC1 as close as possible to an in vivo situation. The possibility that the system appeared still more complicated than already known, we aimed at a minimization of variables by restricting our analysis, at least initially, to a single cell lineage, the hematopoietic compartment.

6. HEMATOPOIESIS

6.1 Normal hematopoiesis

Hematopoiesis is the process in which progenitor cells give rise to all mature blood cells. It is highly dynamic because mature cells has limited life-span and must be continuously replaced. This process take place in a bone marrow however, mature cells are migrating to secondary hematopoietic organs as thymus, spleen and blood for terminal differentiation. The most primitive cell type, the hematopoietic stem cell (HSC) has the highest self-renewal potential and gives rise to all hematopoietic cell type. In the adult, HSCs locate predominantly in the bone marrow, where they reside for the entire life of organism. HSCs exist in minute numbers (0.005% Oguro et al 2013), compared to more differentiated cells. As all stem cells, HSCs undergo symmetric and asymmetric divisions to generate daughter HSCs (self-renewal) (Morrison & Kimble, 2006) or cells that, upon successive divisions, will become a complex set of progenitors differentially primed for distinct cell lineages (Cabezas-Wallscheid et al., 2014; Hérault et al., 2017; A. Wilson et al., 2008). Following the committed cell fate, progenitors become the precursors of fully differentiated mature cells. Lacking any of surface molecules

termed lineage markers, some of which univocally identify cell lineages (for example, CD19 on lymphoid precursors of B cells, or Ter119, on erythroid cells, progenitors are referred to as the pool of lineage negative (Lin-) cells in the bone marrow. Another cell population of relevance is one expressing c-kit, the receptor for an important cytokine, the stem cell factor, also known as kit-ligand) present in more or less undifferentiated cells, including many Lin- cells. Figure I1, shows one of the best accepted paradigms of hematopoietic differentiation, noting relationships between progenitors, precursors and mature cells. It contains three major lineages: megakaryo-erythroid, myeloid and lymphoid. Maturation within the first two is attained within the bone marrow from where platelets, erythrocytes and a variety of myeloid cells, such as neutrophil, granulocytes or macrophages leave for the blood stream. The lymphoid lineage, on the other hand, i.e. B and T-cells leave the bone marrow to house in secondary hematopoietic organs, spleen and thymus, respectively (lymph nodes, too), where their fully functional capacities are acquired. In general, lymphoid cells have a much longer lifespan than myeloid cells, implying that most hematopoiesis is spent generating short-lived myeloid cell types. B-cells arriving to the spleen constitute a major component of splenic cell population.

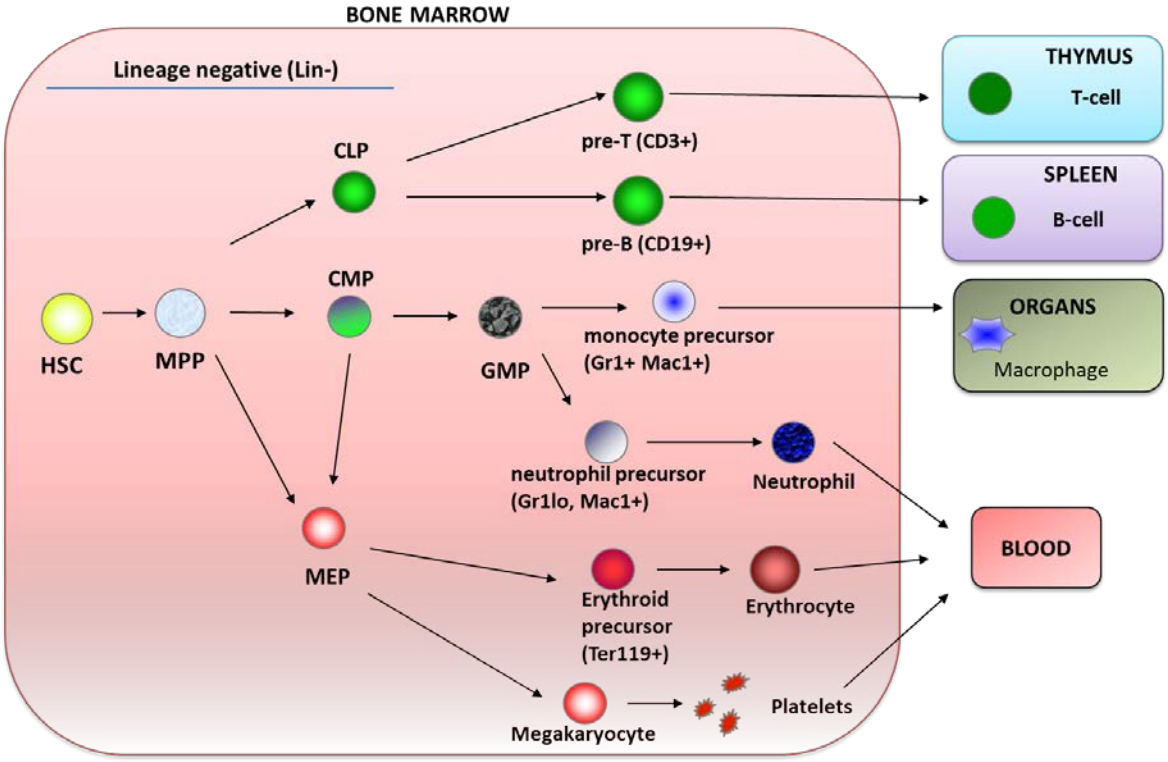

Figure I1. Hematopoietic differentiation. HSC- hematopoietic stem cell, MPP – multipotent progenitor, CLP – Common lymphoid progenitor, CMP – common lymphoid progenitor, MEP-megakaryo-erythrocytic progenitor, GMP- granulocyte/macrophage progenitor.

They are primed for death from where a subset of them are rescued and maintained in a quiescent state before engaging full immune activity activated by antigens (Osmond, 1993). Likewise, T-cell precursors arriving at the thymus are selected for survival upon successful recognition of complexes between self-peptide and proteins of the major histocompatibility complex, a prior step to their final maturation (Tough & Sprent, 1996).

6.2 Aberrant hematopoiesis

Probably the best studied cell compartment, networks of transcription factors and cis-control regions have been identified with roles in hematopoiesis (Calero-Nieto et al., 2014; Gottgens, 2015; Huang et al., 2013; Paul et al., 2015). This knowledge has provided an understanding, in molecular terms, of many of the events associated to aberrant hematopoiesis, the malignization of hematopoietic cell types characteristic of the hematopoietic disease. Characteristically, the differentiation process is wired, within defined transcriptional programs, to the cessation of cell proliferation. In malignant hematopoiesis, alterations of normal regulators with roles in transcription, usually fusion proteins resulting from chromosomal translocations (Yokoyama, 2016), changes their regulatory properties and corrupts the program, often blocking cells in an intermediate differentiation state endowed with proliferation capacity(Y. W. Lin & Aplan, 2004). It is the case of myeloid leukemias, in which the product of the Trithorax group gene Mll1/KMT2A fuses its 5'-sequences to those segments of genes encoding, for example, elements of the transcription elongation machinery. Examples are Mll-ENL or Mll-Af9 proteins, which are actively used in the generation of mouse models of acute leukemia (AML) (Somervaille & Cleary, 2006)

7. FUNCTIONS OF PRC1 IN HEMATOPOIESIS

Chromatin regulators play critical functions in differentiation and tissue homeostasis and as such, perturbation of the Polycomb system, through both loss-of and gain-of-function mutations in genes encoding PcG subunits, leads to hematopoietic alterations.

In general, the genetic analysis showed, initially, a consistent association with the promotion of cell proliferation. More recent evidence points also to functions restricting cell proliferation. Sought after alterations of cell fate, however, are reared and not as prevalent as those related to deregulated proliferation. Focusing on mutations in genes encoding PRC1 subunits, the phenotypes could be considered within two large sets of functions:

7.1 Role in self-renewal

Loss of PCGF4 leads to decreasing of HSC number in mice (Oguro et al., 2010; Park et al., 2003) and this protein has been found to regulate self-renewal of HSC (Iwama et al., 2004) CBX family members were found to regulate balance between self-renewal and differentiation during hematopoiesis (Klauke et al., 2013). Loss of CBX2 leads to exhaustion of HSC and progenitors cells (van den Boom et al., 2013). CBX7 is necessary for HSC self-renewal (Klauke et al., 2013; van den Boom et al., 2013) and overexpression of this protein leads to enhanced expansion of hematopoietic progenitors (Klauke et al., 2013; Scott et al., 2007).

7.2 Role in proliferation and differentiation

RING1B, regulate cell proliferation during hematopoiesis and could act as positive or negative regulator (Calés et al., 2008). In vivo inactivation of this protein leads to hypocelularity of bone marrow (Calés et al., 2008) but also to reduced size of thymus and spleen (Raaphorst, Otte, & Meijer, 2001) Mice deficient in RING1B and their homolog RING1A suffer for aplastic anemia (Vidal & Starowicz, 2017) what is probably related to DNA replication in which both proteins are involved (Bravo et al., 2015; Piunti et al., 2014). Animals lacking CBX2 have hypoplastic lymphoid organs, defective expansion of T-cells and impaired differentiation of B-cells (Coré et al., 1997; Iwama et al., 2004). Overexpression of CBX2 leads to enhanced differentiation (Iwama et al., 2004; Klauke et al., 2013). PCGF family members also plays role in proliferation and differentiation of hematopoietic cells. Loss of PCGF1 leads to enhancement of progenitor expansion (Ross et al., 2012; van den Boom et al., 2013). Lack of PCGF2 result in hypocellular bone marrow, spleen and thymus and also enhance proliferation of HSC (present in reduced number) (Park et al., 2003; Van Der Lugt et al., 1994). Loss of PCGF4 leads to enhanced lymphoid differentiation which is caused by activation of genes which control differentiation in this compartment and in normal situation are repressed by PCGF4 (Oguro et al., 2010).

KDM2B regulates lineage commitment of HSC, loss of this protein results in defected lymphoid differentiation (Andricovich et al., 2016). BCOR deficiency leads to higher cell proliferation rate and enhanced myeloid differentiation (Q. Cao et al., 2016).

Knockout of L3MBTL3 is embryonic lethal and impairs maturation of cell to granulocytes and erythrocytes (Arai & Miyazaki, 2005). Most of Polycomb function were investigated in HSC or progenitor/precursor cells, however in more differentiated cells these proteins also plays

fundamental role. Inactivation of Ring1A and Ring1B in lymphoid lineage results in block of T-cells differentiation and conversion of these cells in functional B-cells (Ikawa et al., 2016). RYBP was found to regulate B-cell precursors differentiation (Calés et al., 2016).

7.3 PRC1 in malignant hematopoiesis

Considering how important role play PRC1 proteins in normal hematopoiesis, some groups also investigate their role in malignant situation. Deficiency of RING1B in absence of *Ink4a* products accelerates lymphomas (Calés et al., 2008) whereas in human progenitors lead to impaired leukemic transformation. Leukemic cells after loss of RING1B are incapable to maintain transformed phenotype (van den Boom et al., 2016). LSC which do not express PCGF4 lost capacity of self-renewal and are going to apoptosis (Lessard & Sauvageau, 2003; Rizo, et al., 2008). CBX family member also were found to regulate leukemogenesis, overexpression of CBX7 cause T lymphomas (Klauke et al., 2013) and CBX8 is necessary for initiation and maintenance of leukemic cells (Tan et al., 2011). Deficiency of CBX8 in transformed cells results in their impaired expansion (Maethner et al., 2013) and also in induce their differentiation (Beguelin et al., 2016).
KDM2B and BCOR were found to be essential factor for induction of leukemogenesis and also for maintenance of leukemic cells. Overexpression of KDM2B leads to leukemia in mice (Andricovich et al., 2016; Ueda et al., 2017).

As a starting point in our attempt to evaluate whether the established knowledge of PRC1 holds in primary cell types or derived from them after ex-vivo expansion we focused on a PRC1 subunit that was common to all complexes. Only two candidates appeared the pair of paralogs RING1A and RING1B. We chose RING1B, given its larger functional impact (see above). We managed to get hold on a mouse model that expressed a form of tagged-RING1B that, on paper, looked ideal for our purposes. The reason is that such a RING1B modification was achieved by knocking-in the tag, through homologous recombination. In this way, regulation and expression of the tagged variant would be as close as they get to physiological RING1B levels. The tag, a short sequence biotinylated in vivo, was advantageous because allowed for efficient isolation by using immobilized streptavidin, a system previously used in the laboratory (Sánchez et al., 2007). This set up was used to investigate RING1B-containing assemblies, with a focus on Polycomb complexes in hematopoietic cells.

Objectives

OBJECTIVES

1. To characterize expression levels and protein assemblies of PRC1 subunits in cell types with a defined (hematopoietic) cell lineage.

2. To identify PRC1 subunits present in RING1B complexes in primary, ex-vivo expanded and immortalized hematopoietic cell types.

3. To explore the role of RING1A and RING1B in the stability of PRC1 assemblies.

Materials and methods

MATERIALS AND METHODS

1. Mouse models

BirA - This mouse line carries a cDNA encoding the E. coli biotin ligase BirA inserted into the Rosa26 locus, a transcriptional unit of ubiquitous expression. It was kindly shared by Dr Koseki (RIKEN Center for Integrative Medical Sciences, Yokohama, Japan). We used mice homozygous for the insertion.

Ring1B^{bio} - This mouse model carries a modified Ring1B locus in which a sequence encoding 23 amino acids was inserted, through homologous recombination in embryonic stem cells, right before the stop codon of the Ring1B locus. It was also generated in Dr. Koseki's lab. The C-term tag can be biotinylated by BirA in mice that combine the BirA and Ring1Bbio alleles, as shown in Fig. M1

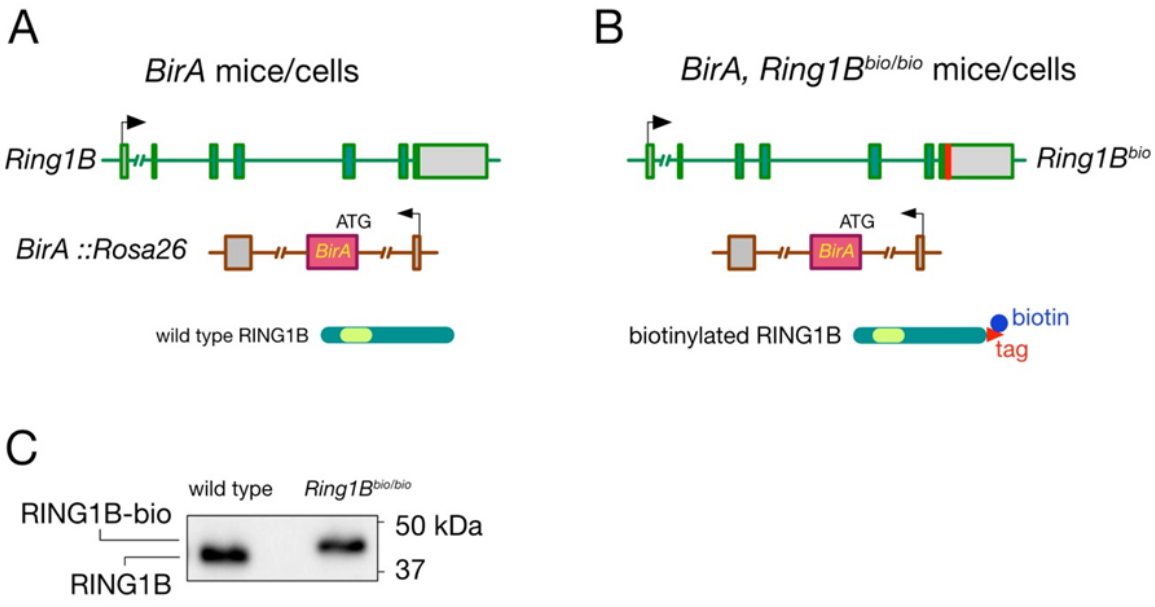

Figure M1. Controlled characterization of RING1B bound proteins in a close-to-physiological set up. (A) Genetically modified BirA mice, showing altered Rosa26 locus and, schematically, the RING1B product from wild type *Ring1B* locus. (B) Genetically modified Bird and Ring1Bbio mice showing altered Ring1B and Rosa26 loci. The biotinylated, tagged-RING1B expressed in these mice is also shown. (C) Representative western blot from total extracts prepared from spleen of mice of the indicated genotypes.

Ring1B $^{fl/fl}$ – This mouse line was designed in our laboratory by Dr Vidal as a model of conditional inactivation of RING1B. A modified Ring1B locus, *Ring1B*^{fl} in which an exon encoding sequences N-terminal to the RING finger is flanked by loxP sequences, leads to gene inactivation in the presence of Cre recombinase from P1 bacteriophage. The *Ring1B*^{fl} allele

also contains a PGKneo cassette which, together with the floxed exon, is removed upon recombination (Calés et al. 2008).

Mx-Cre - It is a transgenic lined in which a Cre recombinase cDNA, fused to elements of the Mx-1 promoter responsive to the interferon signaling pathway, is used to drive Cre activity in (predominantly) hematopoietic bone marrow cells (Gu et al., 1994). These mice were crossed with *Ring1*$^{fl/fl}$ animals for inducible (after Polyinosinic-polycytidylic acid, p(I:C) injections) inactivation of RIng1B in vivo. The structure of p(I:C) mimics a double stranded RNA as in viral infections that trigger an interferon response.

CreER^{T2} – In this mouse line a hybrid cDNA encoding a Cre recombinase fused to the ligand binding domain of the human estrogen receptor, is inserted in 3'-UTR sequences of the Polr2a gene (Mijimolle et al., 2005). Expression of the Cre-ER^{T2} recombinase is ubiquitous but its activity can be regulated by the estrogen analog, 4'-hydroxytamoxifen (4'-OHT) that induces its translocation to the cell nucleus and its relocation to the cytoplasm in the absence of 4'-OHT. Mice homozygous for *Ring1B*^{fl} and *CreER*^{T2} were used as a source of cells for studies in vitro that required *Ring1B* inactivation.

Ring1A$^{-/-}$–. A mouse line carrying a deletion of most coding exons of the Ring1A locus, i.e. a null mutation, reported by our laboratory (del Mar Lorente et al., 2000).

Ring1A$^{-/-}$ *Ring1B*$^{fl/fl}$ *CreERT2* – Mice carrying the indicated alleles were generated by successive mattings. These mice were a source of cells for the compound inactivation, in vitro, of *Ring1A* and *Ring1B* genes.

2. Isolation of genomic DNA

A crude preparation of genomic DNA was prepared from a biopsy of small part of tail from 21 day age mice. Tissue was lysed in 50mM Tris-HCl pH 8.0, 100mM EDTA, 100mM NaCl, 1% SDS containing 0.5 mg/ml Proteinase K (Roche) and incubated overnight at 55^{0}C. Most protein and detergent was precipitated by adding one third of a saturated solution of NaCl. After centrifugation in a microfuge, 10 min at 12,000 rpm the supernatant was transferred to a new tube. The DNA was then precipitated with 0.6 volumes of isopropanol and isolated by centrifugation during 10 min at 4^{0}C. The pellet was washed with 70% EtOH, air-dried and resuspend in TE buffer.

3. Genotyping by PCR

DNA was diluted 1/10 with water and 1 µl used per reaction. Oligonucleotides (Table 1) were purcharsed from Sigma. All reagents used for PCR reactions were purchased from Biotools. Polymerization reactions were carried out in a Thermocycler T300 (Biometra).

cDNA	Sequence 5'-> 3'	Size of product	PCR conditions
birA::Rosa26	TGTTGCAATACCTTTCTGGGAGTTC	311 bp	94^0C x 30 sec 60^0C x 30 sec 72^0C x 30 sec X 32 cycles
	GTCCTCCTCCGAGATAAGCTTCTG		
Rosa26	TGTTGCAATACCTTTCTGGGAGTTC	528 bp	
	AGAAGGAGCGGGAGAAATGGATATG		
Ring1B-bio	GCACCCACCAAGGAGCAC	1500 bp (1400 wt)	94^0C x 45 sec 60^0C x 45 sec 72^0C x 1min 30 sec X 34 cycles
	AATCTTATGGCACAGATTAC		

Table 1. Primers and PCR reactions conditions used for genotyping

4. In vivo Ring1B inactivation

Inactivation of Ring1B in vivo was attained by intraperitoneal injection of 8.5mg/kg p(I:C) (GE Healthcare) on three alternate days in 10- to 20-week-old mice. As a control we used animals without *the Mx-Cre* transgene injected with p(I:C) as well. Tissues were used two months after p(I:C) injection so that recombination in peripheral organs could be achieved. Effective inactivation was tested by Western blot.

5. In vitro Ring1B inactivation

Cultures of *Ring1B$^{fl/fl}$ CreER^{T2}* or *Ring1A$^{-/-}$ Ring1B$^{fl/fl}$ CreER^{T2} cells* were given 0.5 µM 4'-OHT(Sigma) from a stock solution in ethanol (EtOH), during 16 hours. After this time, cells were centrifuged and fresh medium added, in order to minimize undesired effects associated to the continuous presence of the Cre recombinase within the cell nucleus. Usually, RING1B

levels decreased dramatically within 36-48 hours after treatment. As a control, cells of the same genotype received an equivalent volume of EtOH.

All mouse procedures were institutionally approved and were performed in accordance with national and European regulations.

6. Tissue culture cell lines

293 PlatinumE - It is a retroviral packaging cell line based on the human kidney embryonic 293 cell line. These cells contain genes codifying for viral structure proteins (*gag, pol and env*) under control of EF1α promoter (Morita, Kojima, & Kitamura, 2000)

293 BirA-bioRING1B – Clones of 293T cells transfected, sequentially, with plasmids that confer expression of BirA ligase and of a tagged-RING1B variant that can be biotinylated were generated by standard procedures.

7. Purification of murine hematopoietic cells

7.1 Immature, lineage negative cells (Lin-)

They were purified using mouse Lineage Depletion Kit (Miltenyi Biotech) according to manufacturer protocol. In brief, bone marrow was harvested from femurs, tibias and hips of 10- to 20-week mice. Cells were filtered and antibody cocktail was added to the suspension. After 15 minutes of incubation, cells were washed and secondary antibody was added for 10 minutes. After antibody binding and subsequent washes, cells suspensions were passed through LD column and Lin- cells were collected in the flowthrough. When used in transduction experiments, $2{,}5x10^4$ cells per well, were seeded in 24-multiwell non-treated tissue culture plates (Costar) in IMDM containing 15% fetal calf serum (FCS), 10 ng/m IL-6 (Immunotools), homemade IL3 (10% of WEHI-conditioned medium) and 5% of homemade SCF (conditioned medium of CHO SCF-expressing cell line).

7.2 Primitive, CD117 (c-kit) positive cells

Cells were purified using mouse CD117 MicroBeads (Miltenyi Biotech) according to manufacturer protocol. In brief, bone marrow was harvested from femurs, tibias and hips of 10- to 20-week old mice. Cells were filtered and beads were added to the cell suspension.

After 15 minutes of incubation, cells were washed and passed through LS column. For transduction purposes, c-kit+ cells were seeded $2,5x10^5$ cells per well in a 24-multiwell plates in the same medium as indicated for Lin- cells.

8. Retroviral transduction of hematopoietic cells

Viral particles

293 PlatinumE cells were seeded the day before transfection at density $3x10^6$ cells per 10 cm dish. 10 μg of plasmid complexed with TurboFect (Biotools) was added to the cells, and after 16 hours, cells were fed fresh medium. Supernatant containing virus particles were collected after 48, 60 and 72 hours. After filter-sterilization, aliquots were stored frozen at -80ºC. Viral titers of the various preparations were estimated either by cytometry analysis of GFP expression (encoded by the viral genomes) or counting colonies of puromycin- or neomycin-resistant 3T3 cells.

Hematopoietic cells were pre-stimulated during 24 hours in 1ml of medium containing cytokines, in order to obtain a highly proliferative population. Then, 750μl medium was removed and replaced with viral supernatant containing polybrene at a final concentration of 2 μg/ml. Subsequently, cells were centrifuged at 800 x g in A-4-62 rotor (Eppendorf) during 1 hour at room temperature. After centrifugation, 750 μl of medium was replaced by fresh medium containing cytokines. This procedure was repeated 24 hours later.

9. Immortalization/transformation of hematopoietic cells

Two processes, displayed schematically in Fig. M2, were used.

We used the overexpression of a protein in which the N-term of Nup98, a nucleoporin often found translocated in hematological disorders is fused to the DNA binding domain of HOXA10. The cDNA, a gift of R.K. Humphries (Terry Fox Laboratory, Vancouver, Canada) was subcloned into a retroviral plasmid that uses as control elements the mouse stem cell virus LTR (pMSCV). After two rounds of spinoculation-transduction, bone marrow Lin- cells were selected in 1,5 μg/ml of puromycin (TOKU-E).

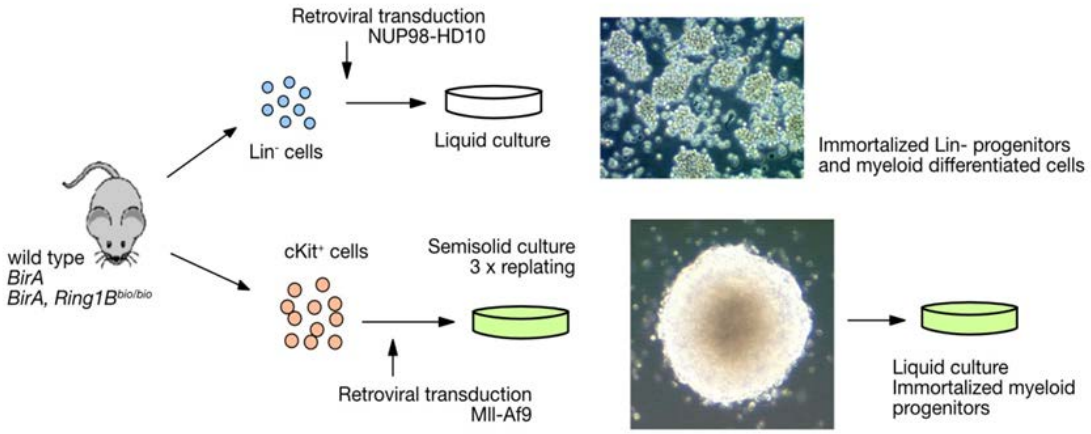

Figure M2. Immortalization/transformation of hematopoietic progenitors. The indicated retroviruses were introduced in bone marrow progenitors (Lin- and c-kit+).Representative images of Nup98-HD10-immortalized cells (top) and a colony of Mll-Af9-transformed cells growing in methyl cellulose are shown.

9.1 Immortal Lin- cells

After 4-5 days of antibiotic selection, the medium was replaced and cells were seeded at a density of $0{,}2x10^6$cells/ml. Cultures were splitted every 2 days. Sixteen days after first round of transduction, the culture was considered immortalized and cell stocks prepared by freezing aliquots in FCS containing 10% DMSO (Sigma). Successful thawing up was an indication of immortalization.

9.2 Immortal, transformed myeloid progenitors

We followed a classical protocol developed to generate cells used for in vivo models of acute murine leukemia (AML)(Somervaille & Cleary, 2006). Isolated c-kit+ cells were transduced with pMSCV-MLL-AF9 (kindly provided by J. Hess, Indiana University School of Medicine, Indianapolis). After 2 rounds of spinoculation, cells were plated in methylcellulose (M3231, Stem Cell Technologies) containing 20ng/ml of IL-3 (Immunotools), 5% of homemade SCF, 10 ng/ml IL6, 10 ng/ml GM-CSF (both from Immunotools) and 0.75 mg/ml of G418 (Gibco), at a density of 10^4 cells per well in 24 multi-well plate. After 6 days, methylcellulose was dispersed and cells replated at the same density but in medium without G418. Five days later, colonies were replated one more time, but at a density of $5x10^3$ per well. After this third round, single colonies were plucked from methylcellulose and transferred, individually, to RPMI1640 medium (Biowest) containing 20% of FCS, IL3 (20% of WEHI-conditioned medium), IL-6, 10 ng/ml, and 5% of homemade SCF. Three days later, cultures derived from single colonies were

transferred to 24-well plates and after 48 hours, actively growing cultures were pooled. As above, cell stocks were stored frozen at -80ºC and immortalization was assessed by ability to successful growth after several freezing-thawing rounds.

10. Isolation of primary cells from spleen ant thymus

Tissues were harvested and smashed in 40 µm cell strainer (Falcon) in cold PBS. Suspension was centrifuged for 10 minutes at 400 x g in A-4-62 rotor (Eppendorf) at room temperature. Cell pellet was resuspended in 2 ml of ACK lysis buffer (150mM NH_4Cl, 10mM $KHCO_3$, 0.1 mM Na_2EDTA, pH 7.2-7.4) and left for 1 minute at room temperature to remove erythrocytes. The tube was then filled up with 13 ml of PBS, mixed and centrifuged for 10 minute at 400 x g in A-4-62 rotor (Eppendorf) at room temperature. Cell pellet was washed with PBS twice to remove erythrocytes debris and used for protein extracts preparation.

11. Generation of murine bone marrow-derived macrophages

Bone marrow from 10- to 20 week mice was harvested in DMEM (Biowest) containing 10% of FCS and 50µM 2-mercaptoetanol (Sigma) and filtered through 40 µm cell strainer. After centrifugation at 400 x g for in A-4-62 rotor (Eppendorf) 10 min at room temperature, cell pellet was resuspended in 1 ml of ACK lysis buffer and incubated for 1 minute. Then tube was filled up to 20 ml with PBS, mixed and centrifuged at 400 x g in A-4-62 rotor (Eppendorf) for 10 min. Cells were resuspended in 14 ml of RPMI 1640 medium and divided into two 10-cm petri dishes. Next day no attached cells were collected and seeded in 9 cm bacterial plates at density $1x10^6$ cells/ml, with 7ml per plate. hrM-CSF (Immunotools) was added to each plate to final concentration 5µg/ml. This procedure was repeated at days +3 and +5. At day +7 cells were recovered from plates and used for further analysis.

12. Isolation of bone marrow neutrophils

Purification of neutrophils was done by Percoll gradient (Amersham Pharmacia Biotech, Uppsala, Sweden) as described previously (Boxio et al., 2004). In brief, bone marrow cells were flushed from bones with Hanks' balanced saline solution (HBSS – without calcium, magnesium and phenol red) containing 15mM EDTA, centrifuged at 400 x g for in A-4-62 rotor (Eppendorf) 5 min and resuspended in 1ml of HBSS-EDTA. Cells were laid on top of a three-

layer Percoll gradient, of 78%, 69% and 52% densities, prepared by diluting 100% Percoll with HBSS. Cells were centrifuged at 1500 x g for 30 minutes at room temperature without brake. The neutrophils from the 69%/78% interface and the top of the 78% layer were harvested and washed twice with 2 ml of PBS. Morphology of cells was checked by May-Grunwald-Giemsa (MGG) staining, confirming purity of isolated cells (≥ 95%).

13. Purification of murine Ter119 and CD19 positive cells

Cells were purified using mouse Ter119 and CD19 MicroBeads (Miltenyi Biotech) according to manufactured protocol. In brief, bone marrow was harvested from 10- to 20-week mice. Cells were filtered and beads were added to the cell suspension. After 15 min of incubation, cells were washed and passed through LS column. Eluted cells were used for loading buffer extract.

14. Activation of splenocytes with lipopolysaccharide (LPS)

Splenocytes were harvested and resuspended in 10 ml of RPMI1640 with 15% of FCS and 50µM 2-mercaptoetanol. 2,5 ml of Ficoll Histopaque (GE Healthcare) was layered at the bottom of the tube. Sample was centrifuged at 800 x g in A-4-62 rotor (Eppendorf) for 10 min at 20^0C without brake. Obtained buffy coat in interphase, containing splenic cells was recovered and washed with 5 ml of medium. Cells were counted and seeded at density $4x10^5$/ml in medium containing 10µg/ml LPS (Sigma). After 72 hours cells were harvested and used for further experiments.

15. Cytometry analysis of hematopoietic cells

For the phenotypic analysis of hematopoietic progenitors, cells were resuspended in staining buffer (PBS with 2% of FCS and 0.01% sodium azide) and blocked for 5 min in 4^0C with anti-mouse BD Fc Block (Becton Dickinson). Subsequently cells were centrifuged at 300 x g in A-4-62 rotor (Eppendorf) for 5 minutes and further incubated for 20 min with appropriated antibodies conjugated with different fluorochomes. All antibodies used were purchased from Becton Dickinson: anti-CD117 (ckit, 2B8)- phycoerythrin (PE), anti-CD11c (Mac-1, M1/70)-peridinin chlorophyll protein (PerCP)-Cy5.5, anti-Sca1(D7)-PerCP-Cy5.5, anti- Gr1 (RB6-8C5)-biotin. After labelling, cells were washed with staining buffer and centrifuged. Cells stained

with antibodies conjugated with biotin were subsequently incubated with streptavidin conjugated with PE for 10 min at 4^0C and washed with staining buffer. Fluorescence-activated cell sorter (FACS) analysis from 5,000 to 10,000 cells was performed on a FACScan instrument (Becton Dickinson). Data were analyzed with FlowJo software v.8.8.6 (Tree Star, Ashland,OR).

16. Loading buffer extracts

Cells were lysed in Laemmli buffer with protease inhibitors for 5 min at 95^oC and sonicated with a Bioruptor Diagenode. Lysates were cleared from cell debris by centrifugation at 11,000 x g for 10 minutes in I6F24-11 rotor (Eppendorf). For protein levels analysis, volume equivalent to $2x10^5$ cells was used.

17. Nuclear extracts

Cells were harvested and washed with ice-cold PBS and centrifuged for 5 minutes at 400xg. Cells were resuspended in 5 volumes of ice-cold buffer A (10mM HEPES-KOH pH7.9, 1.5mM $MgCl_2$, 10mM KCl, 0.5mM DTT supplemented with protease (Biotools) and phosphatase (PhosStop, Roche) inhibitors, and incubated on ice for 10 minutes. Suspension was centrifuged for 5 minutes at 400 x g in A-4-62 rotor (Eppendorf) at 4^0C, and subsequently, pellet was resuspended in 2 volumes of buffer A with added 0.15% Igepal. Suspension was then transferred to a Dounce homogenizer and cells were homogenized with pestle type b with break every 10 strokes. Efficiency of nuclei isolation was checked with Trypan Blue (Sigma). Nuclei suspension was transferred to a new tube and centrifuged for 15 minutes at 3200xg at 4^0C. Supernatant was discarded and 5 volumes of ice-cold PBS were gently added to the pellet. Pellet was detached by flicking tube a few times and then centrifuged for 5 minutes at 3200xg at 4^0C. Supernatant was discarded and nuclear pellet resuspended in 2 volumes of buffer C (420mM NaCl, 20 mM HEPES-KOH pH7.9, 20% glycerol, 2mM $MgCl_2$, 0.2mM EDTA, 0.1% Igepal, 0.5mM DTT, protease and phosphatase inhibitors). Suspension was incubated at 4^0C on rotating wheel for 60 minutes and subsequently centrifuged at 11,000 x g at 4^0C I6F24-11 rotor (Eppendorf) for 40 minutes. Concentration of obtained nuclear extract was determined by Bradford assay. Extract aliquots were snap-frozen and stored at -80^0.

18. Binding to streptavidin beads (pull down)

Nuclear extracts were transferred to low-binding tubes (Eppendorf), and salt concentration was adjusted to 150mM with HENG buffer (20 mM HEPES-KOH pH7.9, 20% glycerol, 2mMMgCl$_2$, 0.2mM EDTA, 0.1% NP40, 0.5mM DTT, protease

Cell type	Washes
Splenocytes	3 times for 5 minutes with 0,25% Igepal and 0,1M NaCl
Thymocytes	3 times for 5 minutes with 0,25% Igepal and 0,2 M NaCl
Splenocytes + LPS	3 times for 5 minutes with 0,25% Igepal and 0,2 M NaCl
Macrophages	3 times for 5 minutes with 0,25% Igepal and 0,2 M NaCl
NUP98HD	3 times for 5 minutes with 0,1% Igepal

Table 2. Washes used in pull downs for each cell type.

and phospathase inhibitors). 5% of total protein was taken as input. Benzonase (Novagen) was added to diluted extract (250U/1mg of extract) Paramagnetic streptavidin beads (Dynabeads M-280, Invitrogen), 80 µl/mg of nuclear extract, were washed three times with HENG buffer and incubated with 1 hour at 4^{o}C on a rotating wheel. The beads were washed differently depending on the cell type, as indicated in Table 1. Bound material was eluted by resuspension in Laemmli sample buffer and boiling of the suspension for 5 min at 96ºC.

For mass spectrometry analysis, proteins were eluted from beads with 1% of SDS for 10 min at 95^{o}C. Freshly prepared DTT was added to samples and further boiled for 2 min. Indol 3-acetic acid (IAA) was added and were incubated for 30 min at room temperature in the dark. Finally, lithium dodecyl sulfate (LDS)-containing loading buffer was added, samples were loaded on Novex Bis-Tris gel (Invitrogen) and run for 20 min at 200V. Gel was stained with Colloidal Blue Staining Kit (Invitrogen), cut into pieces and liofilized for 4 hours.

19. LC-MS/MS Analysis

Peptide analysis by nano-LC-ESI-MS/MS with LTQ Orbitrap Velos (Thermo Fisher Scientific, Waltham, MA, USA) was performed as published follows: the instrument was coupled to Agilent 1200 HPLC nanoflow systems (dual pump with one precolumn and one analytical column; Agilent Biotechnologies, Palo Alto, CA, USA). Data were acquired using Xcalibur

(v2.1.0). HPLC solvents were as follows: solvent A consisted of 0.4% formic acid in water and solvent B consisted of 0.4% formic acid in 70% methanol and 20% isopropanol. From a thermostated microautosampler, 8 µL of the peptide mixture was automatically loaded onto a trap column (Zorbax 300SB-C18 5 µm, 5 × 0.3 mm, Agilent Biotechnologies) with a binary pump at a flow rate of 45 µL/min using 0.1% TFA for loading and washing the precolumn. After washing, the peptides were eluted by back-flushing onto a 16-cm fused silica analytical column with an inner diameter of 50 µm packed with C18 reversed phase material (ReproSil-Pur 120 C18-AQ, 3 µm, Dr. Maisch GmbH, Ammerbuch-Entringen, Germany). The peptides were eluted from the analytical column with a 27 min gradient ranging from 3 to 30% solvent B, followed by a 25 min gradient from 30 to 70% solvent B and, finally, a 7 min gradient from 70 to 100% solvent B at a constant flow rate of 100 nL/min. The analyses were performed in a data-dependent acquisition mode using a top 15 CID method for the LTQ Orbitrap Velos. Dynamic exclusion for selected ions was 60 s. A single lock mass at m/z 445.120024 was employed. Maximal ion accumulation time allowed in MS and MSn mode was 500 and 50 ms, respectively. Automatic gain control was used to prevent overfilling of the ion trap and was set to 106 ions and 5000 ions for a full Fourier transform mass spectrometry scan and MSn, respectively. Peptides were detected in MS mode at 60 000 resolution (m/z 400).

Protein Database Search

The acquired raw MS data files were processed with msconvert (ProteoWizard Library v2.1.2708) and converted into Mascot generic format (mgf) files. The resultant peak lists was searched against the mouse SwissProt database version v2014.07_20141023 (24,862 sequences, including isoforms as obtained from varsplic.pl) with the search engines Mascot (v2.3.02, MatrixScience, London, U.K.) and Phenyx (v2.5.14, GeneBio, Geneva, Switzerland). Submission to the search engines was via a Perl script that performs an initial search with relatively broad mass tolerances (Mascot only) on both the precursor and fragment ions (±10 ppm and ±0.6 Da, respectively). High-confidence peptide identifications were used to recalibrate all precursor and fragment ion masses prior to a second search with narrower mass tolerances (±4 ppm and ±0.025 Da). One missed tryptic cleavage site was allowed. Carbamidomethyl cysteine and oxidized methionine was set as a variable modification. To validate the proteins, Mascot and Phenyx output files were processed by internally developed parsers. Proteins with ≥2 unique peptides above a score T1 or with a single peptide above a score T2 were selected as unambiguous identifications. Additional

peptides for these validated proteins with score >T3 were also accepted. For Mascot and Phenyx, T1, T2, and T3 were equal to 16, 40, 10 and 5.5, 9.5, 3.5, respectively (p value $<10^{-3}$). Following the selection criteria, proteins were grouped on the basis of shared peptides, and only the group reporters are considered in the final output of identified proteins. Spectral conflicts between Mascot and Phenyx peptide identifications were discarded. The whole procedure was repeated against a reversed database to assess the protein group false discovery rate (FDR). Peptide and protein group identifications were <0.1 and <1% FDR, respectively

20. Glycerol gradients

For glycerol gradient analysis, 500 µg of nuclear extract was added to the top of 4 ml 15-35% gradient. The sample was then centrifuged at 35,000 rpm at 4^0C for 16 hours in a SW55Ti rotor (Beckman). Gradient was then fractionated every 180 µl. Four volumes of cold acetone (-20^0C) were added and thoroughly mixed by vortexing. Protein was then precipitated for 2 hours at -20^0C and subsequently centrifuged at 11,000 x g at 4^0C I6F24-11 rotor (Eppendorf) for 10 minutes. Supernatant was removed and protein pellet was air dried at room temperature. Dry pellets were resuspended in Laemmli sample buffer and resolved on SDS-PAGE gels.

21. Western blotting analysis

Proteins were subjected to SDS-PAGE and transferred to nitrocellulose membrane (Amersham Protran, GE Healthcare) on a wet transfer apparatus (Bio-Rad). After blocking in 5% nonfat dry milk (Blotto, Santa Cruz Biotechnology) in Tris-buffered saline containing 0.1% Tween20 (TTBS), filters were incubated with primary antibodies diluted in blocking solution for 1-2 hours at room temperature. After three washes with TTBS, filters were incubated with horseradish peroxidase-conjugated secondary antibodies (Dako). Signals were detected using ECL Prime detection reagent (GE Healthcare).

22. Western blot quantification

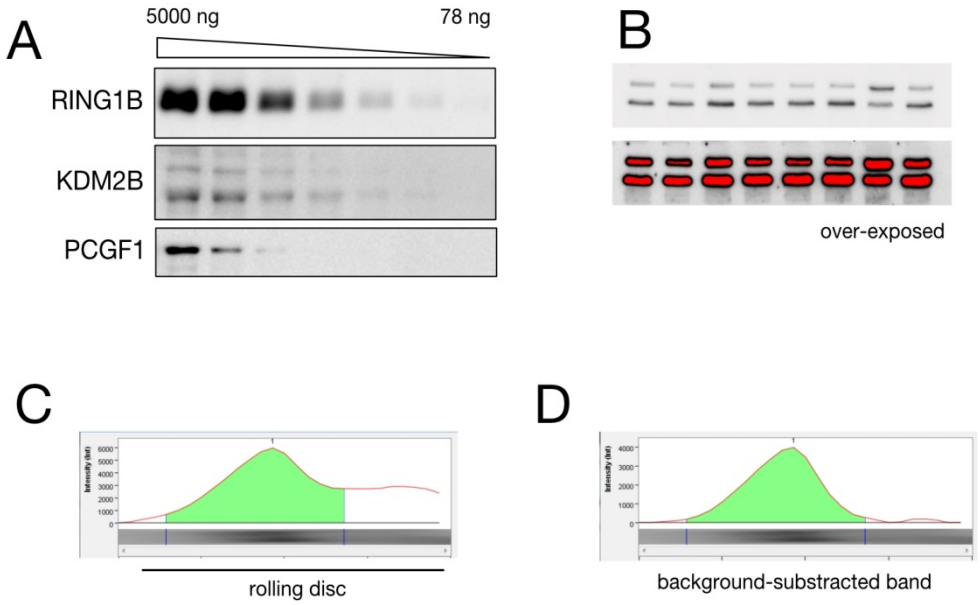

Figure M3. Western blot quantification. (A) Serial dilution of spleen extracts to show signal responses to variations in protein concentrations for the indicated antibodies.(B) Digital images showing signals appropriated (top) and saturated, useless (bottom) acquisition times. (C) Window of Image Lab 5.2.1 software to select values for band and rolling disc algorithm and (D) result of background subtraction.

Only good quality Western blots were used for quantitative analysis. Chemiluminiscence signals were digitalized with a ChemiDoc Touch system (BioRad) and then analyzed with Image Lab 5.2.1 software (BioRad). Acquired signals were within the linear dynamic range of loading, to ensure responses to changes in amount of protein. Figure M4A shows variations of intensities obtained with different antibodies on serially diluted samples. In addition, the software allowed the identification of overexposed images, which turned red when containing saturated pixels (Fig. M3B). For normalization purposes, we used signals for histone H2A as a reference, except in pull-down experiments in which input (nuclear extract) signals were used.

An important step during quantification was the account for background. We used a so-called rolling disc algorithm and a lane profile tool provided by the software for essential, careful background lane by lane subtraction. When employed side by side, it allows for an appropriate selection of band width and lane background for each lane. Using the "Lane and bands" tool, the band dimension and the volume under the peak were visualized two-dimensionally (Fig M3C) and assisted in choosing a rolling disc value to perform the

background subtraction per band (Fig. M3D). Similar steps were carried out with normalization signals (normalization channel) with determine values that then are factored into the intensities computed for sample bands. To homogenize for experimental variation and antibody idiosyncrasy, samples were compared within stripes incubated with the same antibody.

Analyses were carried out a minimum of two times (one exception indicated) with extracts prepared from independent cell preparations. Average values and standard deviation were plotted as bar graphs.

23. May-Grünwald-Giemsa staining (MGG)

Glass slides were covered with poly-L-lysine (Sigma) for 1 hour and air-dried. Cells were counted and resuspended in PBS at a density of $5x10^5$/ml. For each sample, we used 5 x 10^4 cells. After centrifugation in a Cytospin 3 device (Shandon), for 2 min at 800 rpm, cells were fixed with methanol for 5 min and subsequently air-dried Slides with fixed cells were incubated with May-Grünwald (Sigma) solution for 5 minutes, washed with distilled water and incubated with Giemsa solution (Sigma) diluted 1:20 for 20 minutes. Slides were washed with distilled water, air-dried and inspected under microscope. Pictures were acquired with Zeiss Axiocam (Carl Zeiss, Inc).

23. Antibodies used in this study

Antibody	source	host	clone
RING1B	Garcia et al. 1999	rabbit	
RING1A	Schoorlemmer et al., 1997	rabbit	
CBX2	Schoorlemmer et al. 1997	rabbit	
CBX7	SCBT	mouse	G-3
CBX8	Cell Signalling	rabbit	D2O8C
PCGF4	Cell Signalling	rabbit	D242B3

PHC2	Kyoichi et al. 2013	mouse	
RYBP	Garcia et al. 1999	rabbit	
YAF2	homemade	rabbit	
PCGF1	SCBT	mouse	E-8
KDM2B	GeneTex (GTX104868)	rabbit	polyclonal
SKP1	Abcam (AB10546)	rabbit	polyclonal
PCGF5	Sigma (HPA038349)	rabbit	polyclonal
DCAF7	homemade	rabbit	
CKIIa	Cell Signalling (2656)	rabbit	polyclonal
PCGF6	Thermo Scientific (PA5-35222)	rabbit	polyclonal
L3MBTL2	Sigma (HPA000815)	rabbit	polyclonal
H3	Abcam (AB1791)	rabbit	polyclonal
H2A	Milipore (07-146)	rabbit	polyclonal
H2AK119ub	Cell Signalling	rabbit	D27C4

Results

RESULTS

1. Cellular models and PRC1 subunits studied

The description of PRC1 subunits and ways in which they associated in hematopoietic cells constitutes the largest part of this study. We think it is convenient to use the classification of PRC1 complexes after Reinberg's lab (identified by their content in one or another member of the PCGF family) (Gao et al., 2012). We chose subunits for which reliable antibodies were available and that could tell about most of the canonical and non-canonical complexes (the less known of them, PRC1.3 was left out). Thus, beyond RING1A and RING1B, we analyzed PCGF4 and three of the CBX proteins to characterize canonical complexes; for non-canonical complexes, in addition to paralogs RYBP and YAF2, thought to be present in all of them, we studied PCGF1, KDM2B and SKP1 for PRC1.1, PCGF5, DCAF7 and CK2a for PRC1.5 and PCGF6 and L3MBTL2 for PRC1.6 complexes. Fig. R1 shows the subunits investigated, as coloured components within accepted classes of PRC1 complexes. Why did we allocate CK2a in PRC1.5? In fact, based on its presence among proteins coimmunoprecipitated with CBX subunits (Vandamme et al., 2011) we could have also included it as a component of canonical PRC1 assemblies. However, although CK2a cannot be taken as a PRC1.5-specific subunit, we decided to refer to it as a PRC1.5 member because it is only there where some PRC1-related functionality, phosphorylating RING1B, has been reported for CK2a (Gao et al., 2012).

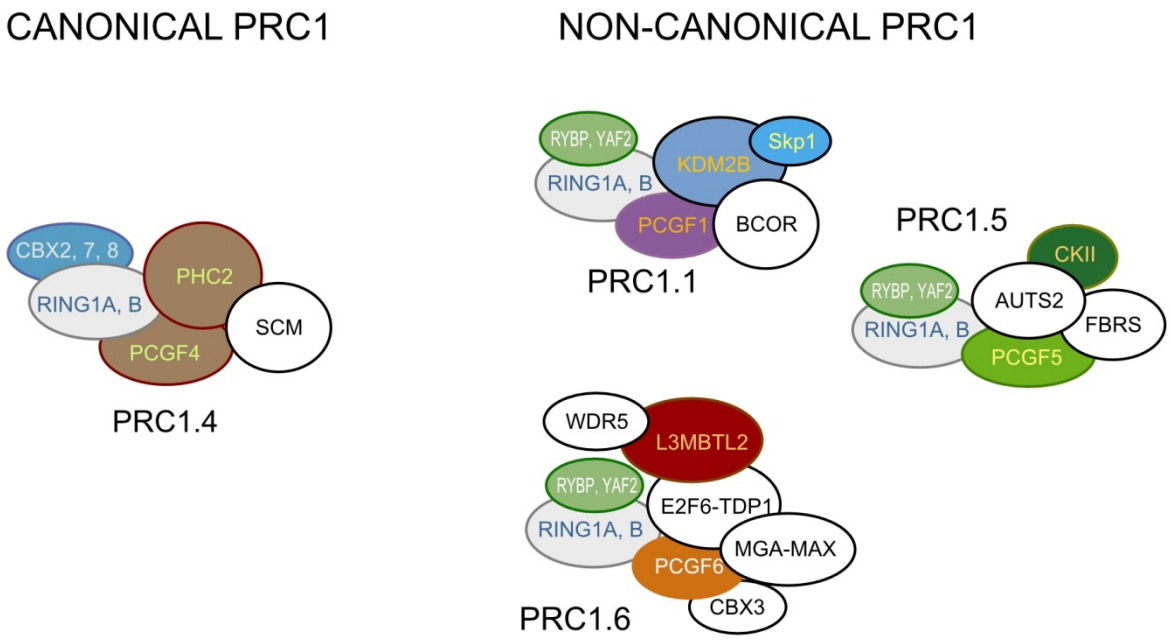

Figure R1. Conventionally accepted PRC1 complexes, showing, in color, the component investigated in this study.

Some antibodies identified more than a single polypeptide. In three cases, at least, the possibility of translating alternate mRNAs has been documented and evidence for the existence of protein variants characterized. This is the case of the Kdm2b gene, known to encode long and short forms, depending on the presence/absence of 5' exons in the corresponding mRNAs (see Fig. R2). The antibody used recognizes structures encoded by sequences in the common 3' half of the mRNAs, explaining the identity of the two bands observed (Fig. R2A). For CBX7 and PCFG5, again, mRNAs predict the presence of, at least,

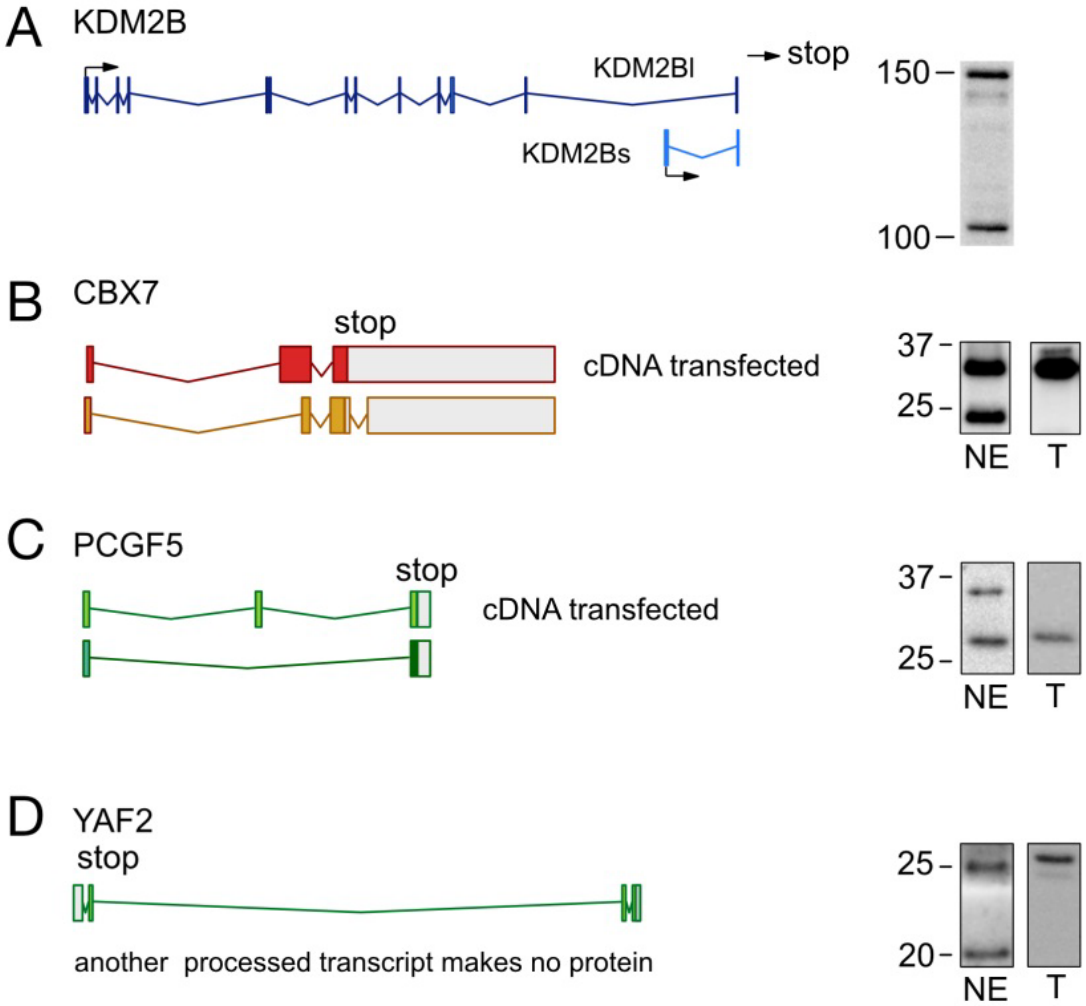

Figure R2. Discerning products recognized by a subset of antibodies not showing univocal identification of antigens. Cartoons show schematic representations (not at the same scale) of intact (or truncated) the indicated genomic loci that could yield more than a polypeptide. Western blots on the right side show bands recognized by anti-KDM2B, anti-CBX7, anti-PCGF5 and anti-YAF2 antibodies in nuclear extracts (NE) and in extracts of transiently transfected (T) 293 cells expressing the indicated cDNAs. Figures on blots indicate molecular weight markers in kDa

two proteins both of which would have been recognized by the antibodies used. Since the mobilities in denaturing polyacrylamide gels of most PRC1 subunits departs from that expected from conceptual translation of sequences, we transfected Cbx7 and Pcgf5 cDNAs to try to correlate mobilities to known sequences. Both of our Cbx7 and Pcgf5 cDNAs encode for the long forms of CBX7 and PCGF5. Analysis of cells extracts from transfected cells showed that the long forms of either protein corresponded to the band of lower mobility recognized by anti-CBX7 and to the band of higher mobility labeled by anti-PCGF, respectively (Fig. R2B,C). We have no explanation for the identities of the second band in both cases, but a reassuring result was that the identified bands were the prevalent species associated to RING1B pull down experiments.

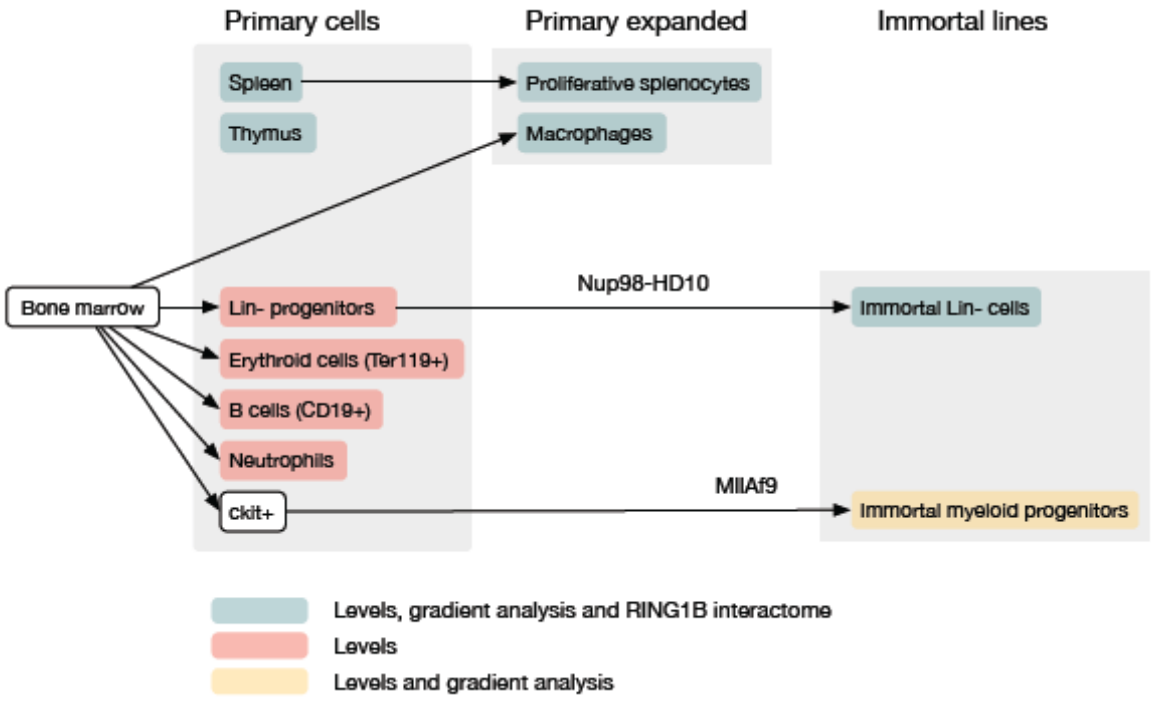

Figure R3. Cellular models used in this work. Colors indicate type of analysis performed with every cell type as described in the legend

Another protein for which we obtained two bands was YAF2. In this case, the only product predicted from known mRNAs would encode a very small polypeptide that would not be recognized by our antibody. As before, to make sure the identity of the visualized bands we

verified that the one of lower mobility was the product encoded for full length Yaf2 cDNA (Fig. R2D) Indeed, the expression of a Yaf2 cDNA identified the full, larger product, as the band of lower mobility, leaving no answer about the identity of the other band. In the opposite situation, we might have expected an additional species for PHC2 but it never appeared in our blots, possibly because the full-length form is expressed below detection levels in hematopoietic cells.

To investigate PRC1 complexities we have used a variety of hematological cell types indicated in Fig. R3. Cells were derived from wild type mice or from any of the strains

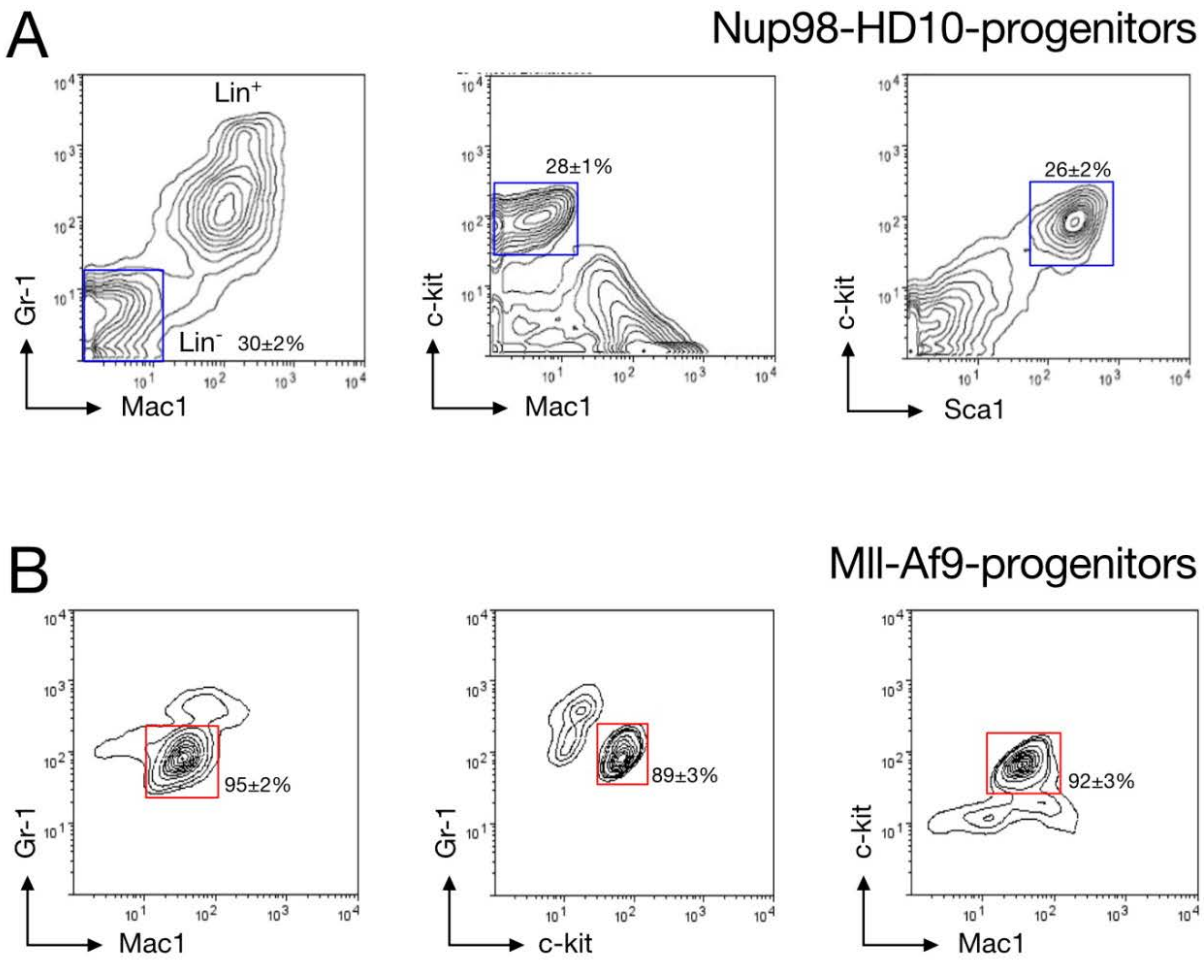

Figure R4. Immunophenotype of expanded progenitors. (A)Representative flow cytometry plot of NUP98-HD10-immortalized cultures labeled with the indicated antibodies; select populations containing Lin- cells are shown.(B) Labelled Mll-Af9 transduced cells showing a predominant population of c-kit, Gr1 and Mac1-expressing cells characteristic of transformed myeloid progenitors. Figures are mean values ± SD of 3 determinations

mentioned in materials and methods section. Primary cells were as taken from the animal, pooled from several animals when if required to get enough numbers of them. Primary expanded refers to cells that underwent some time in culture, either to enrich (macrophages) or to obtain (proliferative splenocytes) specific cell types. Finally, in order to generate immortalized progenitors we used published strategies that provide enlarged populations that can be characterized by their surface markers. Nup98-HD10-immortalized cultures contain a mixture of undifferentiated (Lin-) and differentiated (Lin+, mostly expressing low levels of myeloid markers Mac1 and Gr1) cell populations (Ohta et al., 2007), which can be separated by immunodepletion techniques (Fig. R4A). Another immortalized cell population we used was that generated by transduction of the oncogenic Mll-Af9 fusion protein, which gives rise to cells used in murine models of AML, i.e. transformed cells of myeloid flavour (Fig.R4B) (Somervaille & Cleary, 2006).

2. Expression levels of PRC1 subunits in primary cells

Our attempt to determine levels of select PRC1 subunits in hematopoietic cells was done by quantitative western blot.

2.1 Primary cells

We prepared cells suspension from selected bone marrow cells and secondary hematopoietic organs, spleen and thymus. B-cell progenitors and precursors were isolated by magnetic immunoisolation exploiting the expression of lineage-specific marker CD19. Likewise for erythroid precursors were we harvested bone marrow cells positive for Ter119.

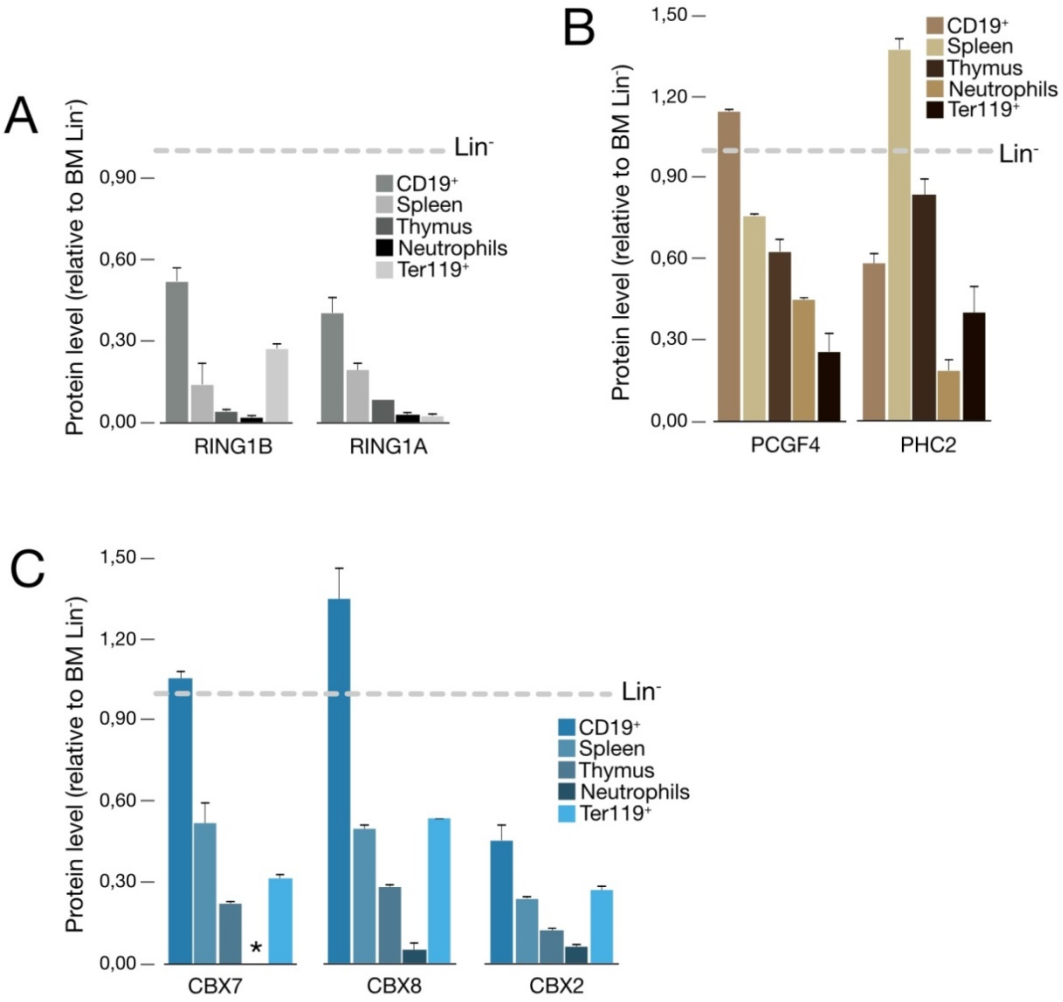

Figure R5. Relative levels of canonical PRC1 subunits in primary hematopoietic cells. Bars represent mean of two experiments ± SD. Values are referred to those in bone marrow Lin- cells (dashed line).

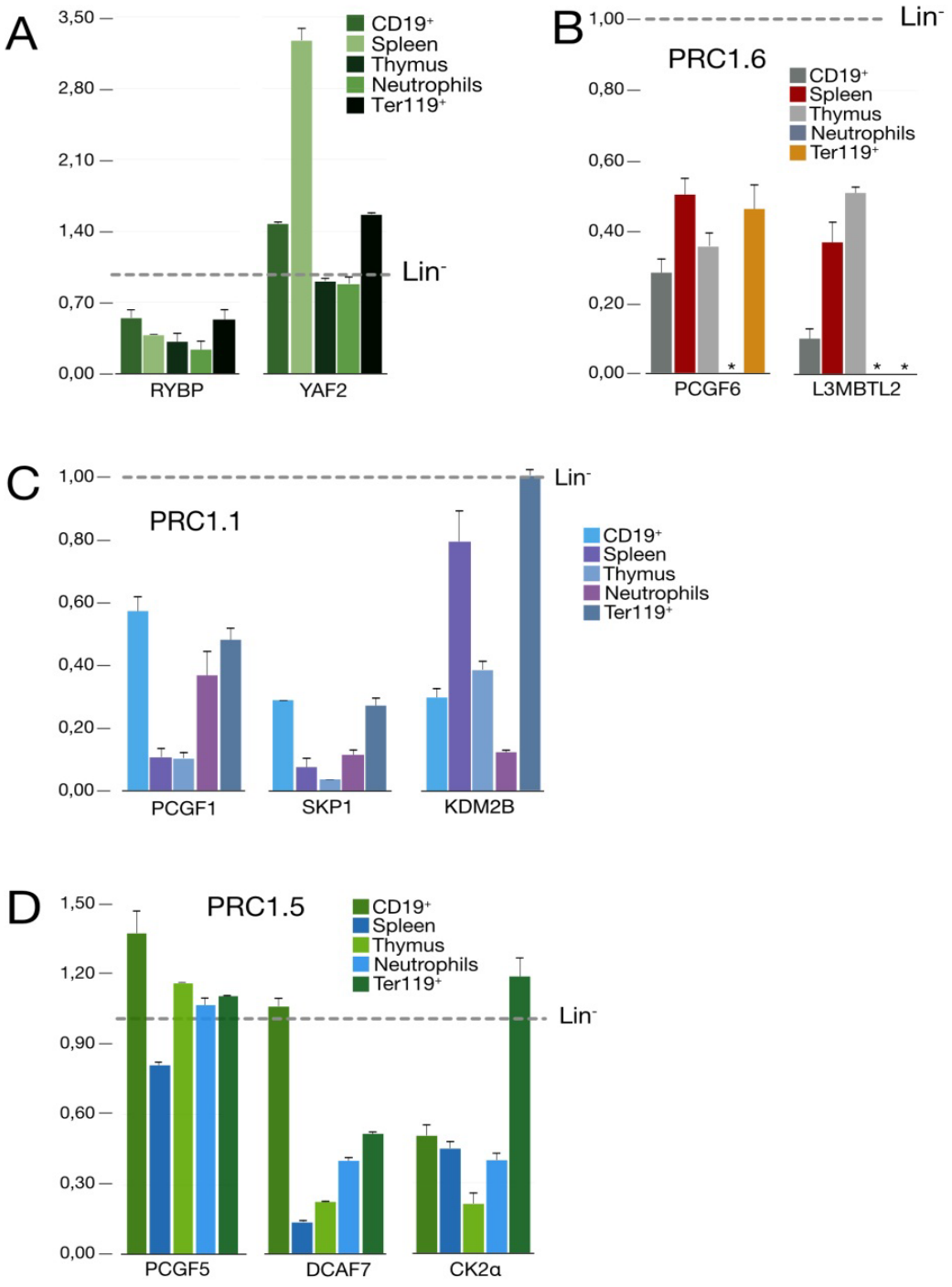

Figure R6. Relative levels of non-canonical PRC1 subunits in hematopoietic primary cells. Bars represent mean of two experiments ± s.d. Dashed line, as in Fig. 5, denotes level of the indicated protein in Lin- progenitors. * denotes, samples where signals were below detection. KDM2B values correspond to the combined contribution of both full-length and truncated forms, both of which associate with RING1B complexes, (see Fig.21B) while PCGF5 values are only those of the faster form, which is the one preferentially present in RING1B complexes (see Fig. 21C).

Neutrophils, instead were isolated by the physical properties that allow their enrichment in Percoll gradients (Boxio et al., 2004). To obtain enough cells, we used material pooled from at least 3 mice per B-cell and erythroid precursors, while enough cells could be obtained from a

single mouse per neutrophils, splenocytes (high content in more differentiated B cells) and thymocytes.

Total cell extracts, prepared as lysates in (denaturing) electrophoresis buffer, corresponding to 2 x 10^5 cells were used per lane. After western blot, signals were quantitated and normalized by content in histone H2A, as described above. Levels of PRC1 subunits in the Lin- population of immature bone marrow cells were used as reference, as shown in Figures 5 and 6.

Subunits of canonical PRC1 complexes were consistently found at the highest levels, but for a few exceptions, in the pool of Lin- cells (Fig. R5). Apart from PCGF4, PHC2, CBX7 and CBX8, that were present at hardly 15-30% excess in B-cell progenitors/precursors, all other subunits were at levels well below of those in Lin- cells (Fig. R5B, C). Of note, erythroid and above all myeloid (neutrophils) cells contained the lowest levels of PRC1 subunits.

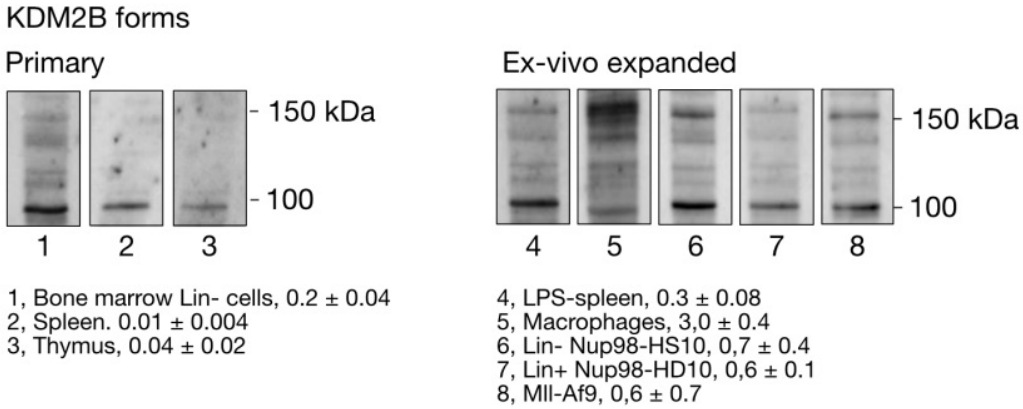

Figure R7. KDM2B forms in hematopoietic cells. Figures following description of cell type indicate ratios, as a mean ± SD of two experiments, of full length to truncated forms of KDM2B

Interestingly, levels of both RING1 proteins were considerable lower in all cells tested, and with few exceptions, the lowest of al PRC1 subunits tested. (Figure R5A).

This tendency towards reduced expression, compared to immature cells, was also seen among subunits of non-canonical complexes (Fig. R6). Exceptions, in all cell types, were YAF2 and PCGF5 (Fig. R6A, D), which were seen at levels similar or higher than in Lin- cells. PRC1.5 subunits were also present at low levels, except DCAF7 and CK2a in B-cell and erythroid precursors, respectively. It was notable the very high levels of YAF2 (3 fold-higher than in bone marrow progenitors) in spleen cells. (Fig. R6A). PRC1.6 subunit L3MBTL2 was below

detection in erythroid precursors and, as PCGF6, in neutrophils (Fig.R6B). PRC1.1 subunits were also at low levels, in all cases, except KDM2B in erythroid precursors below those in Lin- cells (Fig. R6A). Regarding KDM2B, levels were calculated by combining the signals of the long and short forms, where they were present. For instance, levels of the full-length variant were below detection in primary cells from spleen and thymus. In general, the shorter KDM2B form was more abundant, except in macrophages (Fig. R7) which was also the only cell type where total (both forms) KDM2B levels were higher than in bone marrow progenitors.

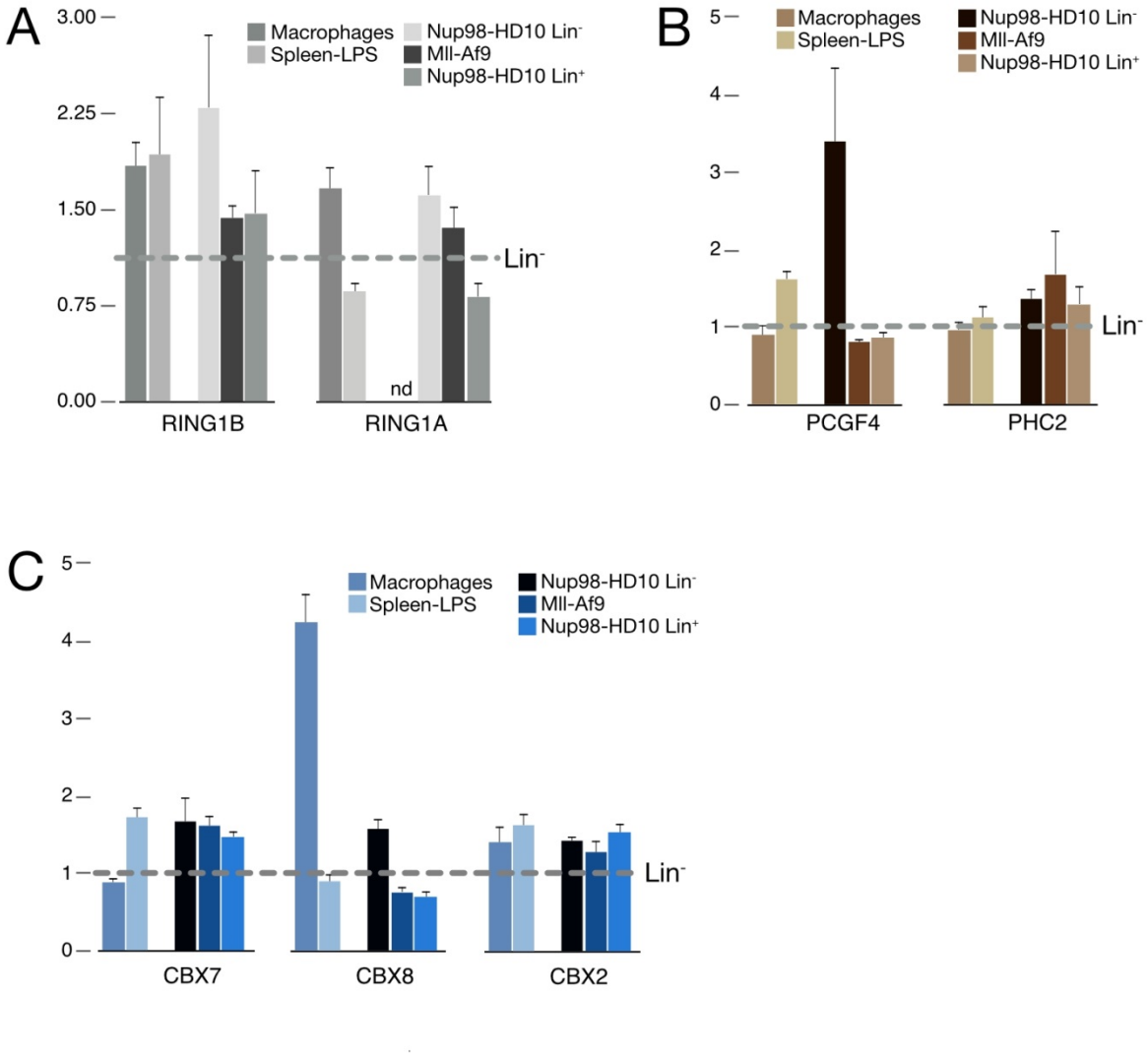

Figure R8. Relative levels of canonical PRC1 subunits in ex-vivo expanded hematopoietic cells. Bars represent mean of two experiments ± SD. As before, the reference is values in Lin- cells.

2.2 Expanded primary cells

All cells expanded ex vivo showed increased levels of PRC1 subunits compared to primary cells (Fig. R8 and R9). Canonical PRC1 subunits were found always at higher than those in primary cells, often higher than those in bone marrow Lin- cells (Fig. R8).

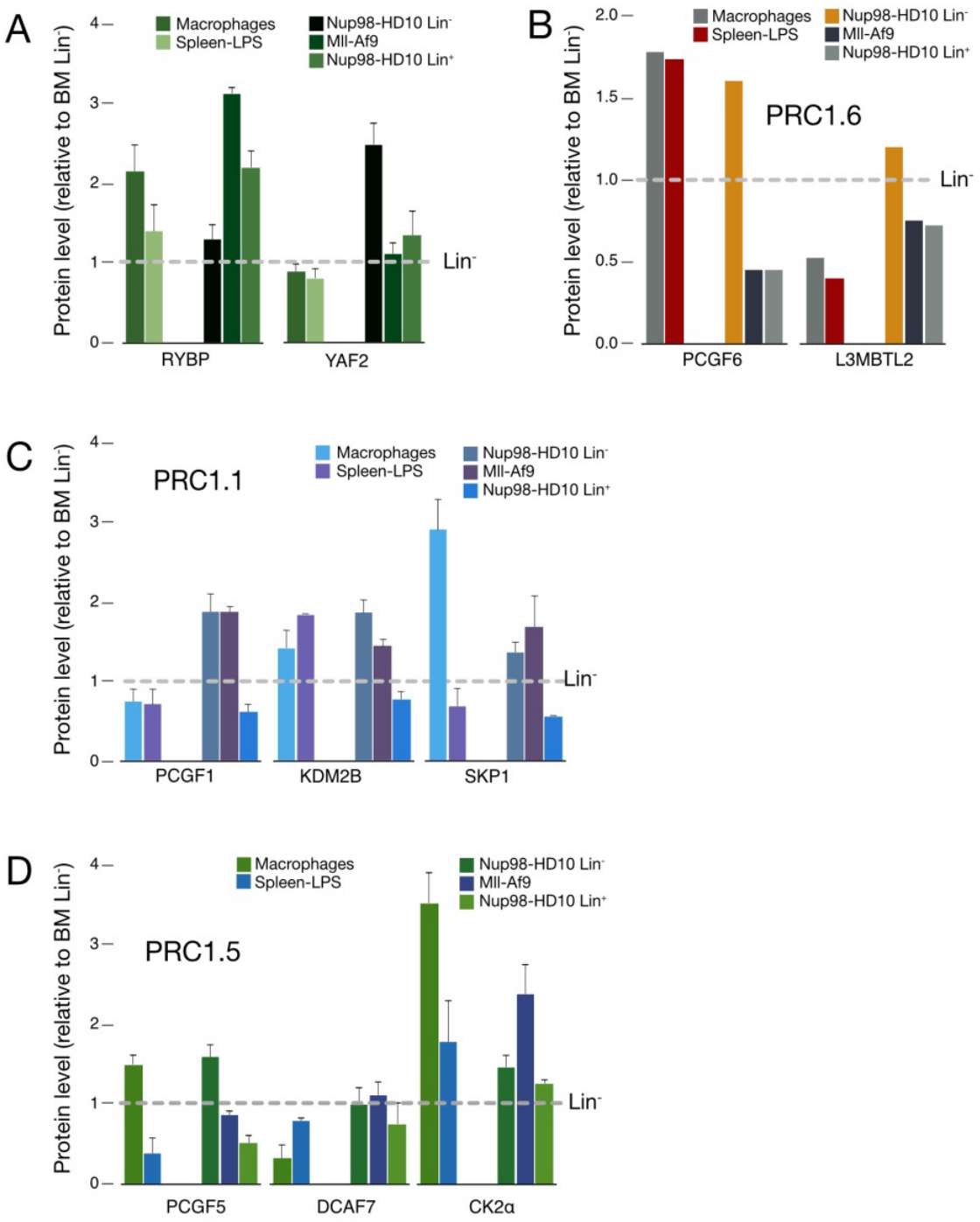

Figure R9. Relative levels of non-canonical PRC1 subunits in ex-vivo expanded hematopoietic cells. Bars represent mean of two experiments ± SD. Values in Lin- cells are shown as a reference.

RING1B, CBX2, CBX7 and PCGF4 were consistently present at higher levels but the content in these subunits was very variable between cell types. Examples are PCGF4 in Nup98-HD10-immortalized cells or CBX8 in macrophages (Fig. R8B, C). Non-canonical PRC1 subunits were found also at higher levels than in primary cells, in the same heterogeneous fashion with some cell types expressing very high levels (RYBP,SKP1 or DCAF7, Fig. R9).

For easy of comparison, the big differences in contents of RING1A and RING1B proteins in primary vs ex-vivo expanded cells is shown in Fig. R10.

Possibly a reason for higher PRC1 levels in expanded versus primary cells is the distinct metabolic status associated to the active proliferative state. In vitro culture effects were maintained to a minimum by analyzing cells at the shortest possible time: 3 or 7 days

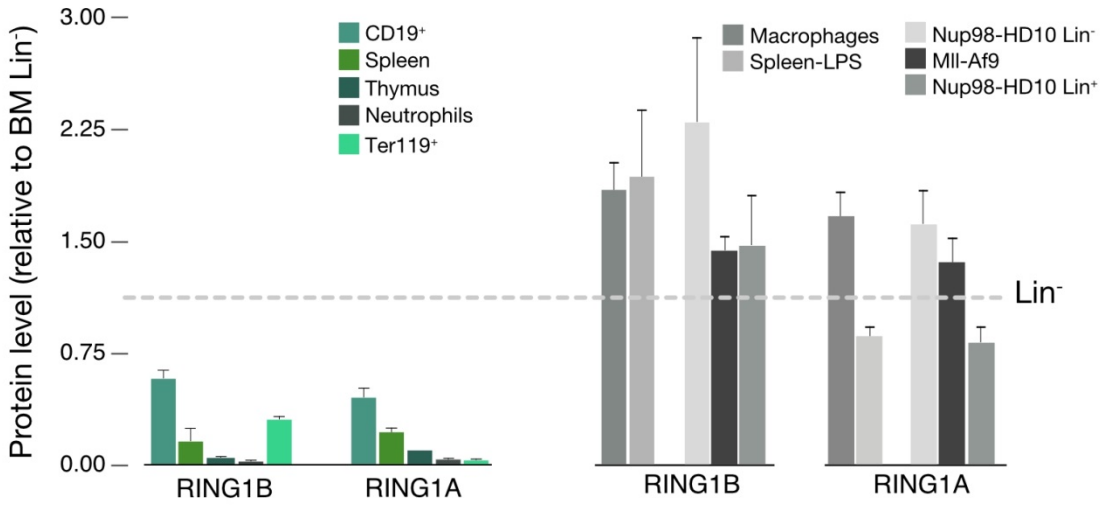

Figure R10. Levels of RING1A and RING1B in primary and expanded cells. Bars represent mean of two experiments ±s.d. Signals are normalized by H2A content. As reference were used levels in lin- cells from bone marrow (BM) which protein levels was considered as =1 and is marked with grey line in all plots.

(LPS- stimulated splenocytes, macrophages, respectively) and 2-3 weeks for cells undergoing immortalization.

To test this notion we chose the best pairs of cell types that could be compared. On the one hand, spleen cells (close to a quiescent population) and proliferative cells derived from them after LPS-induced stimulation (Figs. 11A and 12A). On the other, the proliferative (Lin-) and

non-proliferative (Lin+) populations within cultures of Nup98-HD10-transduced progenitors (Fig. R11B and 12B). The data showed that, almost with no exception, levels were higher for proliferative cells, whether for canonical (Fig. R11) or non-canonical (Fig. R12) PRC1 subunits.

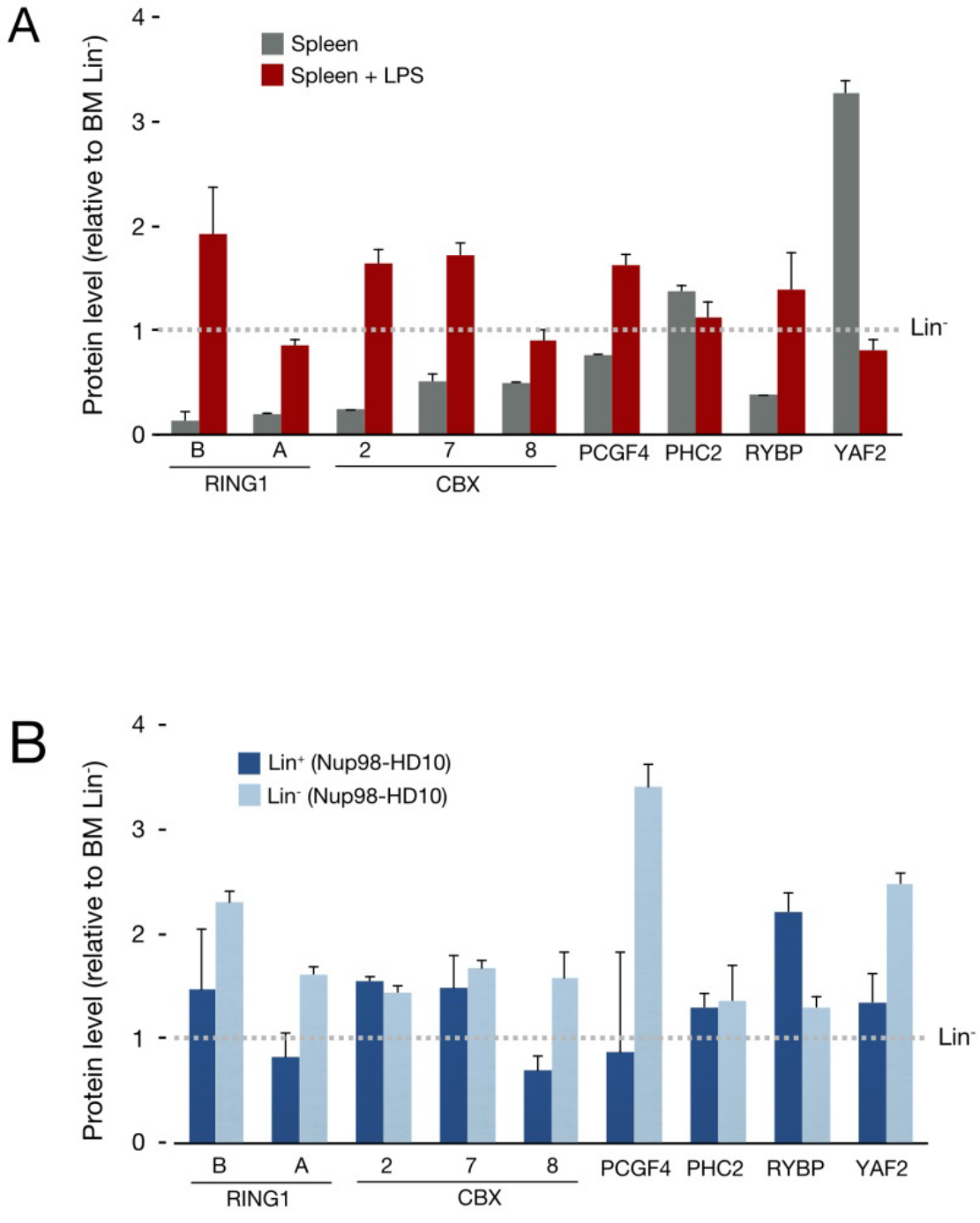

Figure R11. Comparison between levels of canonical PRC1 subunits levels within comparable quiescent/proliferative cell types.

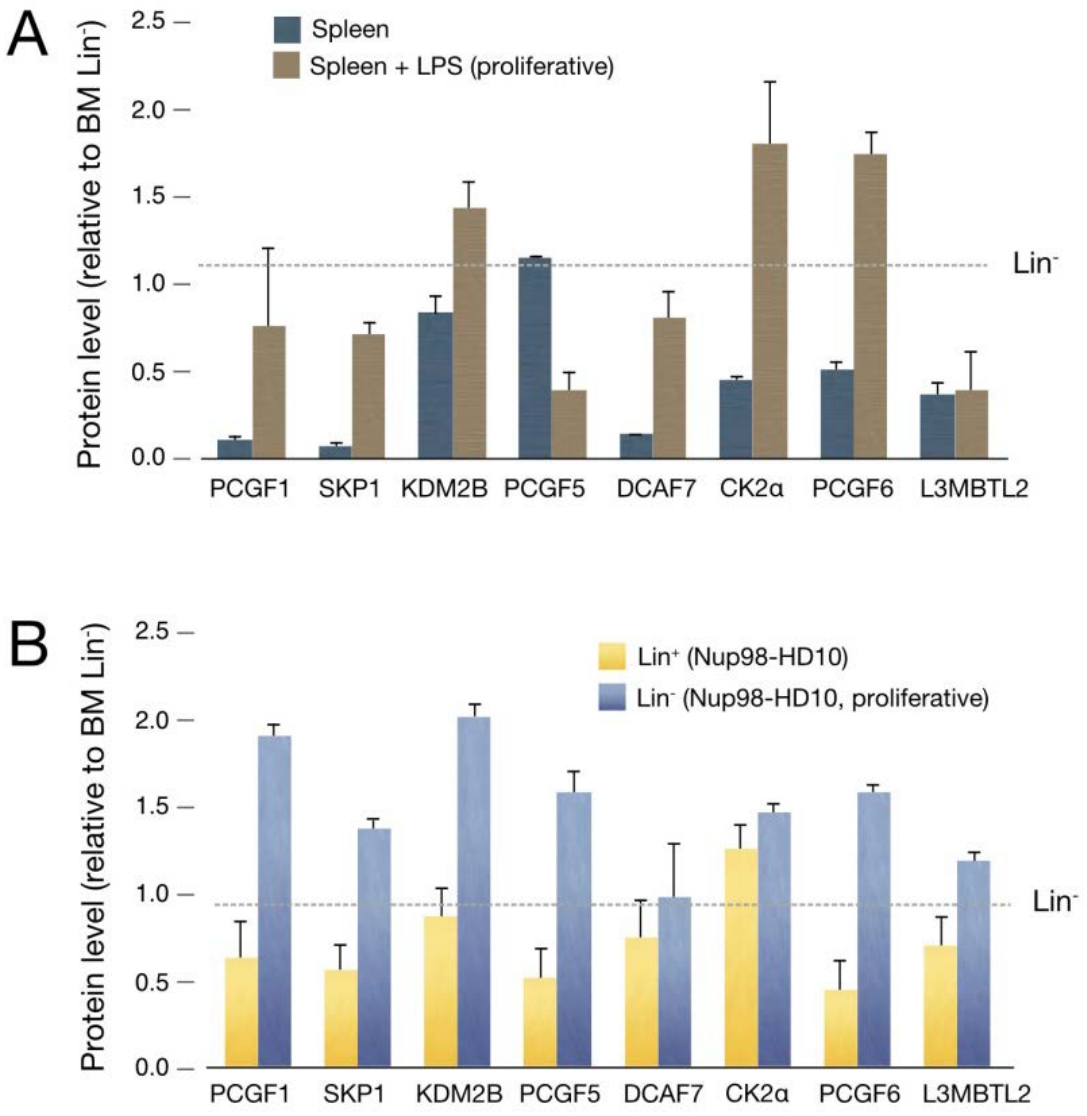

Figure R12. Comparison between levels of non-canonical PRC1 subunits levels within comparable quiescent/proliferative cell types.

3. Diversity of molecular species containing PRC1 subunits

The biochemical nature of chromatin regulator complexes usually is given by the identification of components within purified preparations. Traditionally, in protein isolation procedures, this has been achieved by following an enzymatic activity. However, with exceptions, such as the isolation of PRC1 complexes with histone H2A monoubiquitylation activity, this has not being always the case for chromatin regulator complexes. Instead, two-step affinity purification schemes have been used, followed by mass-spectrometry/western

blot identification. Whereas this may yield preparations relatively free from non-related subunits, it certainly does not resolve different species of complexes.

3.1 Complexes with RING1A and RING1B

To gain insight in the possible intricacies of PRC1 complexes, we decided to analyze the behavior of nuclear extracts in density gradients of glycerol (15% to 35%). At the equilibrium, fractions were taken and orderly analyzed by Western blot. Obviously the resolution power of this method is not ideal but it combines simplicity with the ability to provide a great deal of information. Another important consideration: there is no way to derive quantitative relationships in this analysis because western blot signals are not comparable for different antibodies. Thus, PRC1 subunits present at low concentrations may not appear as such just because acquisition times of chemiluminesce was that sufficient to provide an image. Moreover, it is not only the amount of the different proteins that influence the generated signal, but also the affinity/avidity of the antibodies used. For example, our anti-RING1B antibody was far more sensitive than anti-PCGF1 antibody (Fig M3). Despite the caveats, some relevant conclusions can be drawn for this analysis.

Fig. R13 shows the results obtained for the distribution of RING1B and RING1A in the cell types indicated. Two simple observations are clear. First, each of these PRC1 subunits migrated within gradients as if belonging to very different molecular aggregates: RING1B in spleen extracts is found throughout most of the gradient (and RING1A in thymus extracts or Nup98-HD10 progenitors). Second, when considering high molecular weight species, it is RING1B rather than RING1A the subunits more abundant: a small part of RING1B was present in species migrating with densities as that of 440 kDa marker and above in primary cells from spleen and in cell expanded in vitro such as LPS-stimulated spleen cells and in macrophages (Fig. R13, left). In contrast, only very small amounts of RING1A were found in similarly sized species in spleen or thymus cells and in Nup-98HD10-progenitors (Fig. R13 right). Of note, the presence of high molecular weight species with RING1B did not correlate with proliferative states.

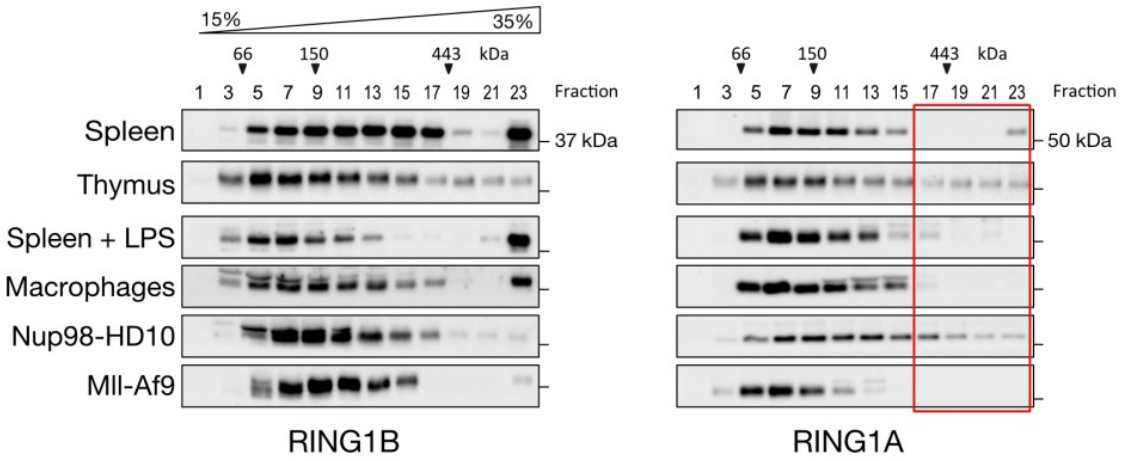

Figure R13. Representative glycerol density mobilities of RING1B and RING1A-containing complexes in nuclear extracts from the indicated cell types. Every other fraction of the gradient analyzed are shown, marking (arrowhead) the one enriched in the marker protein of the molecular weight indicated. The red rectangle, in RING1A westerns, identify fractions containing large molecular assemblies. On the right side, the position of mobilities in electrophoresis of molecular weight markers.

Thus, their residence in these complexes was clear in actively dividing cell types such as stimulated splenocytes or ex-vivo expanded macrophages but not so much in immortalized primitive and myeloid progenitors (Nup9-HD10, MllAf9-transduced). At the same time, samples enriched in quiescent primary cell types, spleen, thymus, contained large species with RING1B. (Fig. R13).

3.2 Species containing subunits that associate competitively to RING1 proteins

We then decided to compare the distribution of chromobox proteins and RYBP/YAF2 paralogs, to see whether it could be perceived that their association to RING1A or RING1B was exclusive (schematized in cartoon R14C) (Tavares et al., 2012). When looking at CBX proteins (Fig. R14A) it was plain that, as seen for RING1A and RING1B, the allocation of each of these proteins varied with the cell type. Compare, for example, the CBX7-containing high molecular weight species in spleen and thymus cells (Fig. R14A middle). And, again, as seen above, there was no correlation between the presence of CBX proteins in large species and the proliferative status of the cell population analyzed: CBX8 in dividing but not quiescent spleen cells, while absent from dividing immortalized cells (Fig. R14A right). Another interesting observation was that high molecular weight species in all cell types contain one (or

more) CBX subunits: CBX7 in quiescent splenocytes, CBX2 and CBX8 in LPS-stimulated splenocytes and

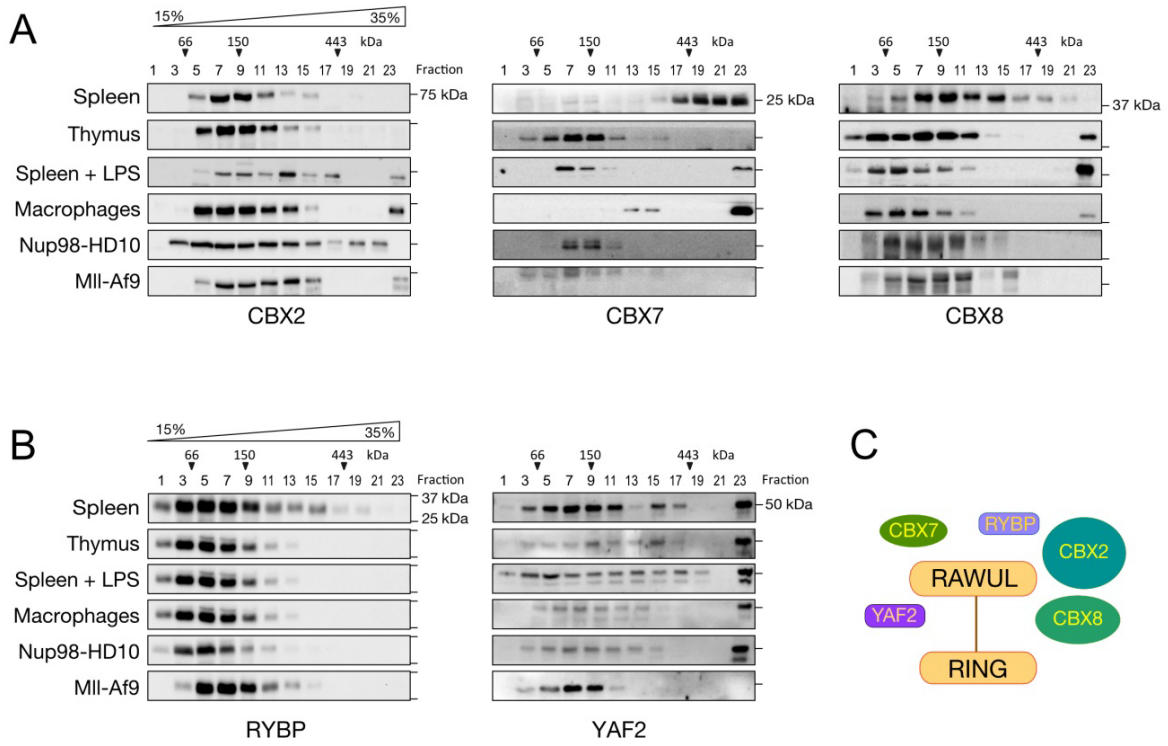

Figure R14. Representative distribution in glycerol gradients of mutually exclusive RING1B/A interactors CBX (A) and RYBP/YAF2 (B). Schematic representation of expected binding competition in their association to the C-term RAWUL domain of RING1 proteins.

macrophages expanded in vitro. Perhaps exceptions were the immortal cell types, where large complexes were almost devoid of CBX proteins but for small amounts of CBX2 (Fig. R14A).

The results for RYBP and its homolog YAF2 led to an unexpected observation: while smaller complexes contained either of them, YAF2, but not RYBP, was present in the largest species (Fig. R14B). Moreover, the intensity of signals in several cell types, suggested as if a large portion of total YAF2 was contained in the large complexes. As an exception, Mll-Af9-immortalized myeloid progenitors were devoid of either RYBP or YAF2. About a possible alternative presence of either RYBP/YAF2 or CBX proteins (Tavares et al., 2012) in large molecular species the data are not conclusive (for instance, large complexes in immortalized myeloid progenitors lack both types of subunits). What the data point is at the coexistence of high molecular weight species containing CBX or YAF2. Assuming that most of YAF2 is part of

PRC1 complexes it follows that large molecular PRC1 species are made of both canonical and non-canonical complexes.

3.3 Complexes with canonical and non-canonical PRC1 subunits

CBX proteins are considered genuine identifiers of canonical PRC1 complexes. However, there is at least a report in which CBX8 is found associated to BCOR-containing complexes (Beguelin et al., 2016), against the accepted consensus. Therefore, we chose to analyze the distributions in glycerol gradients of PCGF4 and PHC2, an interacting pair (Fig. R15B) which together make for good markers of canonical PRC1 complexes.

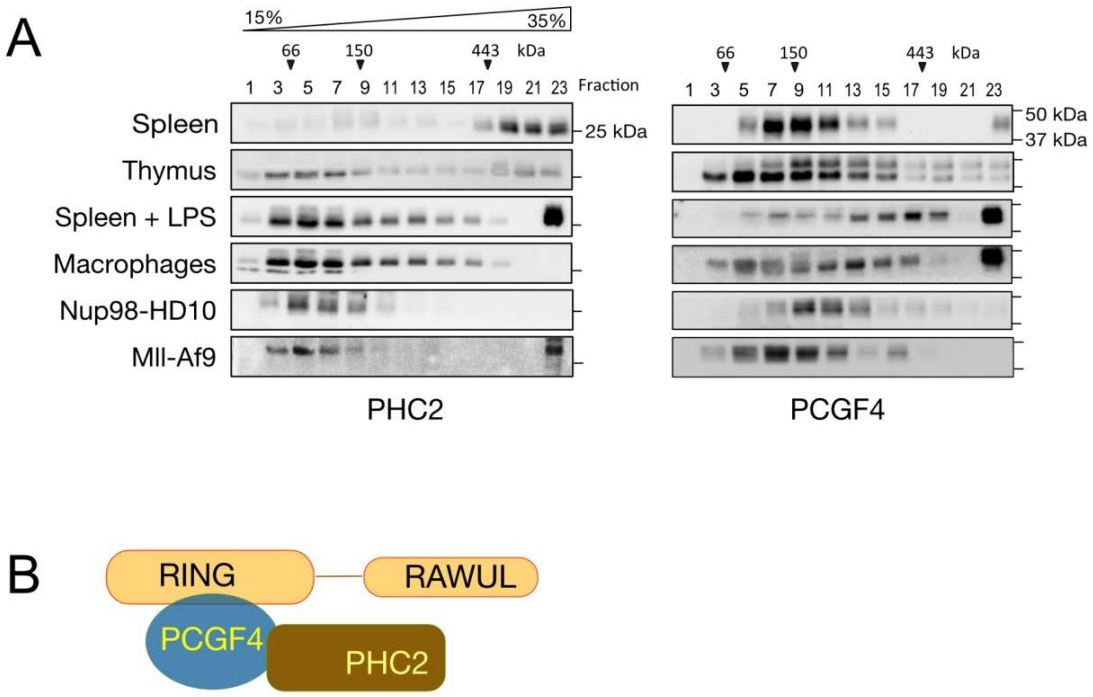

Figure R15. Representative distribution in glycerol gradients of archetypical canonical PRC1 subunits PHC2 and PCGF4 (A) distribution in glycerol density gradient (B) schematic representation of PCGF4 contacting both RING1B and PHC2, although contacts between RINGB and PHC2 cannot be discarded

PHC proteins, as described above, are proteins with shown capacity to generate large aggregates, due to the presence of dual interacting surfaces in their SAM domains. Thus, it was not surprising to see PHC2 as part of very large molecular species (spleen, thymus and dividing splenocytes (Fig. R15A, left). As part of smaller complexes was also seen in extracts of macrophages, but unexpectedly large complexes in immortal, undifferentiated progenitors

(expressing Nup98-HD10) lacked PHC2. PCGF4, on the other hand, was identified in fractions of the gradients corresponding to large species, although not always and not overlapping with fractions containing PHC2. For example, fraction 23 in dividing splenocytes have both PHC2 and PCGF4, but the same fraction in extracts from macrophages while lacking PHC2 is enriched in PCGF4; similar discrepancy was also noticed in spleen and, most surprisingly in immortal, Mll-Af9-transduced myeloid progenitors (top and bottom rows in Fig. R15A). The accepted way of association of PHC2 and PCGF4 in PRC1 canonical complexes is as indicated schematically in Fig. R15B, i.e. PHC2-PCGF4 direct interaction determining its presence in canonical versus non-canonical complexes, and then through known contacts in PCGF4 with the RING finger of RING1A or RING1B. Therefore, the results suggest the existence, at least within the range of large sizes, of complexes of distinct content. Alternatively, PCGF4 and PHC2 in these extracts could be part of complexes not related to PRC1.

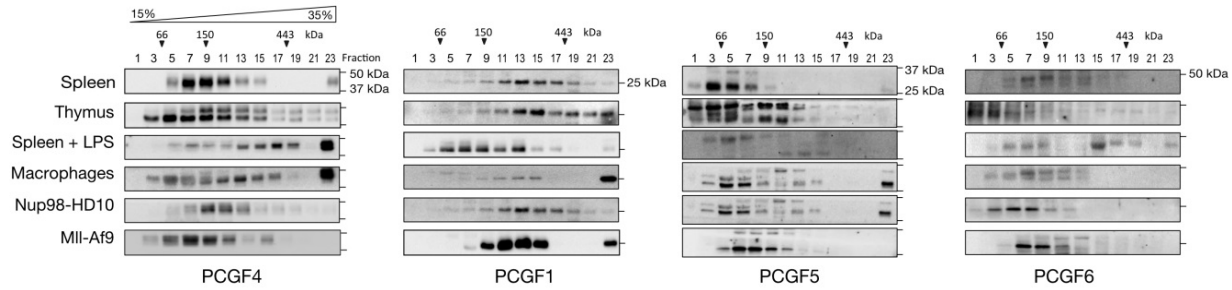

Figure R16. Representative distribution in glycerol gradients of the four PCGF subunits studied.

Examination of distribution of PCGF members characteristic of non-canonical complexes (Fig. R16), as seen before with RYBP and YAF2 supported the existence of variously sized complexes, including some of very high molecular weight. PCGF6, originally described as part of a large complex in HeLa cells (Ogawa et al., 2002) only appeared to be present, partially, among large species in LPS-stimulated splenocytes. PCGF5 complexes, hardly studied, were found in fraction 23 of macrophages and immortal Lin- progenitors. The difficulty in interpreting these data considering the distribution of its direct interactions, RING1A and RING1B, is that whereas in macrophages RING1B co-fractionates, in immortal Lin- cells there are just minor amounts of RING1B or RING1A (Fig. R13). PCGF5 (leaving aside the band of lower mobility, of unknown identity, although it may well be a

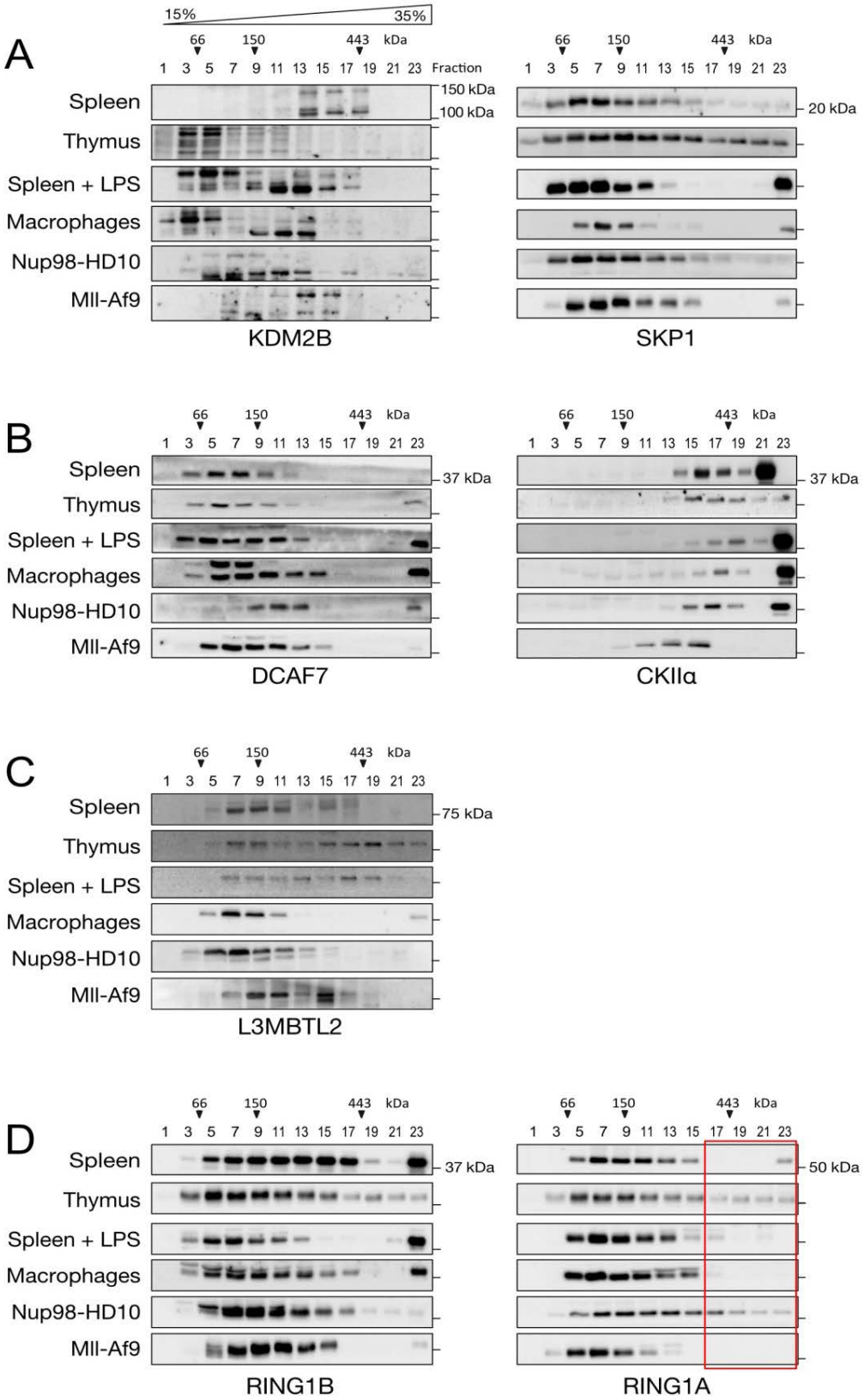

Figure R17. Representative distribution in glycerol gradients of subunits present in non-canonical complexes, PRC1.1 (A), PRC1.2 (B) and PRC1.6 (C). RING1A and RING1B (D) are shown for quick visualization of fractions that contain them.

posttranslational modified PCGF5, appears in large complexes of intermediate size (Fig. R16) complexes in macrophages and transformed progenitors, and as in other cell types.

It was unexpected to find that non-canonical PCGF1 subunit appeared participating of aggregates larger, on average, than those containing canonical PCGF4 (Fig. R16, half left). Also, the presence of PCGF1 in very large complexes in some extracts is perplexing because none of them contain, for instance, its direct interaction KDM2B (Fig. R17A, left). And, as in other instances, there is no correlation with the presence of other direct interactions, namely RING1A and RING1B which are absent from these PCGF1 structures in cells like splenocytes or immortal Mll-Af9 progenitors (Figs. 13 and 16).

Finally, subunits found in PRC1 complexes that appear to not bind directly RING1A or RING1B (SKP1, DCAF7, CK2a and L3MBTL2) were also studied (Fig. R17). Expectancies about obtaining useful information from these analysis were reduced, in part due to the the evidence of some of these proteins being part of non-PRC1 complexes (Hauri et al., 2016)

Most CK2a was present in all cell types, except thymus and Mll-Af9 immortalized progenitors (Fig. R17B) large complexes, perhaps in the same molecular species that also contain RING1B and CBX subunits. The presence, also in high molecular weight complexes, of SKP1 in LPS-stimulated spleen cells is difficult to associate to PRC1 species, because a hypothetical binding to RING1B would be mediated through KDM2B, which is absent from these same species (Fig. 17A, B). The migration of L3MBTL2 fits with that of PCGF6, except in the thymus, although only this evidence does not probe that they are part of the same complex(es).

4. PRC1 subunits associated to RING1B

As stated above, most studies reporting subunits in PRC1 complexes is not of quantitative nature. Whereas the identification of one or another component is valuable in itself, a more quantitative approach permits to speculate about the dynamics of the complexes. Indeed, more recent studies are undertaking such a quantitative approach using sensitive, although expensive mass-spectrometry methods. Here, we have identified PRC1 proteins associated to RING1B by quantitative western blot. We set up an in vivo tagging system for efficient isolation of RING1B expressed as close as possible to physiological levels. To do this, a sequence encoding a peptide that can be biotinylated was knocked in at the Ring1B locus by homologous recombination in ES cells, so that a fusion protein that is modified at its C-term was produced. Mice homozygous for this modification (Ring1B-bio/bio) were normal and

expressed a RING1B protein of lower mobility at levels similar to those in wild type mice (Fig. M1). Ring1Bbio/bio mice were mated to mice generated from ES cells where a cDNA encoding the E. coli BirA ligase was knocked into the Rosa26 locus, so that a ubiquitous biotin ligase activity on the sequence, 23 amino acids, at the C-term extension of RING1B was attained. Endogenously biotinylated RING1B, and associated proteins, were then isolated from nuclear extracts using immobilized streptavidin that shows a very high affinity for biotin. To control for non-specific associations we analyzed proteins bound to streptavidin in extracts that contain wild type, non-tagged RING1B. The animal models used for this study are depicted in figure M1.

4.1 A way to estimate quantitative association to RING1B

Experiments such as the isolation of a tagged protein and bound interactors are usually referred to as co-precipitation (co-immunoprecipitation if using an antibody) or pull-down experiments. For this study, we chose cells from spleen and thymus, proliferative splenocytes and macrophages from ex vivo expanded cultures as described above. As a source of primitive hematopoietic cells we chose the Lin- fraction from Nup-98HD10 immortalized progenitors.

Pull-down experiments are critically dependent on conditions (protein concentrations, binding buffer and removal of non-specifically bound proteins with washes). An example with 293 cells, an established human cell line widely used in the characterisation of protein complexes, including Polycomb complexes, is shown in Fig. R18. Here, a 293-cell clone selected after transfection of plasmids that express E. coli BirA and a biotinylatable RING1B variant was used. Note that this clone expresses amounts of ectopic, tagged-RING1B, comparable to those of the endogenous form (lane 5) which is efficiently captured by streptavidin beads (see the little remaining RING1B in not bound fraction, lane 6). Pulled down material from extracts that only expressed BirA provided the desired estimation of non-specifically bound proteins. Lanes 3 and 4 illustrate how washing conditions can be found that eliminate background interactions by washes that modify ionic (NaCl) and hydrophobic environments (Igepal). At the same time tagged-RING1B and associated proteins after these washes, lanes 7, 8), although of similar appearance within the extremely limited number of binding event analysed, are expected to be free of non-specifically associated interactions after washes with 0.2M NaCl and 0.25% Igepal, lane 8, but not if washed with a buffer or reduced NaCl content, lane 7.

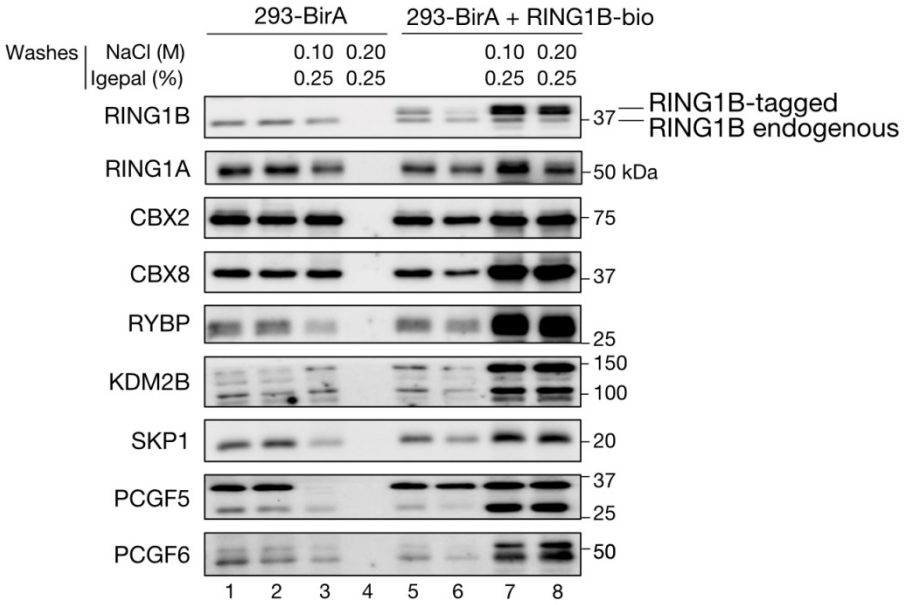

Figure R18. Isolation of RING1B and associated proteins (pull down) in lines of 293 cells that express only biotin ligase BirA (293-BirA) or the biotinilytable RING1B form (BirA-RING1Bbio) under different conditions.

Using these conditions in pull down experiments with the indicated hematopoietic cells we observed somehow unexpected results. These are illustrated in Fig. R19A. Binding of a reduced number of PRC1 subunits to RING1B (in contrast to 293 cells, our hematopoietic cells express only the tagged-RING1B species) illustrates how proteins anticipated to be present as RING1B interactions, as seen with nuclear extracts from thymus cells (Fig. R19A, left) were missing among the material bound to streptavidin beads in extracts from spleen cells or primitive progenitors (Fig. R19 center, right).

Obviously, conditions had to be found, if at all possible, that balanced the removal of non-specifically bound material with the persistence of specifically bound proteins. We found that the conditions used for nuclear extracts from thymus were satisfactory too for macrophages and LPS-stimulated spleen cells. Figure R19B shows some of the results that lead us to identify conditions acceptable for spleen and progenitor cells. We took as controls of total binding the material present in not washed (quick rinse) beads. It can be seen that washes with only Igepal were not enough

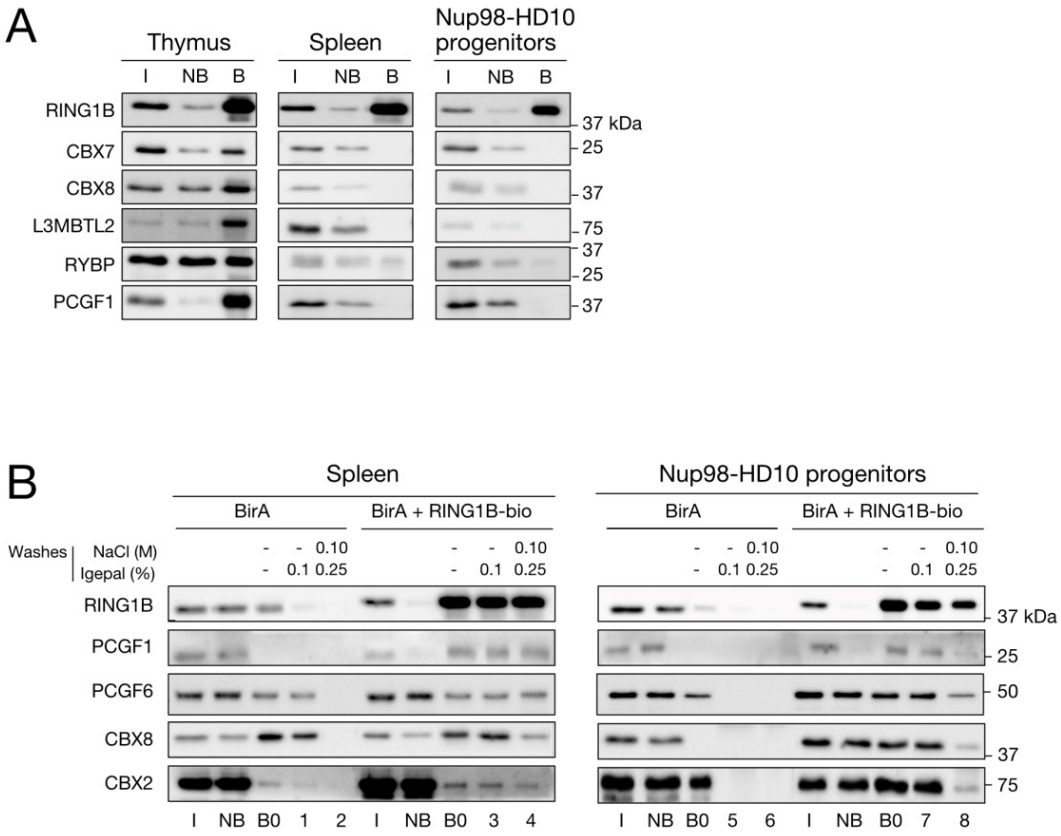

Figure R19. Optimization of streptavidin-pull down experiments with hematopoietic cells. (A) Conditions that are useful for tissue-culture, transformed cells (293) are unsuitable for hematopoietic cells. (B) Cell type-dependent conditions to minimaze background binding. I, input (5% of total extract), NB, not bound fraction or proteins in extract after removal of strepatividin beads and associated proteins; B0, material eluted with loading buffer from beads after a quick PBS rinse, taken as not-washed beads. Eluted material, after indicated washes, is in lanes 1-8.

to remove background (PCGF6, CBX8 from spleen, Fig. 19B, lane 1), not even after increasing Igepal to 0.25% (not shown) and that some NaCl had to be included in the washing buffer with inappreciable losses of specific binding (lane 1, 2 and lanes 3,4 of Fig. R19B). Pull down results with Nup98-HD10-progenitors illustrated how forcing washes lead to unacceptable results that remove much of the proteins bound, included those bound specifically. Thus, only Igepal washed background binding (lane 5) but conditions acceptable for spleen led to severe losses of specifically bound proteins (compare lanes 7 and 8 in Fig. 19B). Optimization of pull down experiments already allowed us to appreciate that the stability of proteins in the RING1B-containing complexes differed greatly among nuclear extracts.

Once, those conditions for pull down experiments were defined we set out to analyze PRC1 subunits bound to RING1B in the indicated cell types. Binding was plotted as a proportion of

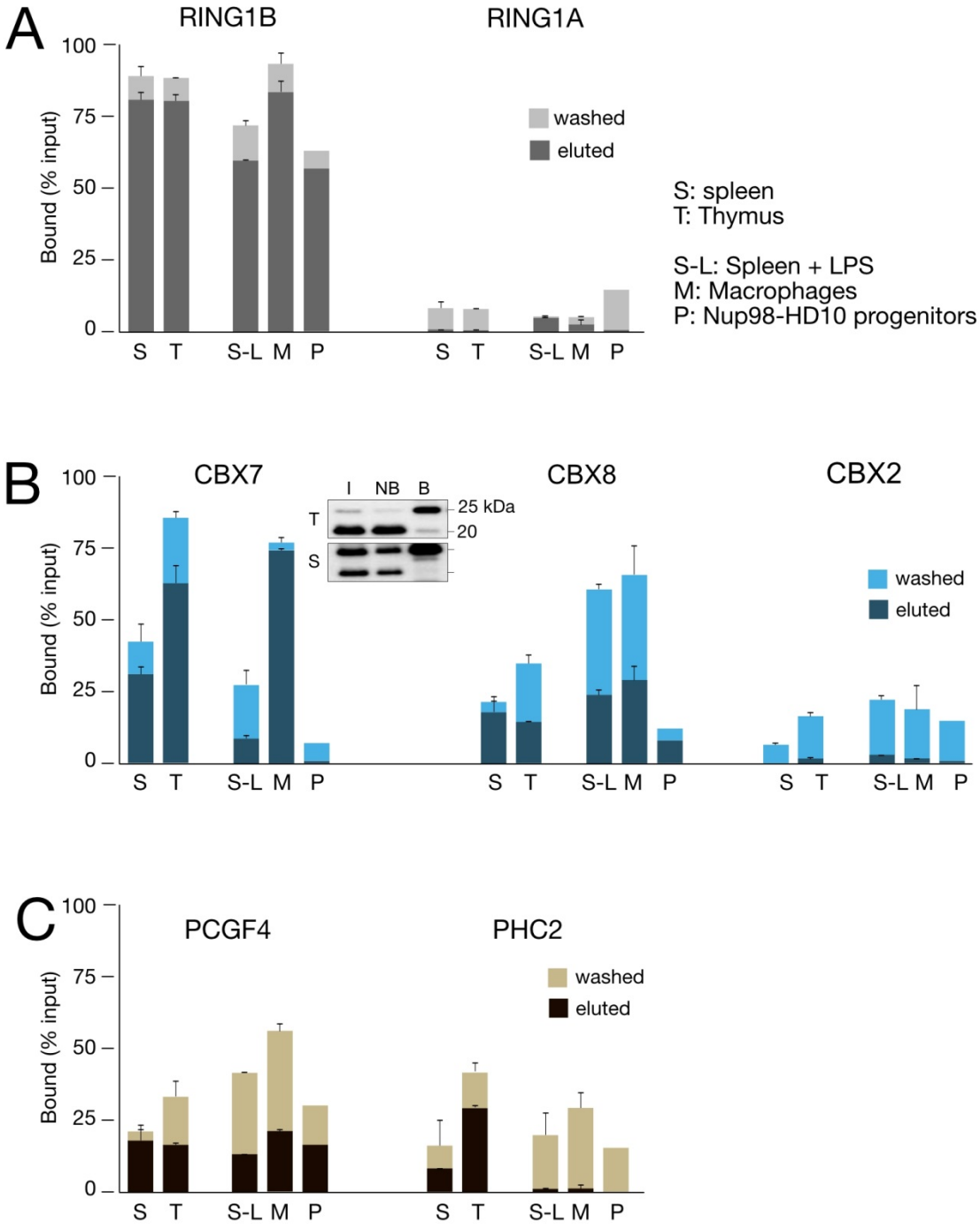

Figure R20. Canonical PRC1 subunits present in RING1B complexes in the indicated hematopoietic cell types. Values are the fraction of the total content in the extract that was removed upon incubation with streptavidin beads. That amount is the combination of material released from beads during washes and eluted after washes. Bars show mean values of two experiments ± SD. Inset in B is a western blot (I, input, NB; not bound and B, bound) showing association of the slow band recognized by our anti-CBX7.

the protein present in the extract. Our quantitative approach was as follows: total content of the protein of interest was calculated from the intensities of signals of a small portion (5%, or input). Then we estimated the fraction of total binding from the difference between the signals for input and not bound fractions (volume of extract, after incubation with streptavidin beads, equal to that of input of the nuclear extract). It was clear that this amount was always larger than that deduced from signals of the material bound to beads after washes, the eluted fraction. The difference was called washed fraction. Thus, two magnitudes are plotted: eluted and washed fractions making the total of bound protein. The data are shown in Figs 20-23). Calculations were done on pixel values after subtracting signals derived from pull down with extracts made out of cells that do not express tagged-RING1B. The so-called washed fraction contains not only protein genuinely washed but also not eluted and/or beads-trapped protein, most likely a small contribution that we decided not to correct for. Besides, as the Fig. 20 and 21 show, the differences among the magnitude of the washed fractions was too big as to be due to trivial reasons. Moreover, differences in the washed fraction also varied for the same protein.

4.2 Striking differences within RING1B-bound PRC1 subunits and RING1B complexes within cell types

Figures 20 and 21 display the data plotted by PRC1 categories, while Figures 22 and 23 compare PRC1 subunits bound within a same cell type. The first observation is the highly efficient binding of tagged-RING1B, ranging from 65 to 90% of the total protein in the extract (Fig. 20A). Also, most of the protein remained after washes. All of which was expected given the high affinity of streptavidin for biotin.

We found that most RING1A was not present among RING1B-bound proteins (maximum binding around 10-15%, most of which lost with washes, Fig R20A). This suggests, that most likely, PRC1 complexes containing RING1A and RING1B are separable entities. Among CBX proteins, it was CBX7, as a whole, the family member prevalent in RING1B complexes (Fig 20B) and while some contained CBX8, the presence of CBX2 was almost negligible, or at least that of the fraction that resisted washes (Fig. 20B, right). Substantial amounts of canonical subunits PCGF4 and PHC2 were also found among RING1B-bound proteins, although the presence of PHC2 in ex vivo expanded cells was minimal (Fig. 20C).

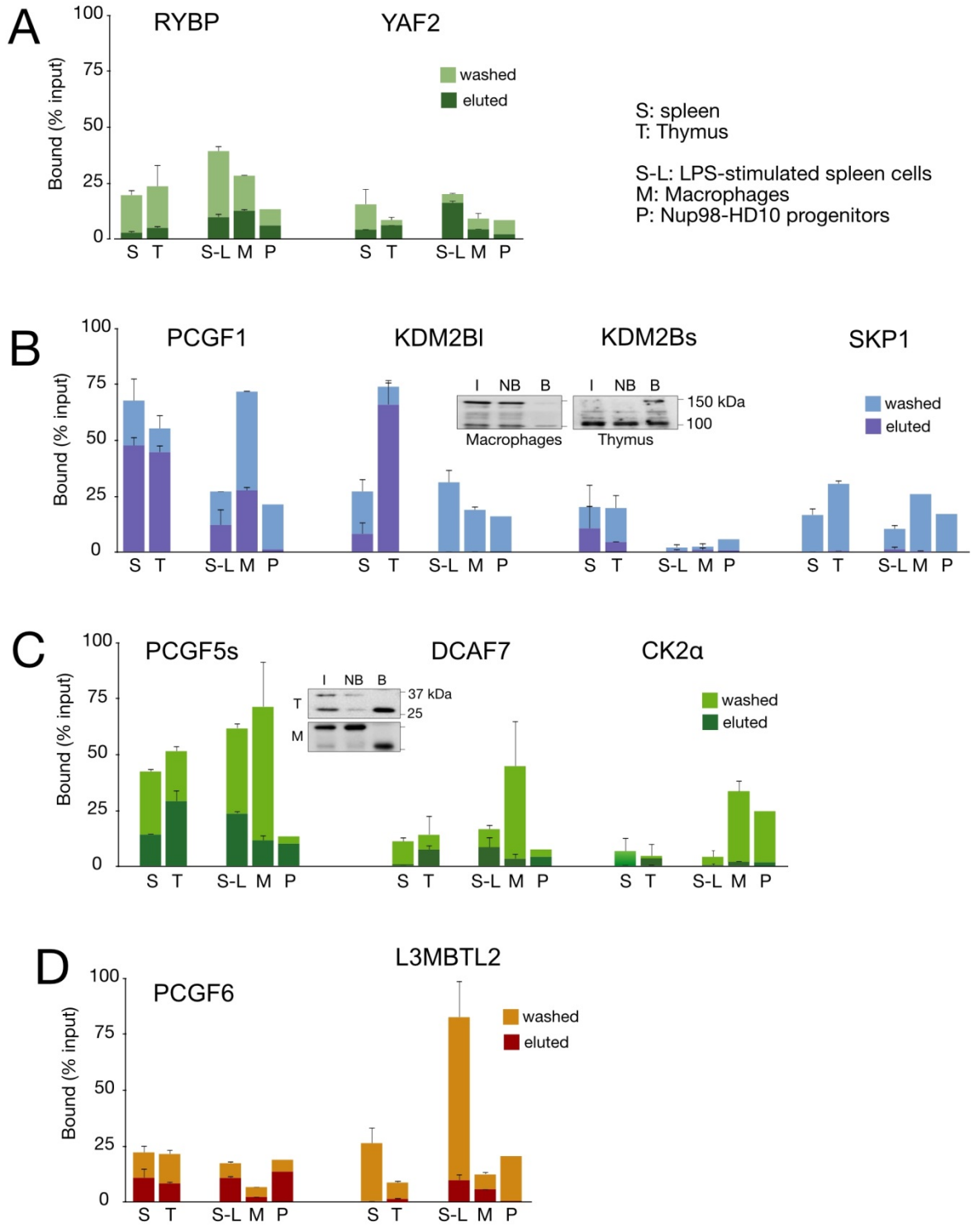

Figure R21. Non-canonical PRC1 subunits present in RING1B complexes in the indicated hematopoietic cell types plotted as in Fig. R20. The inset in B shows differential binding of the full length or truncated KDM2B forms, depending on cell type, which is why the are shown separately. Note that bars indicate fraction of the total present and therefore, despite the larger proportion of full-length form bound, its contribution to total KDM2B is still below that of the, more abundant truncated form. Total binding is separated, as above, in washed and eluted fractions.

The presence of non-canonical PRC1 subunits as part of stably bound RING1B complexes was, in general low. In particular, the presence of RYBP or YAF2, two direct interactors of RING1B was was relatively minor (Fig. R21A), with less than a third of the protein available associated to RING1B. It was as if most PRC1 complexes in these hematopoietic cell types were to be made of canonical species. RING1B-PRC1.6 complexes, as assessed by the presence of PCGF6 and L3MBTL2 (Fig. R21D) were poorly represented. Other direct interactors such as PCGF1 and PCGF5, in contrast, were relatively enriched in RING1B complexes (Fig. R21B, C) but only in primary cells from spleen and thymus. It was unexpected to find the different affinities of KDM2B forms for PRC1 complexes in thymus cells, where despite the low concentration of the full-length form (Fig.R7) most of it was among proteins bound to RING1B (Fig. R21B).

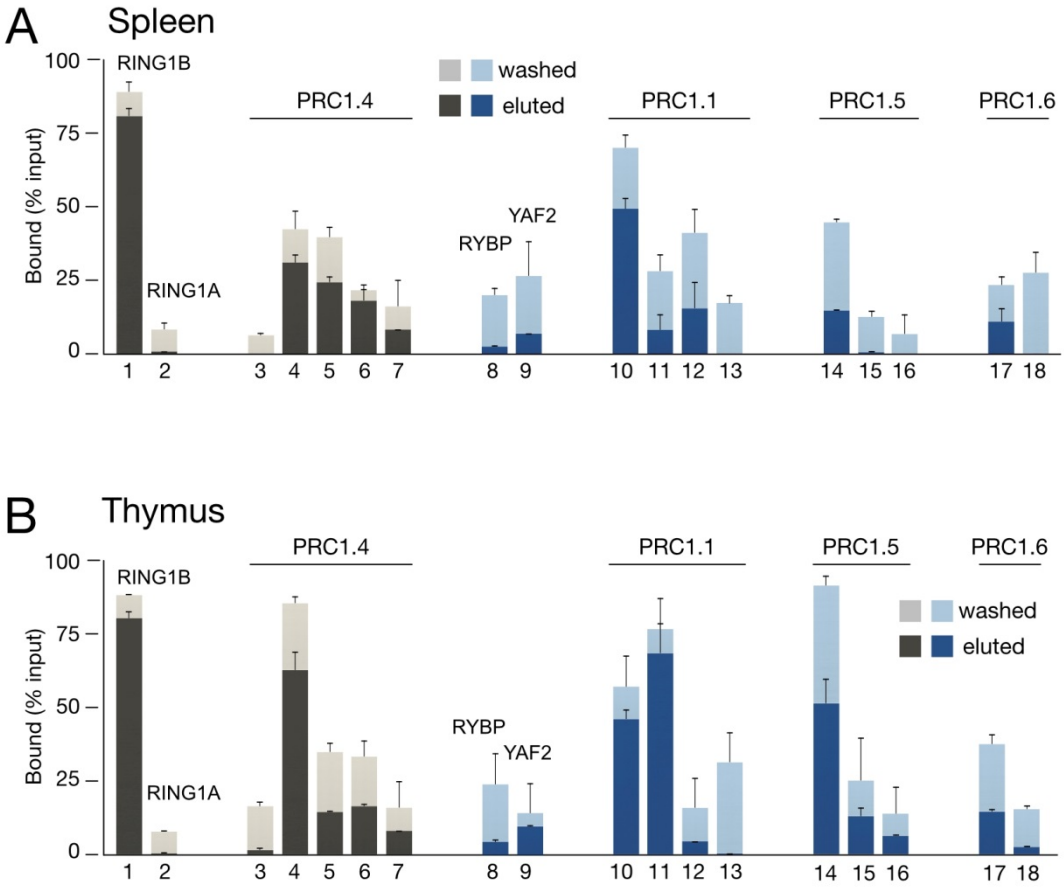

Figure R22. PRC1 subunits bound to RING1B in primary hematopoietic cells. Plots as in Fig. R20. Proteins are 1-RING1B (1), RING1A (2), CBX2 (3), CBX7 (4), CBX8 (5), PCGF4 (6), PHC2 (7), RYBP (8), YAF2 (9), PCGF1 (10), full-length KDM2B (11), truncated-KDM2B (12), SKP1 (13), PCGF5 (14), DCAF7 (15), CKIIa (16), PCGF6 (17), L3MBTL2 (18).

In contrast, in macrophages, where the full-length form is far more abundant, did not associate in an stable manner with the complex(es) (Fig . R21B)

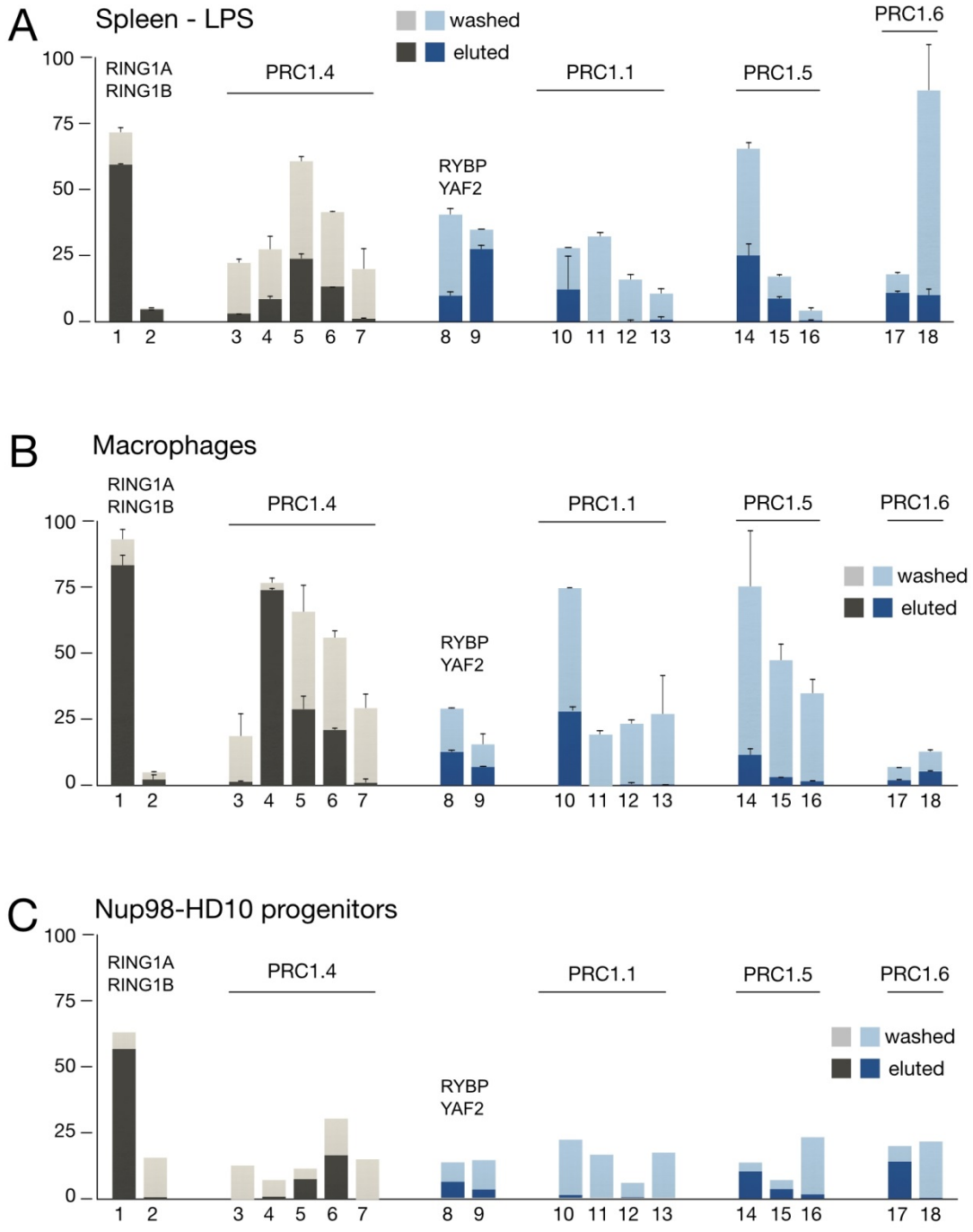

Figure R23. . PRC1 subunits bound to RING1B in primary in expanded hematopoietic cells. Plots as in Fig. R20. Proteins are 1- RING1B (1), RING1A (2), CBX2 (3), CBX7 (4), CBX8 (5), PCGF4 (6), PHC2 (7), RYBP (8), YAF2 (9), PCGF1 (10), full-length KDM2B (11), truncated-KDM2B (12), SKP1 (13), PCGF5 (14), DCAF7 (15), CKIIa (16), PCGF6 (17), L3MBTL2 (18).

The above mentioned trends, that RING1B is present preferentially as part of canonical instead of non-canonical PRC1 complexes, and that PRC1 complexes are more easily captured from extracts from primary cells, can be seen in Figures R22, 23. Another singularity was that

PRC1.1 complexes were hardly present in ex-vivo expanded cells, where only PCGF1, but no KDM2B or SKP1, was found associated to RING1B (Fig. R23). Perhaps an extreme case was that of immortal immature progenitors (induced after Nup98-HD10 expression) were, apart RING1B, binding could be considered to occur mostly for PCGF family members (Fig. R21C). Overall, in many cases the association with RING1B complexes is rather labile and large part of the proteins initially bound, present at the beginning of washes, and are released eventually. Binding of L3MBTL in LPS-stimulated spleen cells (Fig. R23A) or of PCGF1 and PCGF5 in macrophages (Fig. R23B) are good examples.

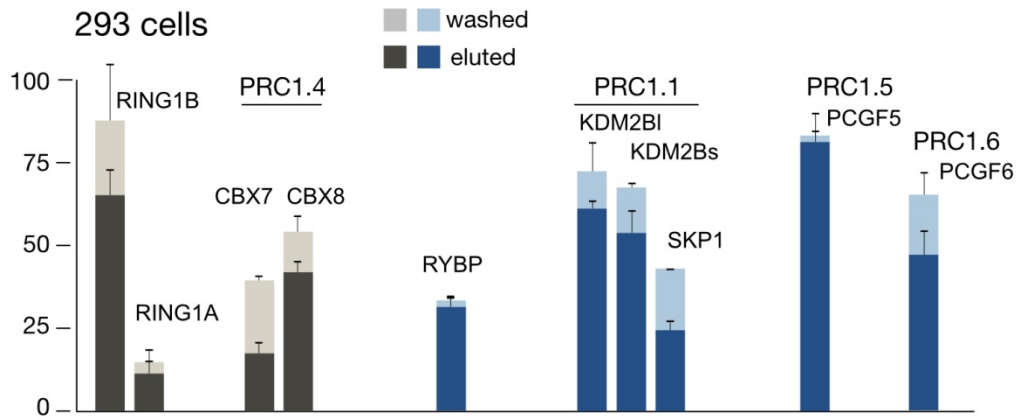

Figure R24. . PRC1 subunits bound to RING1B in a conventional tissue-culture cell lines. The proportion of the total protein for each of the indicated PRC1 subunits associated to RING1B is plotted as the mean value ± SD of two experiments.

Since binding efficiency for many PRC1 subunits was below expectations we thought of a possible contradiction with published evidence about PRC1 complexes. Certainly, much of the reported data are seldom of quantitative nature. Therefore, we asked whether in our hands PRC1 assemblies captured from a "standard" cell type would differ from our data with primary of close-to-primary hematopoietic cell or, on the contrary, it would be that PRC1 complexes might be more dissimilar between cell types than anticipated. Thus, we carried out a quantitative estimation of the content of RING1B complexes in a subset of PRC1 subunits in 293 cells. The data (Fig.R24) showed that binding was, in general, far more efficient than with nuclear extracts of hematopoietic origin, and that the washed fractions were relatively small, indicating a somehow stable association. In particular, the presence of non-canonical subunits in RING1B-assemblies was much more prevalent than that seen with hematopoietic cells. In summary, RING1B-PRC1 complexes are probably highly dynamic

entities whose levels, as well as the stability of the associations of their constituents vary with cell type.

4.3 PRC1 and non-PRC1 RING1B-containing complexes.in thymus

Similarly to our previous attempt at identifying RING1B interactors in MEL cells (Sánchez et al., 2007) and as part of forthcoming analysis of RING1B-bound proteins in hematopoietic cells, we identified interactors contained in thumus cells. The main purpose of the inclusion of these (preliminary) results is to provide an idea of the network of interactions the core component of PRC1 complexes is involved in. Tables I and II display a list of proteins identified from the peptides contained in a pull down experiment as those described above. Spectral counts (a measure of mass), number of different peptides identified and extent of the protein covered by them are indicated. The lists are one of high stringency, in which proteins identified by peptides contained in control beads (material bound from extracts without biotinylated RING1B) were subtracted. Of interest here, a relatively large set of subunits of other chromatin regulators were present among RING1B interactors. Some of them, commonly present in non-PRC1 complexes, were grouped, in table I, with PRC1 subunits on the basis of previous reports (Hauri et al., 2016; Trojer et al., 2011).

It was interesting that many of subunits of chromatin remodelers of the SWI/SNF and NurD families were present almost in their entirety. Subsets of subunits are those in BAF complexes, the subtype of SWI/SNF complex containing ATP-dependent helicase BRG1/SMARCA4. BAF complexes antagonize Polycomb activity (B. G. Wilson et al., 2010) and are involved in the eviction of PRC1 from chromatin (Stanton et al., 2016). The other remodeler whose components were enriched among RING1B interactors was NuRD, a complex with ability to rearrange nucleosomes and deacetylate their histones and has been shown to influence histone H3K27 status (Reynolds et al., 2012). Among DNA binding proteins the presence of Ikaros paralogs (IKZF1, 2 and 3) is probably relevant considering their activity targeting NuRD in lymphoid tissues (Yoshida & Georgopoulos, 2014).

Table I. Polycomb proteins associated to RING1B in thymus

AC	Gene symbol	Protein	UP	SC	COV
Q9CQJ4	Rnf2	E3 ubiquitin-protein ligase RING2	9	88	0,29
O35730-1	Ring1	E3 ubiquitin-protein ligase RING1	2	21	0,11
P25916	Bmi1	Polycomb complex protein BMI-1	2	4	0,08
Q64028-1	Phc1	Polyhomeotic-like protein 1	2	2	0,03
Q9QWH1-1	Phc2	Polyhomeotic-like protein 2	4	4	0,04
Q8CHP6-1	Phc3	Polyhomeotic-like protein 3	4	9	0,06
P30658	Cbx2	Chromobox protein homolog 2	2	7	0,08
O55187-1	Cbx4	E3 SUMO-protein ligase CBX4	6	8	0,11
Q9DBY5	Cbx6	Chromobox protein homolog 6	1	1	0,05
Q8VDS3	Cbx7	Chromobox protein homolog 7	5	9	0,27
Q9QXV1	Cbx8	Chromobox protein homolog 8	11	30	0,35
Q8CCI5	Rybp	RING1 and YY1-binding protein	2	4	0,19
Q99LW6-1	Yaf2	YY1-associated factor 2	1	3	0,13
Q8R023	Pcgf1	Polycomb group RING finger protein 1	4	9	0,15
Q6P1G2-1	Kdm2b	Lysine-specific demethylase 2B	15	27	0,12
Q8CGN4-1	Bcor	BCL-6 corepressor	19	40	0,13
A2AQH4	Bcorl1	BCL-6 corepressor-like protein 1	4	8	0,03
Q9WTX5	Skp1	S-phase kinase-associated protein 1	4	6	0,25
Q3UK78-1	Pcgf5	Polycomb group RING finger protein 5	5	14	0,22
P61963	Dcaf7	DDB1- and CUL4-associated factor 7	5	9	0,13
Q60737	Csnk2a1	Casein kinase II subunit alpha	3	4	0,08
P67871	Csnk2b	Casein kinase II subunit beta	3	4	0,12
Q8R089	Fbrs	Probable fibrosin-1	4	11	0,12
Q6A4J8-1	Usp7	Ubiquitin carboxyl-terminal hydrolase 7	4	7	0,04
Q99NA9	Pcgf6	Polycomb group RING finger protein 6	5	12	0,15
P59178	L3mbtl2	Lethal(3)malignant brain tumor-like protein 2	4	13	0,06
P23198	Cbx3	Chromobox protein homolog 3	3	7	0,14
P61965	Wdr5	WD repeat-containing protein 5	3	5	0,11
A2AWL7-1	Mga	MAX gene-associated protein	21	34	0,09
Q8BLB7-1	L3mbtl3	Lethal(3)malignant brain tumor-like protein 3	2	3	0,03

Ac- accession number, UP- unique peptides, SC-spectral counts, COV-coverage

Highlighted proteins were investigated during this study

Table II. Chosen non-Polycomb proteins associated to RING1B in thymus

AC	Gene symbol	Protein	UP	SC	COV
		CHROMATIN REMODELLERS			
		SWI/SNF			
Q3TKT4-1	Smarca4	Transcription activator BRG1	11	32	0,08
Q91ZW3	Smarca5	SWI/SNF-related matrix-associated actin-dependent regulator of chromatin subfamily A member 5	13	30	0,13
P97496-1	Smarcc1	SWI/SNF complex subunit SMARCC1	8	19	0,08
Q8BSQ9-1	Pbrm1	Protein polybromo-1	9	16	0,06
O54941	Smarce1	SWI/SNF-related matrix-associated actin-dependent regulator of chromatin subfamily E member 1	3	9	0,1
Q99JR8-1	Smarcd2	SWI/SNF-related matrix-associated actin-dependent regulator of chromatin subfamily D member 2	4	8	0,11
A2BH40-1	Arid1a	AT-rich interactive domain-containing protein 1A	5	6	0,04
Q61103	Dpf2	Zinc finger protein ubi-d4	1	1	0,04
		NuRD			
Q6PDQ2	Chd4	Chromodomain-helicase-DNA-binding protein 4	23	57	0,13
Q9R190	Mta2	Metastasis-associated protein MTA2	11	46	0,18
Q60972	Rbbp4	Histone-binding protein RBBP4	9	35	0,21
O09106	Hdac1	Histone deacetylase 1	5	35	0,12
Q62318-1	Trim28	Transcription intermediary factor 1-beta	7	34	0,11
Q60973	Rbbp7	Histone-binding protein RBBP7	8	26	0,19
Q8VHR5-1	Gatad2b	Transcriptional repressor p66-beta	10	24	0,22
P70288	Hdac2	Histone deacetylase 2	4	24	0,12
Q8K4B0	Mta1	Metastasis-associated protein MTA1	7	16	0,11
Q8CHY6	Gatad2a	Transcriptional repressor p66 alpha	6	10	0,14
Q924K8-1	Mta3	Metastasis-associated protein MTA3	5	9	0,09
Q09XV5-1	Chd8	Chromodomain-helicase-DNA-binding protein 8	2	2	0,01
Q03267-1	Ikzf1	DNA-binding protein Ikaros	12	44	0,25
O08900	Ikzf3	Zinc finger protein Aiolos	7	33	0,16
Q920B9	Supt16h	FACT complex subunit SPT16	7	18	0,08
P13864-1	Dnmt1	DNA (cytosine-5)-methyltransferase 1	9	17	0,06
P81183-1	Ikzf2	Zinc finger protein Helios	3	9	0,05
O88379	Baz1a	Bromodomain adjacent to zinc finger domain protein 1A	3	3	0,03
Q60520-1	Sin3a	Paired amphipathic helix protein Sin3a	1	1	0,01
		HISTONE MODIFYING COMPLEXES			
Q80TJ7-1	Phf8	Histone lysine demethylase PHF8	3	9	0,04
Q8VDF2-1	Uhrf1	E3 ubiquitin-protein ligase UHRF1	4	6	0,05
Q8K224	Nat10	N-acetyltransferase 10	4	6	0,05
B2RWS6	Ep300	Histone acetyltransferase p300	3	6	0,02
Q9WTU0	Phf2	Lysine-specific demethylase PHF2	3	4	0,04
Q5DW34-1	Ehmt1	Histone-lysine N-methyltransferase EHMT1	2	3	0,02
Q9Z148-2	Ehmt2	Histone-lysine N-methyltransferase EHMT2	1	1	0,01
Q8CFE3	Rcor1	REST corepressor 1	3	6	0,08
Q8BX09-1	Rbbp5	Retinoblastoma-binding protein 5	1	3	0,02
P55200-1	Kmt2a	Histone-lysine N-methyltransferase 2A	1	2	0
Q9Z2D6-1	Mecp2	Methyl-CpG-binding protein 2	1	1	0,04
		TRANSCRIPTIONAL REGULATORS			
Q61191	Hcfc1	Host cell factor 1	17	49	0,12
Q99PV8-1	Bcl11b	B-cell lymphoma/leukemia 11B	12	48	0,2
Q80YR5	Safb2	Scaffold attachment factor B2	10	25	0,14
D3YXK2	Safb	Scaffold attachment factor B1	11	22	0,14

P53564-1	Cux1	Homeobox protein cut-like 1	9	20	0,09
Q00899	Yy1	Transcriptional repressor protein YY1	6	18	0,13
Q8CH25-1	Sltm	SAFB-like transcription modulator	5	13	0,06
Q03347-1	Runx1	Runt-related transcription factor 1	6	10	0,17
Q08024-2	Cbfb	Core-binding factor subunit beta	3	10	0,18
Q60974-1	Ncor1	Nuclear receptor corepressor 1	2	4	0,01
P42225	Stat1	Signal transducer and activator of transcription 1	3	3	0,05
Q8K0H5	Taf10	Transcription initiation factor TFIID subunit 10	1	2	0,11
P70353	Nfyc	Nuclear transcription factor Y subunit gamma	2	2	0,06
Q61164	Ctcf	Transcriptional repressor CTCF	1	1	0,01
		DNA REPLICATION AND REPAIR			
P11103-1	Parp1	Poly [ADP-ribose] polymerase 1	8	28	0,1
P54276	Msh6	DNA mismatch repair protein Msh6	7	16	0,06
Q99J62	Rfc4	Replication factor C subunit 4	3	11	0,08
Q60596	Xrcc1	DNA repair protein XRCC1	3	8	0,07
P43247	Msh2	DNA mismatch repair protein Msh2	4	8	0,06
P35601-1	Rfc1	Replication factor C subunit 1	3	8	0,03
P97386-1	Lig3	DNA ligase 3	4	7	0,05
P23475	Xrcc6	X-ray repair cross-complementing protein 6	3	4	0,08
P17918	Pcna	Proliferating cell nuclear antigen	1	2	0,05

Ac- accession number, UP- unique peptides, SC-spectral counts, COV-coverage

5. PRC1 alterations in hematopoietic cells deficient in Ring1A, B-gene products

The relative amounts of PRC1 complexes and their composition could be affected by alterations in the concentration of any of their constituent subunits. An example, in ES cells, is the negative regulation of CBX products by CBX7, thus becoming the functionally predominant PRC1 CBX component in these cells. We have addressed the possibility that RING1B or RING1A participate in the stability/composition of PRC1 complexes by quantitative analysis of the protein levels of a number of PRC1 subunits in primary hematopoietic cells lacking either of these homologs.

5.1 RING1B-deficient hematopoietic cells

We took tissues from mice carrying a floxed allele of the Ring1B gene and a Mx-Cre transgene whose expression can be induced in the response to poly (I:C). Total cell extracts were prepared from bone marrow cells, including populations of Lin-, CD19+ and Ter119+ progenitors/precursors and neutrophils, and also from spleen and thymus cell suspensions. We analyzed the same set of PRC1 proteins shown in Fig. R1.

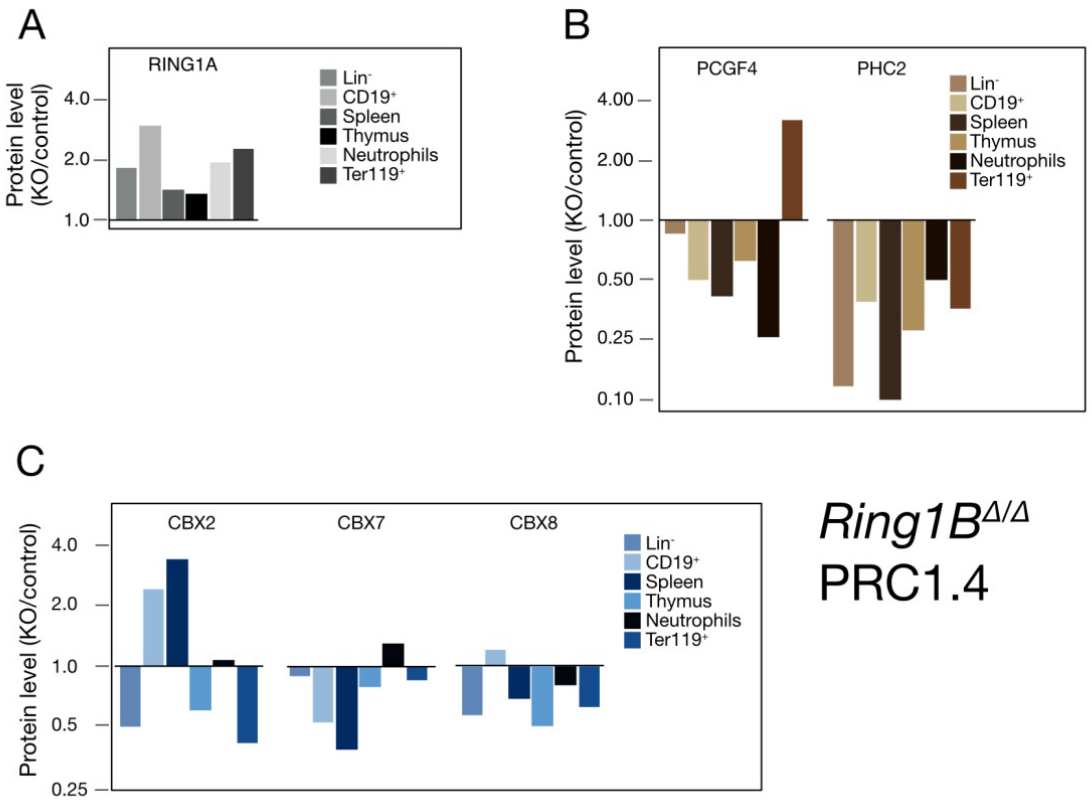

Figure R25. Levels of canonical PRC1 subunits in primary primary hematopoietic cells depleted of RING1B. Bars represent differences from values in control cells in two experiments. A log scale was chosen to better plot the dual (up regulation, down regulation).

Levels of canonical PRC1 subunits in RING1B-deficient cells showed alterations of opposed signs, compared to those in control (tissues from mice without MxCre transgene): up regulation was seen for RING1A, in all cell types, for PCGF4 in erythroid precursors and for CBX2 in primitive progenitors and B-cell precursors (Fig. R25). On the other hand most mutant cell types showed decreased levels of PCGF4, PHC2 and CBX subunits. PHC2 levels were particularly depressed in Lin- progenitors and in splenocytes (Fig. R25B). The magnitudes of these alterations were, in some cases, striking. RING1A levels augmented by 2-3 fold and even more, in erythroid progenitors those of PCGF4 or, in B-cells, those of CBX2. However, the prevalent consequence of RING1B inactivation was a reduction in levels of canonical PRC1 subunits, sometimes by up to 1/4 - 1/8 (PCGF4, PHC2) and to a less degree for CBX subunits. It would appear that some of these changes would imply functional consequences, for instance in Lin- progenitors or spleen cells, which normally expressed the highest PHC2 levels (Fig. R5) and where they are more deeply depressed in the absence of RING1B.

Non-canonical PRC1 subunits were less affected, with exceptions. The magnitudes of alterations were within the half - double range of values in wild type cells. Among the exceptions were neutrophils, where SKP1 and CK2a showed huge opposing changes (Fig. R26B, C). An interpretation of these variations, within a PRC1 context, is very difficult because these are subunits that also belong into other protein complexes. Opposing changes were also observed in the levels of the short form of KDM2B (the full-length variant, as in wild type cells, remained in very low levels) in differentiated cells. KDM2B was augmented by 4-fold in neutrophils and erythroid precursors and decreased, to the same extent, in spleen cells (Fig. R26B).

We have not attempted to investigate the contributions of the possible mechanisms (transcriptional, translational/miRNA or of protein homeostasis) that determine protein levels. Nevertheless, a major conclusion is that the secondary consequences of gene inactivation of RING1B may confound phenotypic analysis.

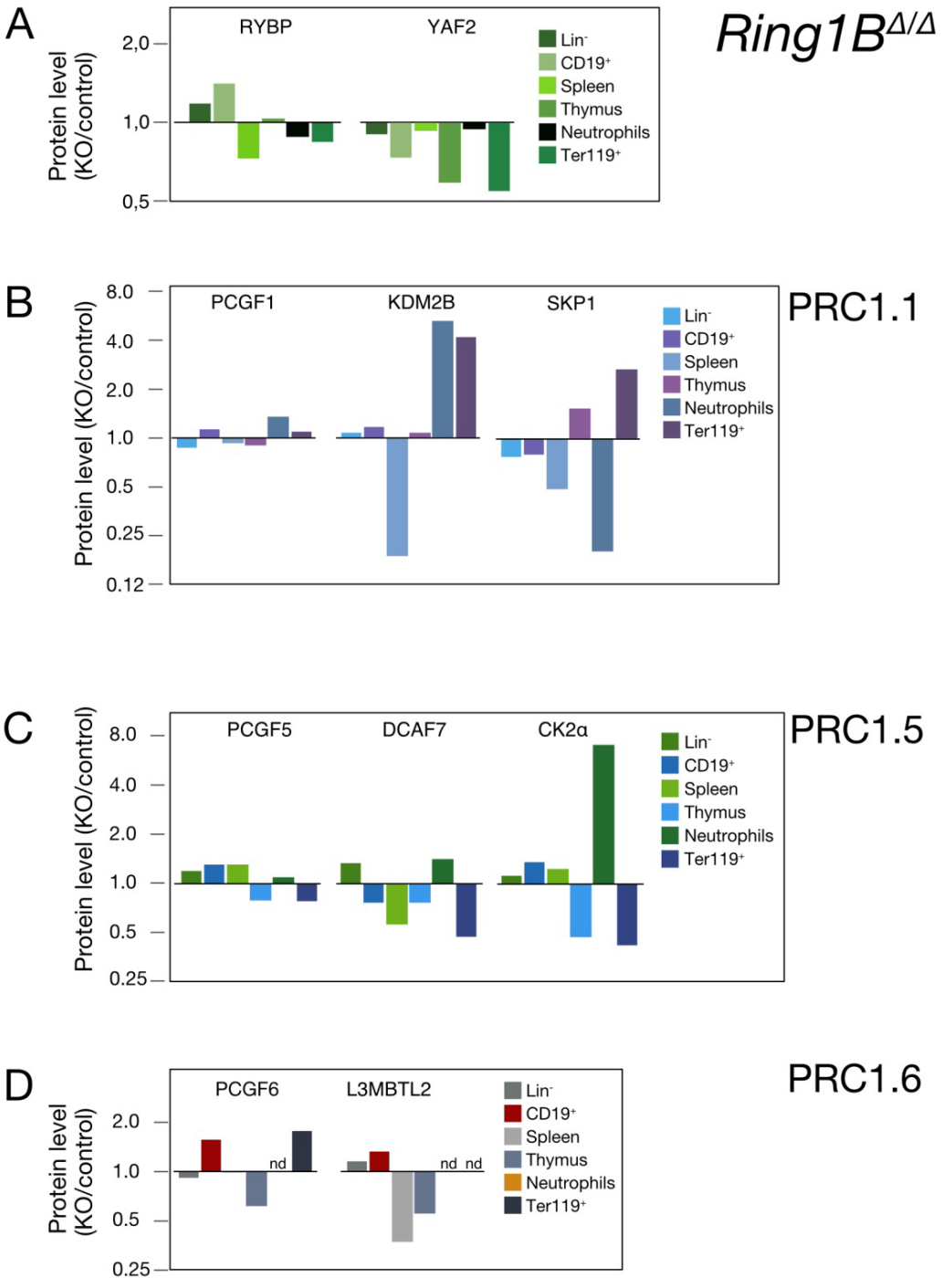

Figure R26. Levels of non-canonical PRC1 subunit in primary hematopoietic cells depleted of RING1B. Data plotted as in Fig. R25

5.2 RING1A-deficient hematopoietic cells

Quantiation of PRC1 subunits in hematopoeitic Ring1A-/- cells also showed some differences with wild type mice (Figs R27 and 28). However, the magnitud of the alterations was modest compared to those seen in RING1B-deficient cells. When the levels increased, the did by a <2 factor. In a few cases, levels were depressed to less than half of those in controls (YAF2 in

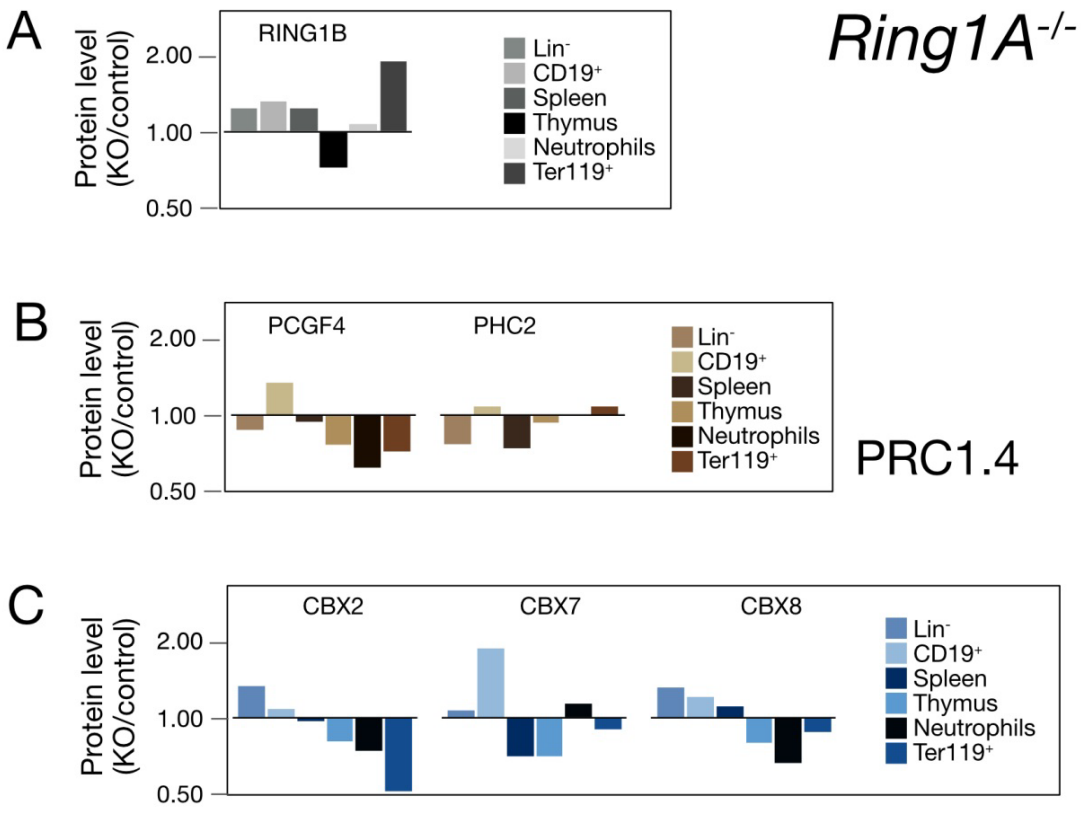

Figure R27. Levels of canonical PRC1 subunits in primary hematopoietic cells depleted of RING1A. Data plotted as in Fig. R25.

thymus, KDM2B in thymus cells or PCGF6 in Lin- progenitors). RING1B levels rose in most cell types, except in thymus, where they even decreased (Fig. R27A) suggesting a complex interrelationship between RING1A and RING1B paralogs. Most surprising was that levels of canonical PRC1 subunits were almost unchanged with the exception of CBX7, which was increased in CD19+ cells, or CBX2, whose expression was reduced in erythroid precursors. Together with data of RING1B-deficient cells, the results showed a larger influence of RING1B in sustaining the PRC1 system, even if these alterations are not dramatically reflected in the global levels of H2AUb (Fig. R29): while RING1B deficiency impacted the extent of H2AUb

more clearly than the absence of RING1A (relative values between 0.4 - 0.76 for RING1B-deficiente cells, compared with 0.75 - 0.99 if RING1A was missing).

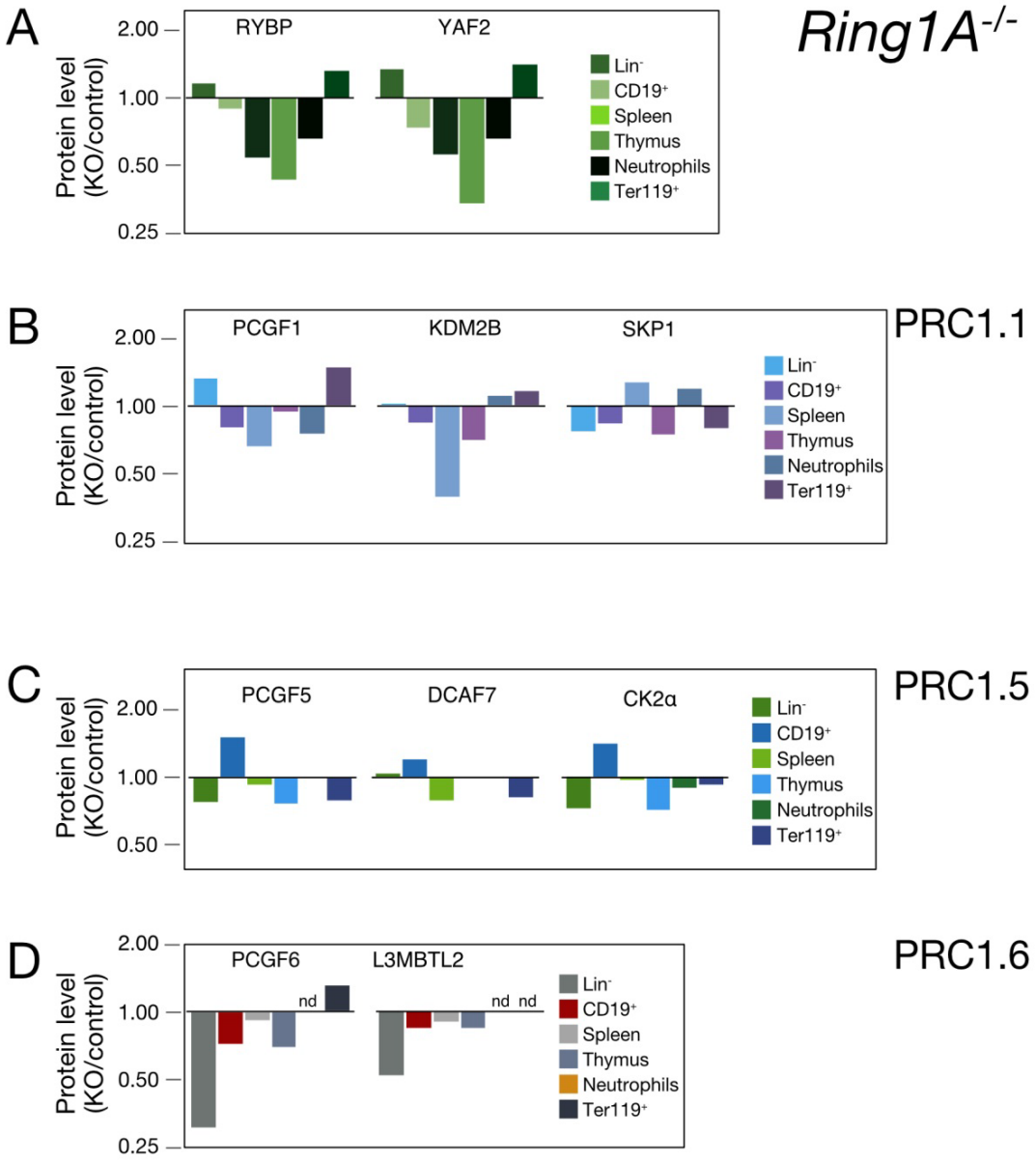

Figure R28. Levels of non-canonical PRC1 subunits in primary primary hematopoietic cells depleted of RING1A. Data plotted as in Fig. R25

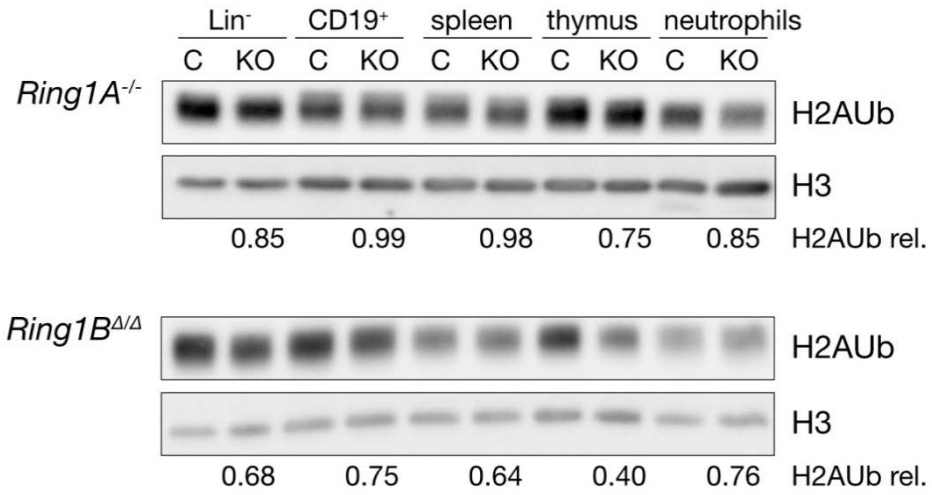

Figure R29. Global H2AUb levels in primary hematopoietic cells depleted of either RING1A or RING1B. Data are mean values of the differences between mutant and control cells, after normalization by histone H3 content. SD values ranged from 0.1 to 0.17.

5.3 Hematopoietic cells double deficient in RING1A and RING1B

An attempt to generate a hematopoietic compartment lacking both RING1 paralogs was done using Ring1A-/- mice that also carry a floxed Ring1B allele and the MxCre transgender. Induction of Ring1B inactivation after Cre-mediated recombination, however, leads to an aplastic scenario whose bone marrow becomes devoid of hematopoietic cells (Vidal & Starowicz, 2017). Then we tried to generate cells depleted of RING1A and RING1B by ectopic expression of Nup98-HD10 in Ring1A-/-, Ring1Bfl/fl, Cre Lin- progenitors (Fig. R30A).

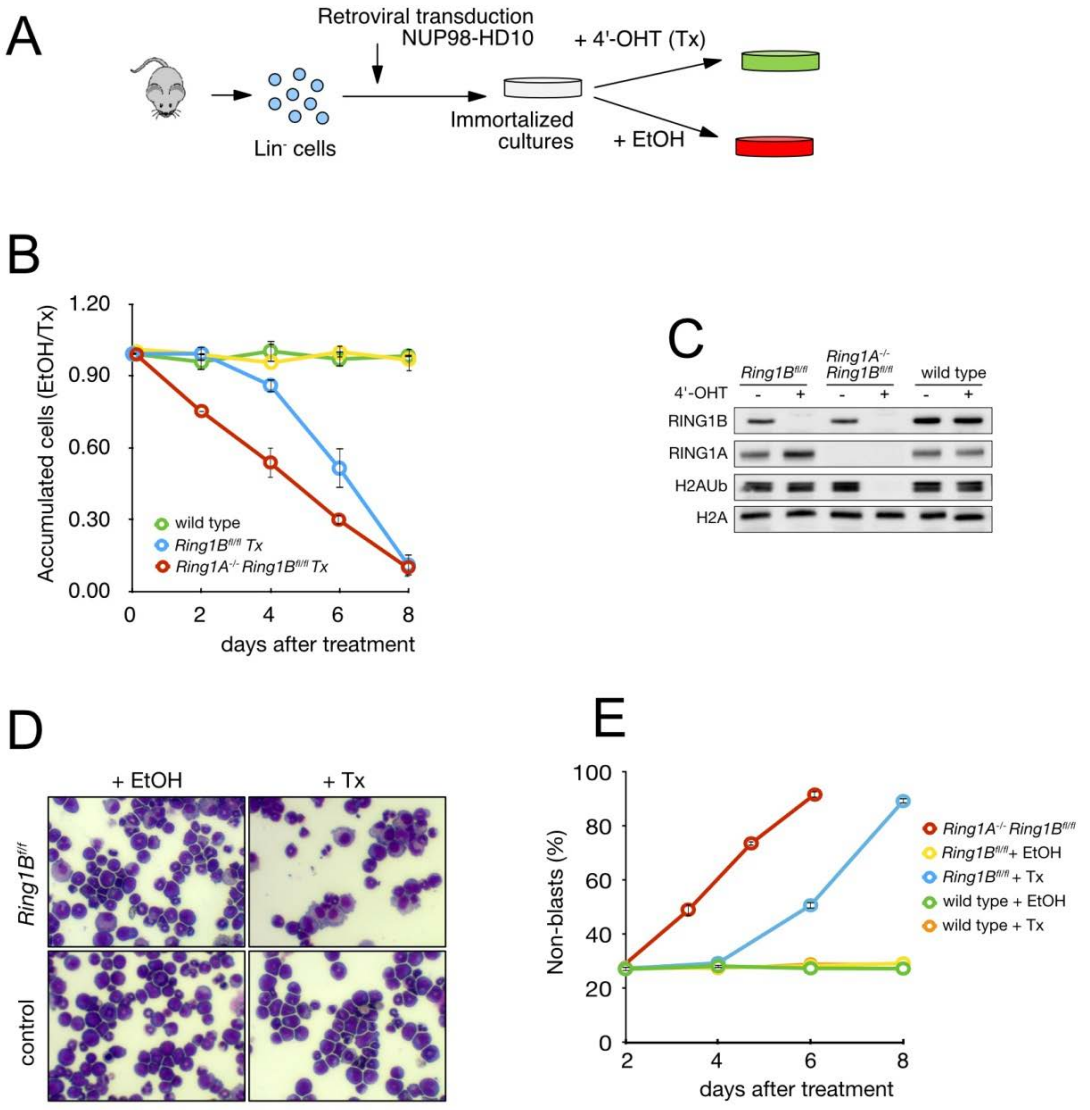

Figure R30. RING1A- and RING1A, RING1B-depleted progenitor cells. Schematic representation of the conditional inactivation of RING1B in Nup98-HD10 immortalized primitive progenitors. (B) Cell accumulation in cultures subject to the indicated treatments.(C) Representative western blot analysis of RING1A and RING1B levels in cells of the indicated genotypes. The effects of RING1 depletion on H2AUb is also shown. Deletion of RING1A and RING1B leads to loss of H2Ak119ub. (D) MGG staining of cytospin preparations from the indicated cultures and treatments. Round, compact, regular nuclei cells correspond to undifferentiated blasts. Flattened, with evident cytoplasm and irregular nuclei, characteristic of differentiated myeloid cell types. (E) Development of differentiation, assessed by MGG staining, over time after treatment in cultures of the indicated genotypes. Tx/4'-OHT, 4'hydroxytamoxifen; EtOH, ethanol (vehicle , used as control treatment). Data in B and C, are mean values ± SD of three experiments.

Once immortal, cultures were given 4'-OHT, to inactivate Ring1B but the consequence of the combined depletion of RING1A and RING1B was senescence and cell death. The evolution of parallel cultures, after transient treatment with 4'-OHT or vehicle (EtOH), showed a steep decline in the rate of cell accumulation, accompanied by quick differentiation, assessed morphologically after MGG staining, in double mutant cultures (Fig. R30D,E). In fact, this occurred just the same even if only RING1B is inactivated (Fig. R30E) although the effects appear slightly delayed compared with the double mutant cells (Fig. R30B,E). In vivo, RING1A (or RING1B) can compensate for the absence of the other paralog (Vidal & Starowicz, 2017) but it appears that the requirements imposed by the immortalizing influence of Nup98-HD10 set a scenario of non-redundancy in which RING1A cannot substitute for RING1B.

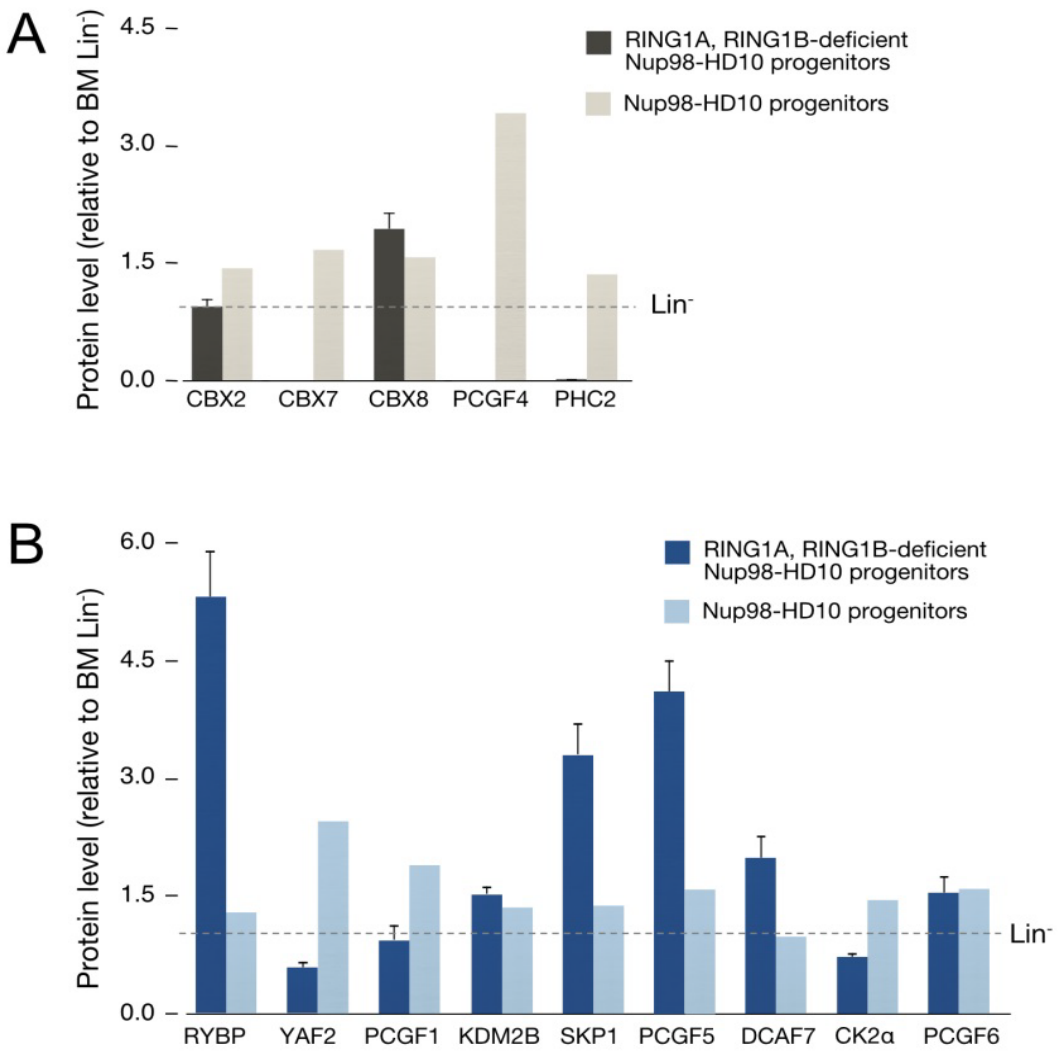

Figure R31. Compared levels of PRC1 subunits in immortal progenitors expressing/lacking RING1A and RING1B. Values are mean ± SD of data normalized to those in bone marrow Lin- cells

During these attempts, we found that, even though at very low frequency, sometime few cells survived and could be expanded in vitro. One of these cultures was then used to quantitate levels of PRC1 subunits and also to investigate whether they associate in complexes in the absence of both RING1 proteins.

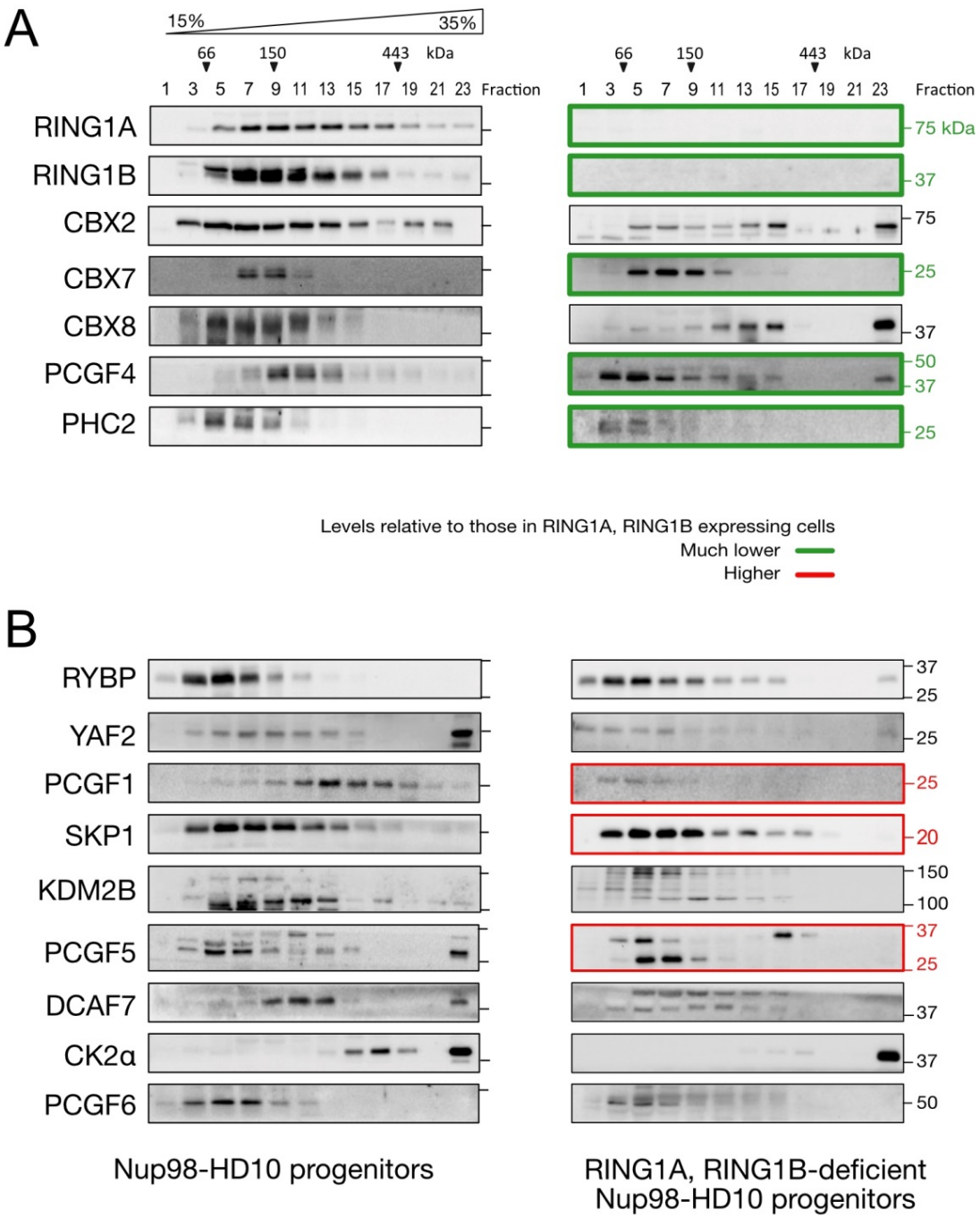

Figure R32. Representative western blots showing the distribution glycerol gradients of PRC1 subunits from RING1A and RING1B-depleted progenitors (right). As a comparison, the distribution of closely related cell type containing both RING1 proteins is included (left). PRC1 subunits have been split in canonical (A) and non-canonical (B) sets.

Figure R32 show levels of PRC1 subunits in Nup98-HD10 immortal progenitors with and without RING1A and RING1B, referred to the levels of these subunits in bone marrow Lin- cells. The results showed that much of PRC1 canonical components were almost gone when the cells lacked RING1 proteins (Fig. R31A). CBX7, PCG4 and PHC2 could be detected only at very low levels. CBX2 and CBX8 levels, perhaps due to their presence in other molecular assemblies, showed little changes. Non-canonical PRC1 subunits, on the contrary not only were little affected but in some cases accumulated at very high levels (Fig. R31B).

In particular, a 5-fold excess of RYBP, compared to Lin- cells that contained RING1A and RING1B, whether from bone marrow of immortalised after Nup98-HD10 expression. YAF2 levels instead were hardly changed. Whether the increase in RYBP, or in SKP1 and PCGF5, reflects transcriptional changes or perturbed proteostasis was not investigated. Whether PRC1 subunits in cells defective in RING1A and RING1B assemble in complexes was examined using migration in glycerol gradients. The data, Fig. R32, have to be examined carefully because the images display no quantitative information. As indicated above, canonical subunits CBX7, PCGF4 and PHC2 were present at very low levels. However, the little of them is present as part of assemblies of unknown nature rather than as free proteins. Subunits normally found in non-canonical complexes also associate to other proteins, except parts of RYBP and YAF2 (Fig R32B). The unavailability of RING1A or RING1B, however, seemed to alter the nature of some complexes as indicated by PCGF1, which been present at levels higher than in cells with RING1 proteins migrates, in mutant cells, as part of smaller assemblies.

Together, the data suggest that, regardless of their E3 ligase activity, RING1A and RING1B play roles stabilizing canonical PRC1 subunits and also as framework subunits within PRC1 complexes.

Discussion

DISCUSSION

In this work we expand the current understanding of interactions between PRC1 subunits that could contribute to clarify mechanisms pertaining chromatin structure and transcriptional control.

We find that steady state levels of PRC1 subunits differ greatly among hematopoietic cell and that these variations result from regulatory events uncoupled, at least in part, from transcriptional mechanisms. The evidence we present also describes heterogeneity of assemblies containing PRC1 subunits. Finally, the associations between subunits known to cohabit PRC1 complexes varied with hematopoietic cell types and were found very different from that of conventional tissue culture cell lines.

1. PRC1 assemblies

Our current appreciation of PRC1 complexes is illustrated by the identities of multi protein assemblies isolated from relatively homogeneous populations of immortal cells or "unusual" cell types, such as ES cells (Gao et al., 2012; Kloet et al., 2016; Ogawa et al., 2002; Sánchez et al., 2007; Vandamme et al., 2011). Based on these findings, in vitro constructions from recombinant subunits provides the information that can be trusted best and that allows for the mapping of interacting domains and, when three-dimensional data exist, determine contact sites, etc. We believe that these results represent a good starting point from where to progress in solving the biochemical complexity inherent to PRC1 complexes, but that they should not dominate our thinking until a better understanding of the system is achieved. For instance, the distribution that we see of PRC1 subunits throughout glycerol gradients indicates that while the accepted structures are probably present in most cell types other, uncharacterized assemblies do exist. An implication of this observation, for example, is that the interpretation of maps with chromatin binding sites for PRC1 subunits becomes difficult. This is illustrated with ChIP data for RING1B in ES cells: along regions with a high density of bound RING1B there were plenty of other regions with much lower occupancy, and the responses to RING1B depletion altered differentially both types of genomic sites (Blackledge et al., 2014). Likewise, ChIP experiments on mesodermal cells derived from mesoderm precursor cells (MES) showed patterns of PRC1 subunits overlapping only partially which were difficult to correlate, beyond a global analysis, with transcriptional activity (Morey et al., 2015)

Some of the complexes predicted from glycerol gradients appear to be made out of interactions not foreseen from the ongoing paradigm. Among the best examples we have seen: large sized complexes, in macrophages, contain PCGF4 but not its direct interaction PHC2 (Gray et al., 2016) and conversely, high molecular assemblies that contain PHC2 count with minor contribution of PCGF4 in MllAf9-transformed progenitors. It is tempting to invoke cell type-specific post-translational modifications that promote/prevent interactions between subunits known to contact each other. In the same line, we have no explanation for the observation that RING1B locates to very large species in some (quiescent and LPS-stimulated spleen cells, macrophages) but not in other (thymocytes, or immortal progenitors). Furthermore, while the presence of RYBP or YAF2 in the complexes is, but a few exceptions, rather homogeneous that of CBX proteins is amazingly diverse. See CBX7: whereas most of it, in macrophages, appears as part of very large complexes, in thymus cells or immortal progenitors appears as constituent of far smaller complexes. We are aware of the caveat that represents not being able to compare molarities for the distinct subunits. We can only achieve an approximation to the proportion of each of the subunits forming part of one or another complex and whether the distributions parallels, qualitatively, that of other subunits. However, for the indicated cases, the segregation of subunits are so extreme that they would appear to support safely the conclusion of cell type-specific assemblies (Klauke et al., 2013; Morey et al., 2012). The results then, are probably manifestations of the, for the most part, unattended aspect of how PRC1 complexes are build up.

The results also show that while both RING1A and RING1B participate of a variety of complexes, and that despite their close structural relatedness these are probably separate entities. It is not only the differences in migration, but also that when pulling down biotinylated-RING1B the amount of RING1A present is just a minor part of all RING1A present. Previous evidence, by us (Sánchez et al., 2007) and other groups (Gao et al., 2012; Vandamme et al., 2011) reported the concurrent presence of RING1A and RING1B in the same complex(es). It is quite possible that a lack of quantitative approach may have contributed to a conclusion of cohabitation. Alternatively, the discrepancy may be cell type-related. However, at least in hematopoietic cells, the observation poses the assemblies would look like, particularly because of (limited) evidence we report supporting question of how RING1A

lack of redundancy between the two paralogs (van den Boom et al., 2013). For example, the inability of RING1A to prevent massive differentiation and promote survival of immortal, primitive progenitors that express Nup98-HD10. Obviously, the uncertainty of the existence of uncharacterized, different from known PRC1 complexes leaves too many unknown variables when proposing non-overlapping activities for RING1A or RING1B-containing complexes.

A very similar situation is that of RYBP and YAF2 paralogs, the subunits that are found in all non-canonical types of PRC1 complexes. Their levels are clearly regulated in distinct fashion and the complexes in which these subunits are found differ too, so that very high molecular weight forms containing only YAF2.

2. PRC1 levels

The large differences in PRC1 protein levels among hematopoietic cell types beg the question of how they might impact PRC1 function. Beyond the general observation that, in primary cells, levels of PRC1 subunits decreased to a different extent compared to those in primitive progenitors contained in the Lin- population, no clear pattern could be established. The exception, for canonical subunits, was the population of B-cell precursors (CD19+ cells). In particular, it was unexpected to determine the magnitude of the fall in RING1A and RING1B levels with differentiation. The lowest levels of canonical subunits in neutrophils may not need of an interpretation considering their short lifespan but only if PRC1 function is considered under the usual perspective of "memory maintenance". Indeed, most functions in differentiated cell types, unveiled through loss-of-function mutations, are associated to longer lived, lymphoid cells (Beguelin et al., 2016; Ikawa et al., 2016). A switch of CBX subunits, from CBX7 to CBX8 has been shown in primitive hematopoietic progenitors (Klauke et al., 2013) so that CBX7 expression in the most undifferentiated type is silenced to turn on that of its paralog CBX8. The process parallels that previously shown in ES cells and its differentiated descendents (Morey et al., 2012). Also, during the progress of this thesis, a systematic comparison between the contents of PcG proteins in ES cells and neural progenitors shows that the differences were reflected in the nature of the complexes formed (Kloet et al., 2016). Here, is worth insisting in that the differences in content reported refer

only to individual subunits and that quantitatively are independent of each other, due to limitations in the methodology used.

Looking at the expression of mRNAs encoding these subunits (Fig. D1) it is plainly evident the lack of correlation with protein levels. The comparison shown in Fig. D1 includes only primary cells since we have no data for immortalized progenitors (de Graaf et al., 2016). As it has been mentioned above, protein levels, whether of canonical or non-canonical PRC1 subunits are lower in every cell type tested when compared with those in primitive, Lin- progenitors. And yet, mRNA levels in the two groups of progenitors that make that pool are not consistently higher than those measured in more differentiated cell types which, in contrast contain much reduced levels of protein. Taking more differentiated cell types the conclusion is similar even though in some cases the correlation between mRNA and protein levels may hold, at least in part.

Whichever regulatory pathway is involved we think it is affected by the proliferative status of the cell. Our comparison of spleen cells between the quiescent population and that of cells taken into proliferation by LPS, however, is affected by the very different conditions the cells are: in the first case they were simply taken from the mouse whereas, in the second, the cells had grown in enriched media under non-physiological dosages of oxygen. The latter conditions are bound to altermetabolic/energetic rates. However, the comparison of immortal progenitors growing in the same rich medium but differing extremely in their proliferative rates also sustains the conclusion that, on average, dividing cells tend to be equipped with higher levels of PRC1 subunits. Of note, among the primary cells studied, even if not actively dividing, the Lin- population enriched in PRC1 subunits contains the larger proportion of cells undergoing proliferation.

Lastly, it was surprising the realization of how the content of PRC1 subunits was altered by the depletion of RING1B, and how the deficiency in RING1A, instead, turned out to produce very mild effects. Thus, although the levels of most subunits in RING1B-deficient cells decreased/increased by half/double compared to control cells, in some cases variations were far more extreme with opposing alterations depending on the cell type.

The minor effects seen in RING1A-deficient cells could be argued that is the consequence of adaptations associated to the nature of the mutation: tissues depleted of RING1A throughout development where some adjustment may have taken place to ameliorate negative effects of the mutation.

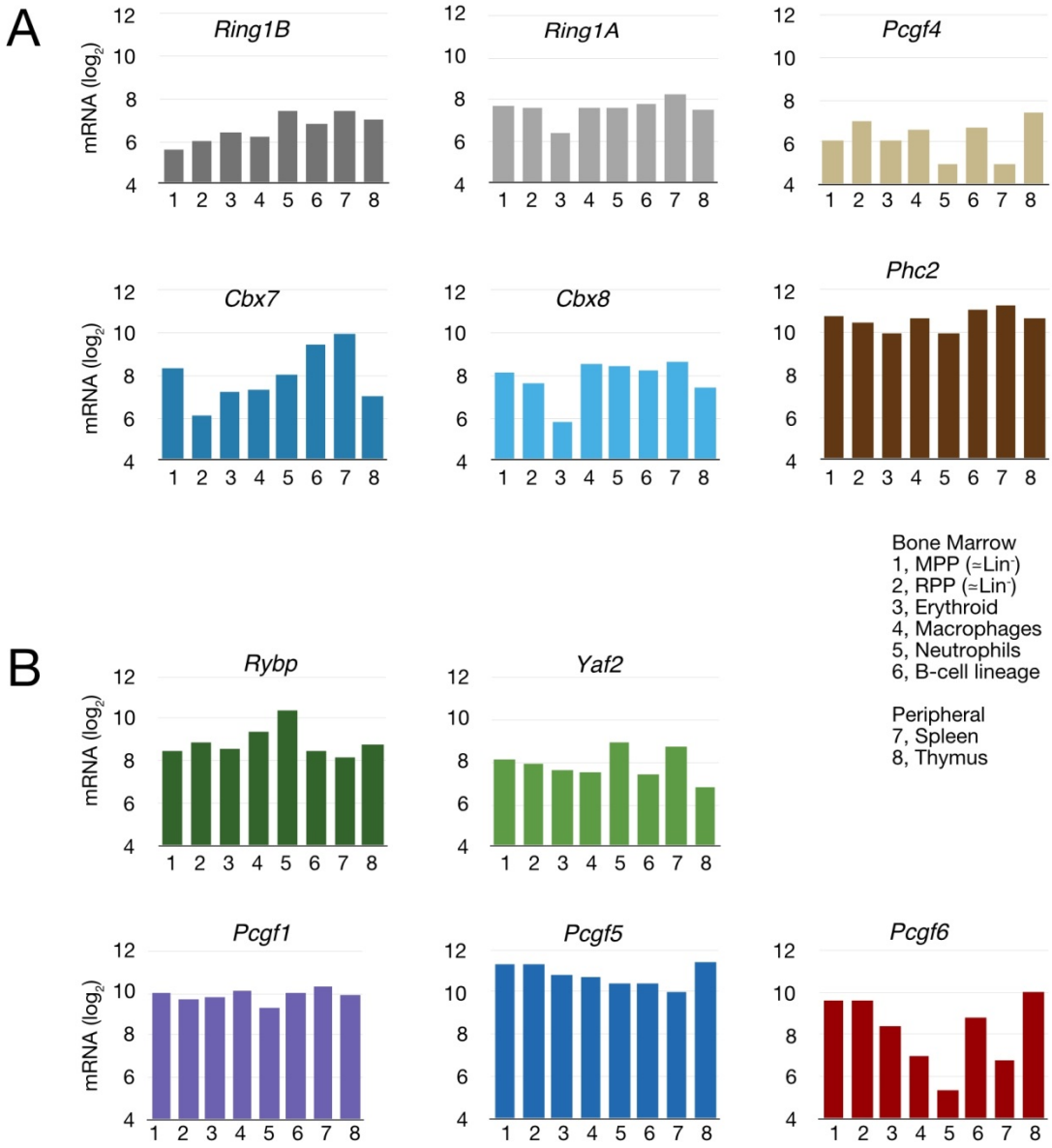

Figure D1. mRNA expression of chosen Polycomb products in hematopoietic cells.(A) RING proteins and canonical subunits. (B) non-canonical subunits. MPP- multipotent progenitor, RPP - restricted potential progenitor

Compared to such a constitutive depletion, our conditional deletion of RING1B may appear more as an acute inactivation. However, our in vivo depletion of RING1B differs from an abrupt inactivation as that seen after 4'-OHT-induced depletion in cultured cells. The reason is that in our protocol, we waited for a substantial period, 8-10 weeks, of time pass after RING1B depletion, in order to ensure complete loss of RING1B in the longer-lived lymphoid compartment. Not having examined mRNA levels encoding PRC1 subunits in mutant cells we cannot elaborate on the nature of the mechanism involved. It is worth noting, however, that

whereas RING1A protein levels are unregulated in all cell types studied, other subunits showed changes towards accumulation or reduction. Therefore, a lineal relationship with transcriptional activity is difficult, more so considering the residence, in differentiated cells, of PRC1 complexes on both, silent and active loci (Frangini et al., 2013; Kloet et al., 2016; Loubiere et al., 2016; Morey et al., 2015; Schaaf et al., 2013).

3. PRC1 complexes as seen in pull-down experiments

In this work we have attempted to identify, among known PRC1 components, possible cell type-selective interactions. PRC1 complexes, with few exceptions, have been identified in isolation procedures that involve affinity steps with one, and often two tags present in one of the members of the complex(es). Following protocols devised long time ago for the extraction of transcription factors, perhaps an epitome of nuclear proteins, antibodies or, as in our case, streptavidin bind the tagged protein and pull down with it the associated subunits. Our choosing of streptavidin was based in the very high affinity for biotin, which allowed for efficient binding of most biotinylated protein. Coupled with a parallel process in which an equivalent extracts but with no tagged protein is used for an estimation of material retained non-specifically during the experiment, it appears, on paper, as an ideal approach. Indeed, 65-95% of RING1B present in extracts (of all, in fact, considering that cells expressed only tagged RING1B) was isolated from the nuclear extracts. Such an efficient purification would facilitate the (quantitative) study of the association of chosen PRC1 subunits. Here a clarification is due and is that our pull down analysis cannot discriminate among biochemical entities since we consider everything eluted from the beads. The identification mentioned above makes use of biochemical fractionation techniques, such as column chromatography (see Ogawa et al., 2002)

As it could be expected, if PRC1 subunits are part of RING1B-free complexes, a more modest fractions of the total amount of these subunits present in each cell was found bound to RING1B. The option that a population of molecules is not in protein complexes can be ruled out from the glycerol gradient data. Given that hardly any RING1A is part of RING1B-complexes, a major source of these assemblies, would be "parallel" PRC1 complexes nucleated around RING1A. This, however, is a prediction remaining to be tested and, certainly, the differences in distribution of RING1A- and RING1B-containing complexes

evidenced in glycerol gradients suggest that PRC1 containing assemblies containing one or another RING1 parlog will be similar only in part. Additional signs of such a dissimilar architectures are the skewed presence of direct interactors in RING1B complexes. Depending on cell type, CBX7 or PCGF1 are subunits pulled down with very high efficiency, as if associated preferentially with RING1B and, therefore, unavailable to be part of RING1A-complexes. This is surely one of the leads to follow, the characterization of PRC1 complexes containing RING1A. This would help clarifying whether the poor presence of RYBP/YAF2 or of CBX2 on RING1B-complexes is a consequence of a preferential engagement with RING1A or, simply that they belong into alternative assemblies. The presence of CBX8 in non PRC1 complexes (Chung et al., 2016) is an example.

An interesting observation in our pull down experiments is the unexpected instability of the associations between PRC1 subunits. As a measure of this, we estimated the proportion of protein initially bound to beads and subsequently lost following washes required to remove non-specifically bound proteins. In other words, they are associated as if they were part of the background binding. Being known RING1B interactors (whether direct or indirect) such an interpretation is ruled out and, instead, we favor the possibility that contacts within the RING1B-complexes are labile. This implies a methodological problem that we will deal with below, but the extent to which binding was more or less robust showed a dependency on the subunit and also with the cell type. In particular, it could not be anticipated that, for instance, so few of the PRC1 subunits and so little of them remained bound to RING1B in pull down experiments with extracts from immortalized Nup98-HD10 progenitors. Note that during the optimization steps, washing conditions were mild, without increased ionic strength! Less extreme situations, however, involved both indirect and also direct RING1B interactions. In LPS-stimulated spleen cells, for instance, it is more CBX7 and CBX8 that are washed away than that remains bound to beads. If a tendency is to be shown, perhaps the subunits thought to form non-canonical complexes interact in a more labile fashion. Moreover, not even the assumption that unstable associations, usually considered to take place among non-core subunits of complexes, are restricted to proteins that bind indirectly RING1B. It is the case of RYBP, which does not withstand washes and a large fraction of it initially bound to the beads is lost with washes. Perhaps the abundant presence of PRC1 subunits in fractions of the glycerol gradients corresponding to the migration of proteins of ≤150 kDa is an indication of

dynamic association-dissociation which, at concentrations much lower of those within the nucleus results in being washed away when removing background binding. The question that arises is whether this dynamic behavior is regulated, as part of a controlled activity of PRC1 (and other) assemblies. Certainly, the "strength" of binding differed among subunits and also varied with cell types. It is not rare that binding of >60% of the protein present in the extract was reduced to a much smaller fraction after washes, eventually. Obviously, even if this determined physiologically it poses a serious concern when attempting quantitative analysis, say using mass-spectroscopy, because much of the bona fide bound protein in vivo is being lost during pull down experiments. Perhaps this would demand a clever usage of cross-linking agents which would complicate analysis in extreme. Currently, such a cross-linking step is usually carried out on protein bound to beads, i.e. after washes, with the intention of detecting contacts protein-protein (Kloet et al., 2016). That would not be a solution because labile associations would be lost prior to cross-linking. That we have not come across a trivial artifact (other labs would have identified already!) is clear from the fact that our analysis with one of the cell types most commonly used, 293 cells, resulted in the expected scenario of robust binding. Extending pull down experiments to other, physiological/primary cell types, should assist in determining the actual behavior of PRC1 complexes in vivo. Together with the observations that just the depletion of a given subunit may lead to secondary effects, the results call for a more patient approach using allelic series as the effective way to study function of PRC1 and that of other complexes that regulate chromatin.

Conclusions (Conclusiones)

CONCLUSIONS

1. Although known PRC1 subunits assemblies were identified in hematopoietic cells, increased complexity was also found, suggesting that accepted notions are but a simplification of physiological settings much harder to accommodate to idealized models.

2. Overall levels of canonical and non-canonical subunits decrease with differentiation of primary hematopoietic cells, in ways apparently uncoupled from transcriptional control. Only ex-vivo expanded and immortal cell types contain levels equal or higher than those of immature progenitors.

3. A large proportion of each PRC1 subunit forms assemblies of size and complexities that vary with cell type. Their identities do not match that of described complexes. Thus, cells of different lineages seem endowed with distinct, only partially overlapping sets of PRC1 assemblies.

4. Core PRC1 subunits RING1A and RING1B, as well as paralogs RYBP and YAF2, common to all non-canonical complexes, associate in very different types of assemblies, with only RING1B and YAF2 present among the largest assemblies.

5. Some of the (uncharacterized) complexes detected do not conform to interactions expected from known PRC1 assemblies.

6. Associations between PRC1 subunits in hematopoietic cells are far more unstable than those in tissue culture cells that lay the foundations of our current understanding of PRC1 assemblies.

7. Association lability affects direct interactors in cell types such as immortal progenitors instability is extreme. Besides possible biological implications, the observation poses a serious challenge to quantitative characterization of PRC1 complexes.

8. Steady-state levels of PRC1 subunits are altered, severely in some cases, in the absence of RING1B, but not of RING1A. This implies that a targeted genetic analysis, i.e. allelic series, may be required to solve uncertainties of the common, global loss-of-function analysis.

CONCLUSIONES

1. Aunque las subunidades conocidas de PRC1 y sus interacciones se han identificado en células hematopoyéticas, nuestros resultados también muestran una complejidad de elementos PRC1 que precisa de modificaciones del modelo idealizado del paradigma actual.

2. Los niveles de subunidades PRC1, en complejos canónicos y no canónicos, disminuyen con la diferenciación hematopoyética. Estos niveles parecen desacoplados, al menos en parte, del control transcripcional. Sólo los cultivos de células expandidas ex-vivo contienen niveles de subunidades PRC1 que igualan o son superiores a los de progenitores.

3. Una parte considerable de cada subunidad PRC1 forma parte de complejos de tamaño y heterogeneidades que varían con el tipo celular; algunos de dichos complejos difieren claramente de los conocidos. Parecería, entonces, que cada tipo celular está dotado de un conjunto de complejos PRC1 compartido sólo parcialmente con otros tipos celulares.

4. Algunos de los complejos que contienen RING1B no contienen RING1A y, análogamente, los que contienen YAF2 no contienen RYBP, de modo que sólo RING1B y YAF2 forman parte de complejos de alto peso molecular.

5. Algunos de los complejos observados no responden a las interacciones esperables de complejo conocidos PRC1.

6. En células hematopoyéticas, las asociaciones entre subunidades PRC1 son mucho más inestables que las descritas en las líneas celulares utilizadas en estudios previos.

7. La inestabilidad de las asociaciones afecta incluso a proteínas que interaccionan directamente. Además de posibles implicaciones biológicas, la observación deberá ser tenida en cuenta para la caracterización cuantitativa de complejos PRC1.

8. Los niveles estacionarios de las subunidades se alteran, severamente en algunos casos, en ausencia de RING1B pero no de RING1A. En consecuencia, un análisis genético dirigido, por

ejemplo, de series alélicas, puede ser necesario para resolver incertidumbres del análisis común de pérdida de función global.

Bibliography

BIBLIOGRAPHY

Alonso, A. G. D. A., Gutiérrez, L., Fritsch, C., Papp, B., Beuchle, D., & Müller, J. (2007). A genetic screen identifies novel polycomb group genes in drosophila. *Genetics*, *176*(4), 2099–2108. http://doi.org/10.1534/genetics.107.075739

Andricovich, J., Kai, Y., Peng, W., Foudi, A., & Tzatsos, A. (2016). Epigenetic regulation of lineage commitment in normal and malignant hematopoiesis by histone demethylase KDM2B, *126*(3), 905–920. http://doi.org/10.1172/JCI84014.

Arai, S., & Miyazaki, T. (2005). Impaired maturation of myeloid progenitors in mice lacking novel Polycomb group protein MBT-1. *The EMBO Journal*, *24*(10), 1863–73. http://doi.org/10.1038/sj.emboj.7600654

Aranda, S., Mas, G., & Croce, L. Di. (2015). Regulation of gene transcription by Polycomb proteins. *Science Advances*, *2*(December), 1–15. http:// doi: 10.1126/sciadv.1500737

Beguelin, W., Teater, M., Gearhart, M. D., Calvo Fernández, M. T., Goldstein, R. L., Cárdenas, M. G., … Melnick, A. M. (2016). EZH2 and BCL6 Cooperate to Assemble CBX8-BCOR Complex to Repress Bivalent Promoters, Mediate Germinal Center Formation and Lymphomagenesis. *Cancer Cell*, *30*(2), 197–213. http://doi.org/10.1016/j.ccell.2016.07.006

Bernstein, E., Duncan, E. M., Masui, O., Gil, J., Heard, E., & Allis, C. D. (2006). Mouse polycomb proteins bind differentially to methylated histone H3 and RNA and are enriched in facultative heterochromatin. *Molecular and Cellular Biology*, *26*(7), 2560–9. http://doi.org/10.1128/MCB.26.7.2560-2569.2006

Blackledge, N. P., Farcas, A. M., Kondo, T., King, H. W., McGouran, J. F., Hanssen, L. L. P., … Klose, R. J. (2014). Variant PRC1 complex-dependent H2A ubiquitylation drives PRC2 recruitment and polycomb domain formation. *Cell*, *157*(6), 1445–1459. http://doi.org/10.1016/j.cell.2014.05.004

Boettiger, A. N., Bintu, B., Moffitt, J. R., Wang, S., Beliveau, B. J., Fudenberg, G., … Zhuang, X. (2016). Super-resolution imaging reveals distinct chromatin folding for different epigenetic states. *Nature*, *529*(7586), 418–22. http://doi.org/10.1038/nature16496

Boxio, R., Bossenmeyer-pourie, C., Steinckwich, N., Dournon, C., & Nu, O. (2004). Mouse bone marrow contains large numbers of functionally competent neutrophils. *Journal of Leukocyte Biology*, *75*(April), 604–611. http://doi.org/10.1189/jlb.0703340.1

Bravo, M., Nicolini, F., Starowicz, K., Barroso, S., Calés, C., Aguilera, A., & Vidal, M. (2015). Polycomb RING1A/RING1B-dependent histone H2A monoubiquitylation at pericentromeric regions promotes S phase progression. *Journal of Cell Science*, jcs.173021–. http://doi.org/10.1242/jcs.173021

Buchwald, G., van der Stoop, P., Weichenrieder, O., Perrakis, A., van Lohuizen, M., & Sixma, T. K. (2006). Structure and E3-ligase activity of the Ring-Ring complex of polycomb proteins Bmi1 and Ring1b. *The EMBO Journal*, *25*(11), 2465–74. http://doi.org/10.1038/sj.emboj.7601144

Cabezas-Wallscheid, N., Klimmeck, D., Hansson, J., Lipka, D. B., Reyes, A., Wang, Q., … Trumpp, A. (2014). Identification of regulatory networks in HSCs and their immediate progeny via integrated proteome, transcriptome, and DNA Methylome analysis. *Cell Stem Cell*, *15*(4), 507–22. http://doi.org/10.1016/j.stem.2014.07.005

Calero-Nieto, F. J., Ng, F. S., Wilson, N. K., Hannah, R., Moignard, V., Leal-Cervantes, A. I., … Göttgens, B. (2014). Key regulators control distinct transcriptional programmes in blood progenitor and mast cells. *The EMBO Journal*, *33*(11), 1212–26. http://doi.org/10.1002/embj.201386825

Calés, C., Pavón, L., Starowicz, K., Pérez, C., Bravo, M., Ikawa, T., … Vidal M. (2016). Role of Polycomb RYBP in Maintaining the B-1-to-B-2 B-Cell Lineage Switch in Adult Hematopoiesis. *Molecullar and Cellular Biology, 36*(6), 900–912. http://doi.org/10.1128/MCB.00869-15.

Calés, C., Román-Trufero, M., Pavón, L., Serrano, I., Melgar, T., Endoh, M., … Vidal, M. (2008). Inactivation of the polycomb group protein Ring1B unveils an antiproliferative role in hematopoietic cell expansion and cooperation with tumorigenesis associated with Ink4a deletion. *Molecular and Cellular Biology*, *28*(3), 1018–1028. http://doi.org/10.1128/MCB.01136-07

Cao, Q., Gearhart, M. D., Gery, S., Shojaee, S., Yang, H., Sun, H., … Koeffler, H. P. (2016). BCOR regulates myeloid cell proliferation and differentiation. *Leukemia*, *30*(5), 1155–65. http://doi.org/10.1038/leu.2016.2

Cao, R., & Zhang, Y. (2004). The functions of E(Z)/EZH2-mediated methylation of lysine 27 in histone H3. *Current Opinion in Genetics and Development*, *14*(2), 155–164. http://doi.org/10.1016/j.gde.2004.02.001

Chung, C. Y., Sun, Z., Mullokandov, G., Bosch, A., Qadeer, Z. A., Cihan, E., … Bernstein, E.

(2016). Cbx8 Acts Non-canonically with Wdr5 to Promote Mammary Tumorigenesis. *Cell Reports*, *16*(2), 472–486. http://doi.org/10.1016/j.celrep.2016.06.002

Coré, N., Bel, S., Gaunt, S. J., Aurrand-lions, M., Pearce, J., Fisher, A., … S, L. (1997). Altered cellular proliferation and mesoderm patterning in Polycomb-M33- deficient mice. *Development*, *729*, 721–729.

Creppe, C., Palau, A., Malinverni, R., Valero, V., & Buschbeck, M. (2014). A Cbx8-Containing Polycomb Complex Facilitates the Transition to Gene Activation during ES Cell Differentiation. *PLoS Genetics*, *10*(12). http://doi.org/10.1371/journal.pgen.1004851

Czermin, B., Melfi, R., McCabe, D., Seitz, V., Imhof, A., & Pirrotta, V. (2002). Drosophila enhancer of Zeste/ESC complexes have a histone H3 methyltransferase activity that marks chromosomal Polycomb sites. *Cell*, *111*(2), 185–196. http://doi.org/10.1016/S0092-8674(02)00975-3

de Graaf, C. A., Choi, J., Baldwin, T. M., Bolden, J. E., Fairfax, K. A., Robinson, A. J., … Hilton, D. J. (2016). Haemopedia: An Expression Atlas of Murine Hematopoietic Cells. *Stem Cell Reports*, *7*(3), 571–582. http://doi.org/10.1016/j.stemcr.2016.07.007

de Napoles, M., Mermoud, J. E., Wakao, R., Tang, Y. A., Endoh, M., Appanah, R., … Brockdorff, N. (2004). Polycomb group proteins ring1A/B link ubiquitylation of histone H2A to heritable gene silencing and X inactivation. *Developmental Cell*, *7*(5), 663–676. http://doi.org/10.1016/j.devcel.2004.10.005

Deaton, A. M., & Bird, A. (2011). CpG islands and the regulation of transcription. *Genes & Development*, *25*(10), 1010–22. http://doi.org/10.1101/gad.2037511

del Mar Lorente, M., Marcos-Gutiérrez, C., Pérez, C., Schoorlemmer, J., Ramírez, A., Magin, T., & Vidal, M. (2000). Loss- and gain-of-function mutations show a polycomb group function for Ring1A in mice. *Development (Cambridge, England)*, *127*(23), 5093–5100.

Elderkin, S., Maertens, G. N., Endoh, M., Mallery, D. L., Morrice, N., Koseki, H., … Hiom, K. (2007). A phosphorylated form of Mel-18 targets the Ring1B histone H2A ubiquitin ligase to chromatin. *Molecular Cell*, *28*(1), 107–120. http://doi.org/10.1016/j.molcel.2007.08.009

Farcas, A. M., Blackledge, N. P., Sudbery, I., Long, H. K., McGouran, J. F., Rose, N. R., … Klose, R. J. (2012). KDM2B links the Polycomb Repressive Complex 1 (PRC1) to recognition of CpG islands. *eLife*, *1*, e00205. http://doi.org/10.7554/eLife.00205

Frangini, A., Sjöberg, M., Roman-Trufero, M., Dharmalingam, G., Haberle, V., Bartke, T., …

Dillon, N. (2013). The Aurora B Kinase and the Polycomb Protein Ring1B Combine to Regulate Active Promoters in Quiescent Lymphocytes. *Molecular Cell*, *51*(5), 647–661. http://doi.org/10.1016/j.molcel.2013.08.022

Gao, Z., Zhang, J., Bonasio, R., Strino, F., Sawai, A., Parisi, F., … Reinberg, D. (2012). PCGF Homologs, CBX Proteins, and RYBP Define Functionally Distinct PRC1 Family Complexes. *Molecular Cell*, *45*(3), 344–356. http://doi.org/10.1016/j.molcel.2012.01.002

García, E., Marcos-Gutiérrez, C., del Mar Lorente, M., Moreno, J. C., & Vidal, M. (1999). RYBP, a new repressor protein that interacts with components of the mammalian Polycomb complex, and with the transcription factor YY1. *The EMBO Journal*, *18*(12), 3404–3418.

Gearhart, M. D., Corcoran, C. M., Wamstad, J. A., & Bardwell, V. J. (2006). Polycomb group and SCF ubiquitin ligases are found in a novel BCOR complex that is recruited to BCL6 targets. *Molecular and Cellular Biology*, *26*(18), 6880–6889. http://doi.org/10.1128/MCB.00630-06

Gottgens, B. (2015). Regulatory network control of blood stem cells. *Blood*, *125*(17), 2614–2621. http://doi.org/10.1182/blood-2014-08-570226.

Gray, F., Cho, H. J., Shukla, S., He, S., Harris, A., Boytsov, B., … Cierpicki, T. (2016). BMI1 regulates PRC1 architecture and activity through homo- and hetero-oligomerization. *Nature Communications*, *7*, 13343. http://doi.org/10.1038/ncomms13343

Gu, H., Marth, J. D., Orban, P. C., Mossmann, H., & Rajewsky, K. (1994). Deletion of a DNA polymerase beta gene segment in T cells using cell type-specific gene targeting. *Science (New York, N.Y.)*, *265*(5168), 103–6. http://doi.org/10.1126/science.8016642

Hauri, S., Comoglio, F., Seimiya, M., Gerstung, M., Glatter, T., Hansen, K., … Beisel, C. (2016). A high density map for navigating the human Polycomb complexome. *bioRxiv*, *17*(2), 059964. http://doi.org/10.1101/059964

Hérault, A., Binnewies, M., Leong, S., Calero-Nieto, F. J., Zhang, S. Y., Kang, Y.-A., … Passegué, E. (2017). Myeloid progenitor cluster formation drives emergency and leukaemic myelopoiesis. *Nature*, 1–19. http://doi.org/10.1038/nature21693

Huang, H.-T., Kathrein, K. L., Barton, A., Gitlin, Z., Huang, Y.-H., Ward, T. P., … Zon, L. I. (2013). A network of epigenetic regulators guides developmental haematopoiesis in vivo. *Nature Cell Biology*, *15*(12), 1516–25. http://doi.org/10.1038/ncb2870

Ikawa, T., Masuda, K., Endo, T. A., Endo, M., Isono, K., Koseki, Y., … Koseki, H. (2016). Conversion of T cells to B cells by inactivation of polycomb-mediated epigenetic

suppression of the B-lineage program. *Genes & Development*, 1–11. http://doi.org/10.1101/gad.290593.116.which

Isono, K., Endo, T., Ku, M., Yamada, D., Suzuki, R., Sharif, J., … Koseki, H. (2013). SAM domain polymerization links subnuclear clustering of PRC1 to gene silencing. *Developmental Cell*, *26*(6), 565–577. http://doi.org/10.1016/j.devcel.2013.08.016

Iwama, A., Oguro, H., Negishi, M., Kato, Y., Morita, Y., Tsukui, H., … Nakauchi, H. (2004). Enhanced self-renewal of hematopoietic stem cells mediated by the polycomb gene product Bmi-1. *Immunity*, *21*(6), 843–851. http://doi.org/10.1016/j.immuni.2004.11.004

Jadhav, U., Nalapareddy, K., Saxena, M., O'Neill, N. K., Pinello, L., Yuan, G. C., … Shivdasani, R. A. (2016). Acquired tissue-specific promoter bivalency is a basis for PRC2 necessity in adult cells. *Cell*, *165*(6), 1389–1400. http://doi.org/10.1016/j.cell.2016.04.031

Jürgens, G. (1985). A group of genes controlling the spatial expression of the bithorax complex in Drosophila. *Nature*, *316*(6024), 153–155. http://doi.org/10.1038/316153a0

Kalb, R., Latwiel, S., Baymaz, H. I., Jansen, P. W. T. C., Müller, C. W., Vermeulen, M., & Müller, J. (2014). Histone H2A monoubiquitination promotes histone H3 methylation in Polycomb repression. *Nature Structural & Molecular Biology*, *21*(6), 569–71. http://doi.org/10.1038/nsmb.2833

Kaneko, S., Bonasio, R., Saldaña-Meyer, R., Yoshida, T., Son, J., Nishino, K., … Reinberg, D. (2014). Interactions between JARID2 and Noncoding RNAs Regulate PRC2 Recruitment to Chromatin. *Molecular Cell*, *53*(2), 290–300. http://doi.org/10.1016/j.molcel.2013.11.012

Kaustov, L., Ouyang, H., Amaya, M., Lemak, A., Nady, N., Duan, S., … Arrowsmith, C. H. (2011). Recognition and specificity determinants of the human Cbx chromodomains. *Journal of Biological Chemistry*, *286*(1), 521–529. http://doi.org/10.1074/jbc.M110.191411

Klauke, K., Radulović, V., Broekhuis, M., Weersing, E., Zwart, E., Olthof, S., … de Haan, G. (2013). Polycomb Cbx family members mediate the balance between haematopoietic stem cell self-renewal and differentiation. *Nature Cell Biology*, *15*(4), 353–62. http://doi.org/10.1038/ncb2701

Kloet, S. L., Makowski, M. M., Baymaz, H. I., van Voorthuijsen, L., Karemaker, I. D., Santanach, A., … Vermeulen, M. (2016). The dynamic interactome and genomic targets of Polycomb complexes during stem-cell differentiation. *Nature Structural & Molecular Biology*, *23*(7), 682–690. http://doi.org/10.1038/nsmb.3248

Kondo, T., Isono, K., Kondo, K., Endo, T. A., Itohara, S., Vidal, M., & Koseki, H. (2014). Polycomb

Potentiates Meis2 Activation in Midbrain by Mediating Interaction of the Promoter with a Tissue-Specific Enhancer. *Developmental Cell*, *28*(1), 94–101. http://doi.org/10.1016/j.devcel.2013.11.021

Ku, M., Koche, R. P., Rheinbay, E., Mendenhall, E. M., Endoh, M., Mikkelsen, T. S., … Bernstein, B. E. (2008). Genomewide analysis of PRC1 and PRC2 occupancy identifies two classes of bivalent domains. *PLoS Genetics*, *4*(10). http://doi.org/10.1371/journal.pgen.1000242

Lau, M. S., Schwartz, M. G., Kundu, S., Savol, A. J., Wang, P. I., Marr, S. K., … Kingston, R. E. (2017). Mutation of a nucleosome compaction region disrupts Polycomb-mediated axial patterning, *7*(March), 1081–1084. http://doi.org/10.1126/science.aah5403

Lehmann, L., Ferrari, R., Vashisht, A. A., Wohlschlegel, J. A., Kurdistani, S. K., & Careys, M. (2012). Polycomb repressive complex 1 (PRC1) disassembles RNA polymerase II preinitiation complexes. *Journal of Biological Chemistry*, *287*(43), 35784–35794. http://doi.org/10.1074/jbc.M112.397430

Lessard, J., & Sauvageau, G. (2003). Bmi-1 determines the proliferative capacity of normal and leukaemic stem cells. *Nature*, *423*(6937), 255–260. http://doi.org/10.1038/nature01572

Levine, S. S., Weiss, A., Erdjument-Bromage, H., Shao, Z., Tempst, P., & Kingston, R. E. (2002). The core of the polycomb repressive complex is compositionally and functionally conserved in flies and humans. *Molecular and Cellular Biology*, *22*(17), 6070–6078. http://doi.org/10.1128/MCB.22.17.6070-6078.2002

Lewis, E. B. (1978). A gene complex controlling segmentation in Drosophila. *Nature*, *276*(5688), 565–70. http://doi.org/10.1128/AAC.03728-14

Li, Z., Cao, R., Wang, M., Myers, M. P., Zhang, Y., & Xu, R.-M. (2006). Structure of a Bmi-1-Ring1B polycomb group ubiquitin ligase complex. *The Journal of Biological Chemistry*, *281*(29), 20643–20649. http://doi.org/10.1074/jbc.M602461200

Lin, X., Ojo, D., Wei, F., Wong, N., Gu, Y., & Tang, D. (2015). A Novel Aspect of Tumorigenesis-BMI1 Functions in Regulating DNA Damage Response. *Biomolecules*, *5*(4), 3396–415. http://doi.org/10.3390/biom5043396

Lin, Y. W., & Aplan, P. D. (2004). Leukemic transformation. *Cancer Biology and Therapy*, *3*(1), 13–20. http://doi.org/10.4161/cbt.3.1.537

Liu, J., Cao, L., Chen, J., Song, S., Lee, I. H., Quijano, C., … Finkel, T. (2009). Bmi1 regulates mitochondrial function and the DNA damage response pathway. *Nature*, *459*(7245), 387–392. http://doi.org/10.1038/nature08040

Loubiere, V., Delest, A., Thomas, A., Bonev, B., Schuettengruber, B., Sati, S., … Cavalli, G. (2016). Coordinate redeployment of PRC1 proteins suppresses tumor formation during Drosophila development. *Nature Genetics*, (June 2015). http://doi.org/10.1038/ng.3671

Luis, N. M., Morey, L., Benitah, S. A., & Di Croce, L. (2012). Polycomb in Stem Cells: PRC1 Branches Out. *Cell Stem Cell*, *11*(1), 16–21. http://doi.org/10.1016/j.stem.2012.06.005

Maethner, E., Garcia-Cuellar, M.-P., Breitinger, C., Takacova, S., Divoky, V., Hess, J. L., & Slany, R. K. (2013). MLL-ENL Inhibits Polycomb Repressive Complex 1 to Achieve Efficient Transformation of Hematopoietic Cells. *Cell Reports*, *1*(5), 1–14. http://doi.org/10.1016/j.celrep.2013.03.038

Malovannaya, A., Lanz, R. B., Jung, S. Y., Bulynko, Y., Le, N. T., Chan, D. W., … Qin, J. (2011). Analysis of the human endogenous coregulator complexome. *Cell*, *145*(5), 787–799. http://doi.org/10.1016/j.cell.2011.05.006

Metzger, M. B., Pruneda, J. N., Klevit, R. E., & Weissman, A. M. (2014). RING-type E3 ligases: Master manipulators of E2 ubiquitin-conjugating enzymes and ubiquitination. *Biochimica et Biophysica Acta - Molecular Cell Research*, *1843*(1), 47–60. http://doi.org/10.1016/j.bbamcr.2013.05.026

Mijimolle, N., Velasco, J., Dubus, P., Guerra, C., Weinbaum, C. A., Casey, P. J., … Barbacid, M. (2005). Protein farnesyltransferase in embryogenesis, adult homeostasis, and tumor development. *Cancer Cell*, *7*(4), 313–324. http://doi.org/10.1016/j.ccr.2005.03.004

Min, J., Zhang, Y., & Xu, R. (2003). Structural basis for specific binding of Polycomb chromodomain to histone H3 methylated at Lys 27 Structural basis for specific binding of Polycomb chromodomain to histone H3 methylated at Lys 27, 1823–1828. http://doi.org/10.1101/gad.269603

Morey, L., Aloia, L., Cozzuto, L., Benitah, S. A., & Di Croce, L. (2013). RYBP and Cbx7 define specific biological functions of polycomb complexes in mouse embryonic stem cells. *Cell Reports*, *3*(1), 60–69. http://doi.org/10.1016/j.celrep.2012.11.026

Morey, L., Pascual, G., Cozzuto, L., Roma, G., Wutz, A., Benitah, S. A., & Di Croce, L. (2012). Nonoverlapping functions of the polycomb group Cbx family of proteins in embryonic stem cells. *Cell Stem Cell*, *10*(1), 47–62. http://doi.org/10.1016/j.stem.2011.12.006

Morey, L., Santanach, A., Blanco, E., Aloia, L., Nora, E. P., Bruneau, B. G., & Di croce, L. (2015). Polycomb Regulates Mesoderm Cell Fate-Specification in Embryonic Stem Cells through Activation and Repression Mechanisms. *Cell Stem Cell*, *17*(3), 300–315.

http://doi.org/10.1016/j.stem.2015.08.009

Morita, S., Kojima, T., & Kitamura, T. (2000). Plat-E: an efficient and stable system for transient packaging of retroviruses. *Gene Ther*, *7*(12), 1063–1066. http://doi.org/10.1038/sj.gt.3301206

Morrison, S. J., & Kimble, J. (2006). Asymmetric and symmetric stem-cell divisions in development and cancer. *Nature*, *441*(7097), 1068–1074. http://doi.org/10.1038/nature04956

Nakamura, S., Oshima, M., Yuan, J., Saraya, A., Miyagi, S., Konuma, T., … Iwama, A. (2012). Bmi1 confers resistance to oxidative stress on hematopoietic stem cells. *PLoS ONE*, *7*(5). http://doi.org/10.1371/journal.pone.0036209

Neira, J. L., Román-Trufero, M., Contreras, L. M., Prieto, J., Singh, G., Barrera, F. N., … Vidal, M. (2009). The transcriptional repressor RYBP is a natively unfolded protein which folds upon binding to DNA. *Biochemistry*, *48*(6), 1348–1360. http://doi.org/10.1021/bi801933c

Ogawa, H., Ishiguro, K., Gaubatz, S., & Livingston, M. (2002). A Complex with Chromatin Modi ers That Occupies E2F- and Myc-Responsive Genes in G 0 Cells. *Science*, *296*(May), 1132–1136. http://doi.org/10.1126/science.1069861

Oguro, H., Yuan, J., Ichikawa, H., Ikawa, T., Yamazaki, S., Kawamoto, H., … Iwama, A. (2010). Poised Lineage Specification in Multipotential Hematopoietic Stem and Progenitor Cells by the Polycomb Protein Bmi1. *Cell Stem Cell*, *6*(3), 279–286. http://doi.org/10.1016/j.stem.2010.01.005

Ohta, H., Sekulovic, S., Bakovic, S., Eaves, C. J., Pineault, N., Gasparetto, M., … Humphries, R. K. (2007). Near-maximal expansions of hematopoietic stem cells in culture using NUP98-HOX fusions. *Experimental Hematology*, *35*(5), 817–830. http://doi.org/10.1016/j.exphem.2007.02.012

Osmond, D. G. (1993). The turnover of B-cell populations. *Immunology Today*, *14*(1), 34–37. http://doi.org/10.1016/0167-5699(93)90322-C

Otte, A. P., & Kwaks, T. H. J. (2003). Gene repression by Polycomb group protein complexes: a distinct complex for every occasion? *Current Opinion in Genetics & Development*, *13*(5), 448–454. http://doi.org/10.1016/S0959-437X(03)00108-4

Oza, J., Ganguly, B., Kulkarni, A., Ginjala, V., Yao, M., & Ganesan, S. (2016). A novel role of chromodomain protein CBX8 in DNA damage response. *Journal of Biological Chemistry*,

291(44), 22881–22893. http://doi.org/10.1074/jbc.M116.725879

Park, I., Qian, D., Kiel, M., Becker, M. W., Pihalja, M., Weissman, I. L., … Clarke, M. F. (2003). Bmi-1 is required for maintenance of adult self-renewing haematopoietic stem cells. *Nature*, *423*(6937), 302–305. http://doi.org/10.1038/nature01587

Paul, F., Arkin, Y., Giladi, A., Jaitin, D. A., Kenigsberg, E., Keren-Shaul, H., … Amit, I. (2015). Transcriptional Heterogeneity and Lineage Commitment in Myeloid Progenitors. *Cell*, *163*(7), 1663–1677. http://doi.org/10.1016/j.cell.2015.11.013

Piunti, A., Rossi, A., Cerutti, A., Albert, M., Jammula, S., Scelfo, A., … Pasini, D. (2014). Polycomb proteins control proliferation and transformation independently of cell cycle checkpoints by regulating DNA replication. *Nat Commun*, *5*, 3649. http://doi.org/10.1038/ncomms4649

Raaphorst, F. M., Otte, A. P., & Meijer, C. J. L. M. (2001). Polycomb-group genes as regulators of mammalian lymphopoiesis. *Trends in Immunology*, *22*(12), 682–690. http://doi.org/10.1016/S1471-4906(01)02082-8

Ram, O., Goren, A., Amit, I., Shoresh, N., Yosef, N., Ernst, J., … Bernstein, B. E. (2011). Combinatorial patterning of chromatin regulators uncovered by genome-wide location analysis in human cells. *Cell*, *147*(7), 1628–1639. http://doi.org/10.1016/j.cell.2011.09.057

Reynolds, N., Salmon-Divon, M., Dvinge, H., Hynes-Allen, A., Balasooriya, G., Leaford, D., … Hendrich, B. (2012). NuRD-mediated deacetylation of H3K27 facilitates recruitment of Polycomb Repressive Complex 2 to direct gene repression. *The EMBO Journal*, *31*(3), 593–605. http://doi.org/10.1038/emboj.2011.431

Ringrose, L., & Paro, R. (2007). Polycomb/Trithorax response elements and epigenetic memory of cell identity. *Development (Cambridge, England)*, *134*(2), 223–32. http://doi.org/10.1242/dev.02723

Rizo, a, Dontje, B., Vellenga, E., de Haan, G., & Schuringa, J. J. (2008). Long-term maintenance of human hematopoietic stem/progenitor cells by expression of BMI1. *Blood*, *111*(5), 2621–2630. http://doi.org/10.1182/blood-2007-08-106666

Ross, K., Sedello, A. K., Todd, G. P., Paszkowski-Rogacz, M., Bird, A. W., Ding, L., … Buchholz, F. (2012). Polycomb group ring finger 1 cooperates with Runx1 in regulating differentiation and self-renewal of hematopoietic cells. *Blood*, *119*(18), 4152–61. http://doi.org/10.1182/blood-2011-09-382390

Sánchez, C., Sánchez, I., Demmers, J. a a, Rodriguez, P., Strouboulis, J., & Vidal, M. (2007). Proteomics analysis of Ring1B/Rnf2 interactors identifies a novel complex with the Fbxl10/Jhdm1B histone demethylase and the Bcl6 interacting corepressor. *Molecular & Cellular Proteomics : MCP*, *6*(5), 820–834. http://doi.org/10.1074/mcp.M600275-MCP200

Sanchez-Pulido, L., Devos, D., Sung, Z., & Calonje, M. (2008). RAWUL: A new ubiquitin-like domain in PRC1 Ring finger proteins that unveils putative plant and worm PRC1 orthologs. *BMC Genomics*, *9*(1), 308. http://doi.org/10.1186/1471-2164-9-308

Saurin, A. J., Borden, K. L. B., Boddy, M. N., & Freemont, P. S. (1996). Does this have a familiar RING? *Trends in Biochemical Sciences*, *21*(6), 208–214. http://doi.org/10.1016/0968-0004(96)10036-0

Schaaf, C. a, Misulovin, Z., Gause, M., Koenig, A., Gohara, D. W., Watson, A., & Dorsett, D. (2013). Cohesin and polycomb proteins functionally interact to control transcription at silenced and active genes. *PLoS Genetics*, *9*(6), e1003560. http://doi.org/10.1371/journal.pgen.1003560

Schoenfelder, S., Sugar, R., Dimond, A., Javierre, B., Armstrong, H., Mifsud, B., … Elderkin, S. (2015). Polycomb repressive complex PRC1 spatially constrains the mouse embryonic stem cell genome. *Nature Genetics*, *47*(10), 1179–1186. http://doi.org/10.1038/ng.3393

Schoorlemmer, J., Marcos-Gutiérrez, C., Were, F., Martinez, R., Garcia, E., Satijn, D. P. E., … Vidal, M. (1997). Ring1A is a transcriptional repressor that interacts with the Polycomb-M33 protein and is expressed at rhombomere boundaries in the mouse hindbrain. *EMBO Journal*, *16*(19), 5930–5942. http://doi.org/10.1093/emboj/16.19.5930

Scott, C. L., Hernando, E., Teruya-feldstein, J., Narita, M., Martı, D., Visakorpi, T., … By, A. (2007). Role of the chromobox protein CBX7 in lymphomagenesis, *104*(13), 1–6.

Somervaille, T. C. P., & Cleary, M. L. (2006). Identification and characterization of leukemia stem cells in murine MLL-AF9 acute myeloid leukemia. *Cancer Cell*, *10*(4), 257–68. http://doi.org/10.1016/j.ccr.2006.08.020

Sparmann, A., & van Lohuizen, M. (2006). Polycomb silencers control cell fate, development and cancer. *Nature Reviews. Cancer*, *6*(11), 846–856. http://doi.org/10.1038/nrc1991

Stanton, B. Z., Hodges, C., Calarco, J. P., G Braun, S. M., Lim Ku, W., Kadoch, C., … Crabtree, G. R. (2016). Smarca4 ATPase mutations disrupt direct eviction of PRC1 from chromatin. *Nature Publishing Group*, (December). http://doi.org/10.1038/ng.3735

Stock, J. K., Giadrossi, S., Casanova, M., Brookes, E., Vidal, M., Koseki, H., … Pombo, A. (2007). Ring1-mediated ubiquitination of H2A restrains poised RNA polymerase II at bivalent genes in mouse ES cells. *Nature Cell Biology*, *9*(12), 1428–1435. http://doi.org/10.1038/ncb1663

Suzuki, A., Hirasaki, M., Hishida, T., Wu, J., Okamura, D., Ueda, A., … Okuda, A. (2016). Loss of MAX results in meiotic entry in mouse embryonic and germline stem cells. *Nature Communications*, *7*, 11056. http://doi.org/10.1038/ncomms11056

Tan, J., Jones, M., Koseki, H., Nakayama, M., Muntean, A. G., Maillard, I., & Hess, J. L. (2011). CBX8, a Polycomb Group Protein, Is Essential for MLL-AF9-Induced Leukemogenesis. *Cancer Cell*, *20*(5), 563–575. http://doi.org/10.1016/j.ccr.2011.09.008

Tavares, L., Dimitrova, E., Oxley, D., Webster, J., Poot, R., Demmers, J., … Brockdorff, N. (2012). RYBP-PRC1 complexes mediate H2A ubiquitylation at polycomb target sites independently of PRC2 and H3K27me3. *Cell*, *148*(4), 664–678. http://doi.org/10.1016/j.cell.2011.12.029

Tough F. David, & Sprent Jonathan. (1996). Turnover of Naive- and Memory-phenotype T Cells. *Journal of Experimental Medicine*, *179*(April), 1127–1135.

Trojer, P., Cao, A. R., Gao, Z., Li, Y., Zhang, J., Xu, X., … Reinberg, D. (2011). L3MBTL2 Protein Acts in Concert with PcG Protein-Mediated Monoubiquitination of H2A to Establish a Repressive Chromatin Structure. *Molecular Cell*, *42*(4), 438–450. http://doi.org/10.1016/j.molcel.2011.04.004

Ueda, T., Nagamachi, A., Takubo, K., Yamasaki, N., Matsui, H., Kanai, A., … Tg, W. (2017). Fbxl10 overexpression in murine hematopoietic stem cells induces leukemia involving metabolic activation and upregulation of Nsg2. *Blood Journal*, *125*(22), 3437–3447. http://doi.org/10.1182/blood-2014-03-562694

van den Boom, V., Maat, H., Geugien, M., Rodríguez López, A., Sotoca, A. M., Jaques, J., … Schuringa, J. J. (2016). Non-canonical PRC1.1 Targets Active Genes Independent of H3K27me3 and Is Essential for Leukemogenesis. *Cell Reports*, *14*(2), 332–346. http://doi.org/10.1016/j.celrep.2015.12.034

van den Boom, V., Rozenveld-Geugien, M., Bonardi, F., Malanga, D., van Gosliga, D., Heijink, A. M., … Schuringa, J. J. (2013). *Nonredundant and locus-specific gene repression functions of PRC1 paralog family members in human hematopoietic stem/progenitor cells. Blood* (Vol. 121). http://doi.org/10.1182/blood-2012-08-451666

Van Der Lugt, N. M. T., Domen, J., Linders, K., Van Roon, M., Robanus-Maandag, E., Te Riele, H., … Berns, A. (1994). Posterior transformation, neurological abnormalities, and severe hematopoietic defects in mice with a targeted deletion of the bmi-1 proto-oncogene. *Genes and Development*, *8*(7), 757–769. http://doi.org/10.1101/gad.8.7.757

Vandamme, J., Völkel, P., Rosnoblet, C., Le Faou, P., & Angrand, P.-O. (2011). Interaction proteomics analysis of polycomb proteins defines distinct PRC1 complexes in mammalian cells. *Molecular & Cellular Proteomics : MCP*, *10*(4), M110.002642. http://doi.org/10.1074/mcp.M110.002642

Vidal, M., & Starowicz, K. (2017). Polycomb complexes PRC1 and their function in hematopoiesis. *Experimental Hematology*, *48*, 12–31. http://doi.org/10.1016/j.exphem.2016.12.006

Wiederschain, D., Chen, L., Johnson, B., Bettano, K., Jackson, D., Taraszka, J., … Benson, J. D. (2007). Contribution of polycomb homologues Bmi-1 and Mel-18 to medulloblastoma pathogenesis. *Molecular and Cellular Biology*, *27*(13), 4968–79. http://doi.org/10.1128/MCB.02244-06

Wilson, A., Laurenti, E., Oser, G., van der Wath, R. C., Blanco-Bose, W., Jaworski, M., … Trumpp, A. (2008). Hematopoietic Stem Cells Reversibly Switch from Dormancy to Self-Renewal during Homeostasis and Repair. *Cell*, *135*(6), 1118–1129. http://doi.org/10.1016/j.cell.2008.10.048

Wilson, B. G., Wang, X., Shen, X., McKenna, E. S., Lemieux, M. E., Cho, Y. J., … Roberts, C. W. M. (2010). Epigenetic antagonism between polycomb and SWI/SNF complexes during oncogenic transformation. *Cancer Cell*, *18*(4), 316–328. http://doi.org/10.1016/j.ccr.2010.09.006

Yap, K. L., Li, S., Muñoz-Cabello, A. M., Raguz, S., Zeng, L., Mujtaba, S., … Zhou, M. M. (2010). Molecular Interplay of the Noncoding RNA ANRIL and Methylated Histone H3 Lysine 27 by Polycomb CBX7 in Transcriptional Silencing of INK4a. *Molecular Cell*, *38*(5), 662–674. http://doi.org/10.1016/j.molcel.2010.03.021

Yap, K. L., & Zhou, M. M. (2011). Structure and mechanisms of lysine methylation recognition by the chromodomain in gene transcription. *Biochemistry*, *50*(12), 1966–1980. http://doi.org/10.1021/bi101885m

Yokoyama, A. (2016). Transcriptional activation by MLL fusion proteins in leukemogenesis. *Experimental Hematology*, *46*, 21–30. http://doi.org/10.1016/j.exphem.2016.10.014

Yoshida, T., & Georgopoulos, K. (2014). Ikaros fingers on lymphocyte differentiation. *International Journal of Hematology*, *100*(3), 220–229. http://doi.org/10.1007/s12185-014-1644-5

Yu, M., Mazor, T., Huang, H., Huang, H. T., Kathrein, K. L., Woo, A. J., … Cantor, A. B. (2012). Direct Recruitment of Polycomb Repressive Complex 1 to Chromatin by Core Binding Transcription Factors. *Molecular Cell*, *45*(3), 330–343. http://doi.org/10.1016/j.molcel.2011.11.032

Zhen, C. Y., Tatavosian, R., Huynh, T. N., Duc, H. N., Das, R., Kokotovic, M., … Ren, X. (2016). Live-cell single-molecule tracking reveals co-recognition of H3K27me3 and DNA targets polycomb Cbx7-PRC1 to chromatin. *eLife*, *5*(OCTOBER2016), 1–36. http://doi.org/10.7554/eLife.17667.001